Research Experience for Undergraduates
Research Reports
Indiana University, Bloomington
Summer 2011

October 28, 2011

Contents

Preface

During the summer of 2010 eight students participated in the Research Experiences for Undergraduates program in Mathematics at Indiana University. The program ran for eight weeks, from June 20 through August 12, 2011. Six faculty served as research advisers. Two faculty members oversaw a pair of related projects; all other faculty advised one student each.

The program opened with an introductory pizza party. On the following morning, students began meeting with their faculty mentors; these meetings continued regularly throughout the first few weeks. During week one, there were short presentations by faculty mentors briefly introducing the problem to be investigated. Several other IU faculty gave talks on their favorite topics during the first half of the program. Students also received orientations to the mathematics library and to our computing facilities. In week three, students gave short, informal presentations to each other on the status of work on the project; they also enjoyed a party at a local swimming pool, hosted by Dr. Housworth. Brief training sessions on using LaTeXwere given during week four. Housed in a common dorm, the students themselves organized a barbecue and a to see renowned local violinist Joshua Bell. In week five, they received a personal tour of the cyclotron facility. During week six, we hosted the Indiana Mathematics Undergraduate Research conference, which featured 20 lectures by 27 students from Rose-Hulman Institute of Technology, Goshen College, Valparaiso University, and Indiana University, and ended with an hourlong panel discussion on graduate school. The next week ended with a picnic at Rawles Hall; the location moved inside due to the heat and humidity. The program concluded with the students giving formal, hourlong presentations to the REU students and faculty, and the submission of final reports, contained in this volume.

It took the help and support of many different groups and individuals to make the program a success.

We thank the National Science Foundation for major financial support through the REU program through grant DMS-0851852. We also thank Indiana University's Vice President for Diversity, Equity, and Multicultural Affairs, Dr. Edwin Marshall, and Vicki Roberts, Associate Vice President for Administration and Culture, for additional funding. We thank Indiana University for the use of facilities, including library, computers, and recreational facilities. We thank the staff of the Department of Mathematics for support, especially Mandie McCarty for coordinating the complex logistical arrangments (housing, paychecks, information packets, meal plans, frequent shopping for snacks and peanut-free items) and Cheryl Miller (now retired) for her assistance in coordinating the application process; we will miss her. We thank Indiana graduate student Tri Lai for serving as LaTeXconsultant and for compiling this volume.

Thanks to mathematics faculty Chris Connell, Elizabeth Housworth, Matvei Libine, William Orrick, Kevin Pilgrim, and Bruce Solomon for serving as mentors and giving lectures, and to Matthias Strauch for giving lectures. Thanks to Matthias Weber for the plenary talk on minimal surfaces at our annual conference. Thanks to Jillian Hinchcliffe of the Lily Library for her personal tour of

the Slocum collection. Thanks to David Baxter of the Center for Exploration of Energy and Matter (nee IU cyclotron facility) for his personal tour of the cyclotron facility.

KMP
October, 2011

Figure 1: REU Participants, from left to right: Kevin Pilgrim (PI); Nick Edelen, Matthew Mizuhara, Rebecca McCarthy, Frederick Robinson, Clark Butler, Rachel Moger-Reischer, Hanna Astephan. Not shown is Ewain Gwynne.

Negatively Curved Surfaces in $\mathbb{R}^3$

Hanna Astephan

Abstract

We explore Vaigant's surface, the only known negatively curved surface with cuspidal ends. The goal of this project is to find a negatively curved surface with more than four cuspidal ends or surfaces of other topological types with only cuspidal ends. Building on his work, we hope to modify this surface in a variety of ways. The first modification entails adding genus to the surface and exploring the topological ramifications. The next type of modification transforms Vaigant's surface to a six-ended surface, as well as an eight-ended one. We are investigating ways to preserve negative curvature after these modifications. As a part of this, we are looking at the indices of planar slice curves in light of these surfaces' Euler characteristics. The main tool we use, apart from algebraic manipulations, is the Poincaré-Hopf theorem. We also look at how to parametrize negatively curved tubes and what types of conditions must be satisfied for a general plane curve.

I. Introduction

Curvature, in the most intuitive sense, can be thought of as how much a surface bends. In the case of negative curvature, every region of the surface as a graph is locally a saddle.

The following definitions, all taken from [1] unless stated otherwise, will be useful in our analysis of negatively curved surfaces. In this paper, each surface will be interpreted as a graph, or a function $z = f(x, y)$. However, the given definitions apply to surfaces in parametric form.

Assume S is a regular, smooth, and complete surface embedded in $\mathbb{R}^3$ for the following definitions. We write the surface S in parametric form as

$$\vec{x}(u, v) = (x(u, v), y(u, v), z(u, v)),$$

for $(u, v) \in U$, where U is an open subset of $\mathbb{R}^2$.

Definition 0.1. Tangent Vector: At a point $p \in S$, the tangent vector $\alpha'(0)$ is a differentiable parametrized curve $\alpha : (-\epsilon, \epsilon) \longrightarrow S$ such that $\alpha(0) = p$.

Definition 0.2. Tangent Plane: $\forall p \in S$, the set of tangent vectors to the parametrized curves of S, passing through p, defines the tangent plane. The vector subspace of dimension 2, $d\vec{x}_q(\mathbb{R}^2) \subset \mathbb{R}^3$, coincides with set of tangent vectors to S at $\vec{x}(q)$. The tangent plane will be denoted as $T_p(S)$. The choice of the parametrization $\vec{x}$ determines a basis $\vec{x}_u, \vec{x}_v$ of $T_p(S)$, called the basis associated to $\vec{x}$.

Definition 0.3. Normal Vector: Given a parametrization $\vec{x} : U \subset R^2 \longrightarrow S$ of a regular surface S at a point $p \in S$, we can choose a normal vector at each point of $\vec{x}(U)$ by the rule:

$$N(q) = \frac{\vec{x}_u \wedge \vec{x}_v}{|\vec{x}_u \wedge \vec{x}_v|}(q), \text{ for } q \in \vec{x}(U).$$

Definition 0.4. Let $S \subset \mathbb{R}^3$ be a surface with an orientation N. The map $N : S \longrightarrow \mathbb{R}^3$ takes it values in the unit sphere

$$S^2 = \{(x, y, z) \in \mathbb{R}^3;\ x^2 + y^2 + z^1 = 1\}$$

The map $N : S \longrightarrow S^2$ is called the Gauss Map of S.

The differential dN_p at $p \in S$ is a linear map from $T_p(S)$ to $T_{N(p)}(S^2)$. It measures how N pulls away from $N(p)$ in a neighborhood of p. In the case of curves, this measure is given by a number, the curvature k, times the cross product of the tangent vector and normal vector. In the case of surfaces, this measure is characterized by a linear map.

Definition 0.5. Let $p \in S$, and let $dN_p : T_p(S) \longrightarrow T_p(S)$ be the differential of the Gauss map. The determinant of dN_p is the Gaussian curvature K of S at p.

Definition 0.6. Let C be a regular curve in S passing through $p \in S$, k the curvature of C at p, and $cos\theta =< \vec{n}, \vec{N} >$ where $\vec{n}$ is the normal vector to C and $\vec{N}$ is the normal vector to S at p. The number $k_n = kcos\theta$ is then called the normal curvature of $C \subset S$ at p. In other words, k_n is the length of the projection of the vector $k\vec{n}$ over the normal to the surface at p, with a sign given by the orientation $\vec{N}$ of S at p.

Definition 0.7. A point of a surface S is called *hyperbolic* if $det(dN_p) < 0$. In the case, there are curves through p whose normal vectors at p point toward any sides of the tangent plane at p.

Definition 0.8. Let p be a point in S. An asymptotic direction of S at p is a direction of $\vec{T_p}(S)$ for which the normal curvature is zero. An asymptotic curve of S is a regular connected curve $C \subset S$ such that $\forall\ p \in C$, the tangent line of C at p is an asymptotic direction.

At a hyperbolic point there are exactly two asymptotic directions. Thus, these form two independent line fields on a surface of negative curvature.

Definition 0.9. First fundamental form: suppose we have two vectors, $\vec{w}_1, \vec{w}_2$, in the tangent plane of a surface S. We can take the inner product of these vectors, $I_p(w) = \langle w, w \rangle_p = |w|^2 \geq 0$. The quadratic form I_p on $T_p(S)$ defined by this equation, is called the first fundamental form of the regular surface $S \subset R^3$ at $p \in S$. Therefore, the first fundamental form is the expression of how the surface S inherits the natural inner product of $\mathbb{R}^3$.

We can compute the Gaussian curvature of a surface using local coordinates. While there are ways to compute the curvature when a surface is in parametric form, there are also ways to compute the curvature for a graph.

This is done by parametrizing a surface as $\vec{x}(u,v) = (u,v,h(u,v))$, for $(u,v) \in U$, where U in a open subset of $\mathbb{R}^2$. Here, the normal vector is given as:

$$N(x,y) = \frac{(-h_x,-h_y,1)}{(1+h_x^2+h_y^2)^{\frac{1}{2}}},$$

as a unit normal field on the surface. This results in coefficients of the second fundamental form as:

$$e = \frac{h_{xx}}{(1+h_x^2+h_y^2)^{\frac{1}{2}}},\ f = \frac{h_{xy}}{(1+h_x^2+h_y^2)^{\frac{1}{2}}},\text{ and } g = \frac{h_{yy}}{(1+h_x^2+h_y^2)^{\frac{1}{2}}}.$$

Curvature is thus:

$$K = \frac{h_{xx}h_{yy}-h_{xy}^2}{(1+h_x^2+h_y^2)^2}$$

Since the denominator of this fraction is always positive, the numerator, $h_{xx}h_{yy}-h_{xy}^2$, is of interest in determining whether a surface is negatively curved or not.

Another necessary component in our analysis of negatively curved surfaces is studying the ends of such surfaces. We will first distinguish two types of ends from one another–bowl ends and horn ends, taken from [2].

Definition 0.10. Let Σ denote an end of a surface S. We call a simple closed curve Γ on Σ a belt curve if it is homotopic to the boundary of the closure of Σ. Then Σ is called a horn end if there is no belt curve of shortest length on the closure of Σ. Otherwise, Σ is a bowl end. In addition, a horn end is called a cusp if the infimum of the lengths of the belt curves is zero.

In studying these ends, we will also consider their planar slice curves in order to make use of the Poincaré-Hopf theorem.

Definition 0.11. Let $\vec{v} : S \longrightarrow R^3$ be a differentiable vector field on a surface S. Then $p_i \in S$ is called a singular point of the vector field $\vec{v}$ if $\vec{v}(p_i) = 0$. The singular point p is isolated if there exists a neighborhood V of p in S such that v has no singular points in V other than p.

Definition 0.12. Let $\vec{x} : U \longrightarrow S$ be an orthogonal parametrization at $p = \vec{x}(0,0)$ compatible with the orientation of S, and let $\alpha : [0,l] \longrightarrow S$ be a simple, closed, positively-oriented piecewise regular parametrized curve such that $\alpha([0,l]) \subset \vec{x}(U)$ is the boundary of a simple region R containing p as its only singular point. Let $v = v(t)$, $t \in [0,l]$, be the restriction of v along α, and let $\phi = \phi(t)$ be some differentiable determination of the angle from $\vec{x}_u$ to $v(t)$. Since α is closed, there an integer I defined by

$$2\pi I = \phi(l) - \phi(0) = \int_0^l \frac{d\phi}{dt} dt$$

Then I is called the index of v at p.

Similarly, for a line field, we can think of the line field index of a singular point on S as the number of clockwise π turns a line field makes around a simple, closed curve enclosing the singular point, when traversed clockwise. Here, a singular point is a point of which the line field is either not defined or cannot be extended continuously.

Definition 0.13. Let S be a closed, orientable surface. Then the Euler characteristic of S, denoted as $\chi(S)$, is given as $\chi(S) = 2 - 2g$, where g is the genus, or the number of holes on the surface.

From those definitions, we can now state the following theorem:

Theorem 0.14. *Poincaré-Hopf Theorem (line field version): Let S be a closed, orientable surface, and let L be a differentiable line field defined on S, with isolated singular points $p_i \in P$, where P is some finite index set. Then,*

$$\sum_{i=1}^{n} ind_{p_i}(L) = 2\chi(S)$$

Where $ind_{p_i}(L)$ denotes the index of L at the singular point, p_i.

Note that the vector field version would be the same except the right-hand side of the equation is just the regular Euler characteristic, $\chi(S)$, since the index in that curve makes 2π turns instead of π turns.

With the Poincaré-Hopf theorem in mind, we now consider planar slice curves of different types of ends. We do this by slicing a surface transversally with a plane. It is necessary to make the planar slice transverse to the surface S so that the normal of the surface is not the normal of the plane. We can compute the index of the end point at ∞ using this planar slice curve, simply by looking at the number of inflection points of the curve.

There are two cases to consider when looking at the asymptotic line fields of slice curves.

Case 1. The slice curve is convex. There are no inflection points in this case, as shown by this relevant lemma, modified from [3]:

Lemma 0.15. *An asymptotic line crosses through a tangency on a transverse slice curve if and only if the point is an inflection point on the curve.*

Proof: Let $c : [0, 1] \to S$ represent a convex plane curve. If $c'(t)$ is asymptotic for some t then by definition, $\langle dN(c'(t)), c'(t)\rangle = 0$, where dN denotes the derivative of the Gauss map. On the other hand, we have $\langle dN(c'(t)), c'(t)\rangle = k(t)\left\langle \vec{n}(t), \vec{N}(t)\right\rangle$, where $\vec{n}(t)$ is the normal to the curve at $c(t)$, $\vec{N}(t)$ is the surface normal at $c(t)$, and $k(t)$ is the curvature of the curve. However, $k(t) > 0$ since c is convex, and $\vec{n}(t)$ lies in the plane because the curve is planar. Thus, the only way it could be zero is if $\vec{N}(t)$ is perpendicular to the plane at some point. However, then the plane is tangent to the surface at that point on the

curve, which contradicts the assumption that the plane is slicing the surface transversally.

Case 2. The slice curve is non-convex. Then, the number of inflection points varies. The normal curvature of the slice curve changes sign when it crosses through a tangency to an asymptotic line, since these divide up the positive and negative regions of the second fundamental form in the tangent plane to the surface. However, such a change in concavity is also the definition of an inflection point. □

Corollary 0.16. *The index is between* $2-t$ *and* $2+t$ *where* t *is half the number of inflection points, which is always even on a closed curve.*

Note that if there are three inflection points in a row and the field to which each inflection point belongs alternates from one inflection point to the next, then this means that both asymptotic line fields rotated through in succession and return to the starting position by the time the third inflection point is reached. This contributes a positive or negative half turn. However, these can cancel, and we do not have a reason to rule out the possibility of the same field being tangent at consecutive inflection points.

Nevertheless, in our examples the index appears to follow the lower bound, $2 - t$, the case when the line field is consistently rotating counter-clockwise through $2t$ inflection points.

We can now begin our main investigation: does there exist a negatively curved surface in $\mathbb{R}^3$ with more than four cuspidal ends?

II. Vaigant's Surface

Vaigant's surface is the only known example of a negatively curved surface with cuspidal ends. It is given as this graph:

$$(z - u + v)^2(8 + u + v)^2 - \epsilon^2(2 - (u - 1)(v - 1)) = 0$$

Where, $u = \sqrt{1 + x^2}$, $v = \sqrt{1 + y^2}$, and $0 < \epsilon < \frac{1}{2\sqrt{2}}$.

This is what it looks like for ϵ equal to $\frac{1}{2}$.

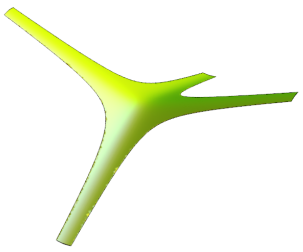

It has four cuspidal ends, its Euler characteristic is 2, and each end has an index of 1. Based on this surface, we are going to modify his surface in a variety of ways: adding genus, adding two more cuspidal ends, and adding four more cuspidal ends. Our main concern will be the index of the ends of these new surfaces in hopes of being able to preserve negative curvature.

It is important to note its planar slice curve:

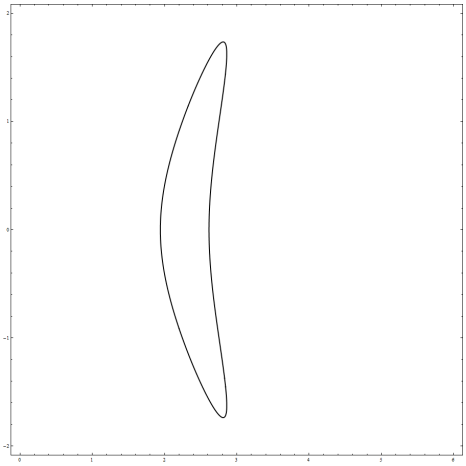

and that this type of cuspidal end has an index of 1. Although it has two inflection points along the non-convex portion of the curve, by symmetry of the asymptotic directions, we only count one of these inflection points. Note that the remaining cuspidal ends in the following surfaces also have an index of 1.

We will begin with our first modification, adding genus.

IIa. Adding Genus.

Suppose we graph Vaigant's surface in (u, v) coordinates, and in particular, the positive root after solving for z:

$$z = u - v + \epsilon \frac{\sqrt{1+u+v-uv}}{8+u+v}$$

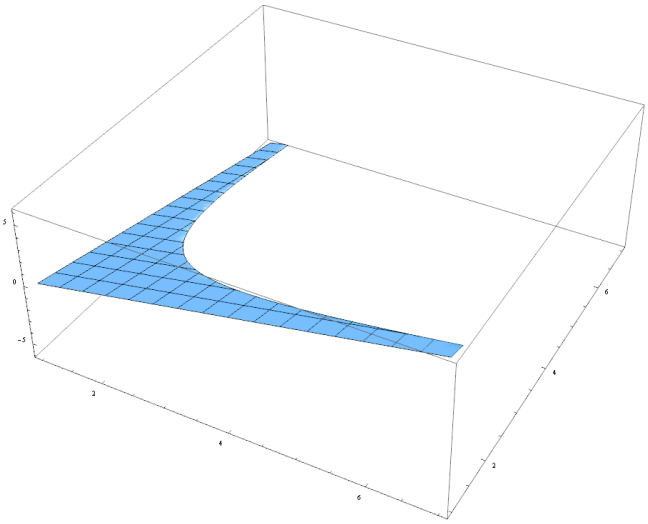

In the positive quadrant, we see a bend that coincides with the bend we see in the surface after we graph it in (x, y) coordinates. Extending the axes, however, in the negative direction of both u and v, shows us that there is a ridge that resembles a portion of a circle like so:

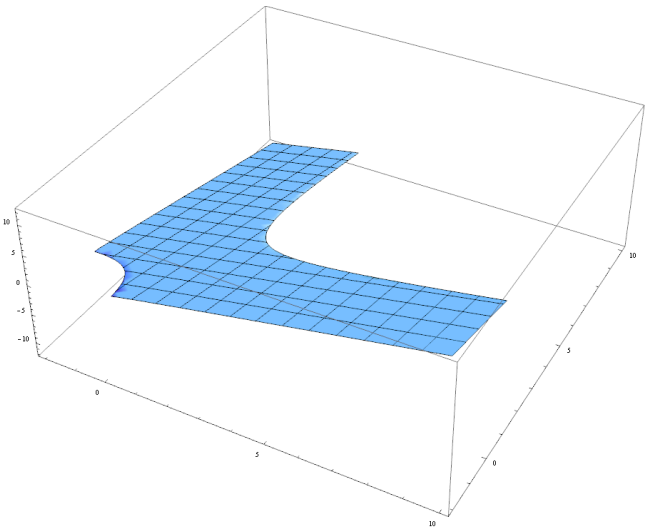

Taking that into consideration, we can shift this piece of the surface so that a hole can be created in the middle of the surface, equivalent to adding genus. The new equation of the surface would be as follows:

$$(z - u + v)^2(8 + u + v)^2 - \epsilon^2(1 + (u - h) + (v - h) - (u - h)(v - h)) = 0$$

Here h is the translation; thus, the size of the hole depends on the value of h. The following shows the surface for when $h = 2$, and $\epsilon = 1/2$.

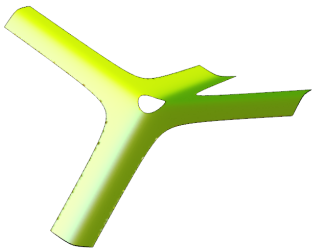

By symmetry, we can compute the curvature of one portion of the surface, the same portion in which the surface lied in the positive quadrant. We will compute the curvature of the following equation:

$$g(x,y) = \sqrt{1+x^2} - \sqrt{1+y^2} - \epsilon \frac{\sqrt{1-2h+\sqrt{1+x^2}+\sqrt{1+y^2}+(\sqrt{1+x^2}-h)(h-\sqrt{1+y^2})}}{8+\sqrt{1+x^2}+\sqrt{1+y^2}}$$

Since we are most interested in the sign of the curvature, we compute the curvature function as:

$$K_g = g_{uu}g_{vv} - g_{uv}^2$$

After replacing $\sqrt{1+x^2}$ as u and $\sqrt{1+y^2}$ as v.

After such computations for small ϵ, we see that there are small regions of nonnegative curvature. This can be seen by graphing both curvature as a function of (u, v) and a plane at 0. The places in which $K_g(u, v)$ lies above the plane are regions in which there is nonnegative curvature. For a specific value of $h = 2$ and $\epsilon = 1/8$, this looks like this:

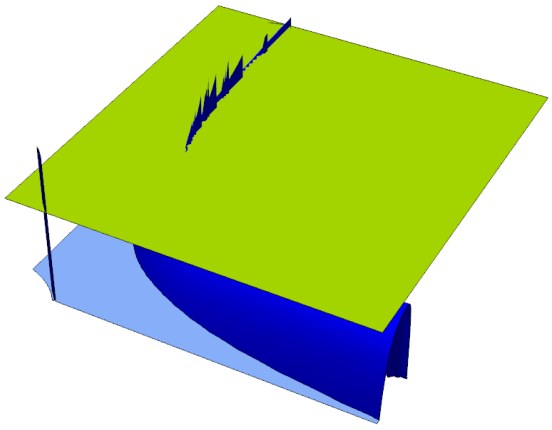

The reason for positive curvature can be explained in a variety of ways. Adding genus changes the Euler characteristic of the surface, and therefore, the surface must also have different ends in order to not violate the Poincaré-Hopf theorem under the assumption of the surface being negatively curved everywhere. However, the process of adding genus only changed the center of the surface; the original Vaigant ends were preserved. Each end, as a result, still has an index of 1, but the surface now has a Euler characteristic of 0 because $\chi(S) = 2 - 2g = 2 - 2(1) = 0$. Thus, the the issue of positive curvature on the surface is likely to be a result of not changing the ends accordingly. Further work in hopes of preserving negative curvature would require changing the ends of the surface, but this remains difficult to do because of the coordinate shift.

IIb. Six Ends.

We now construct a Vaigant surface with six cuspidal ends. For this surface, the Euler characteristic remains the same as 2. Because there are six ends now, though, each end cannot have the same index, since the sum must be 4 and each index has to be an integer.

There were a few ways in which we approached the construction of this surface.

The first approach entailed using the shape of the cruciform algebraic curve. Its implicit equation is given as $x^2y^2 - b^2x^2 - a^2y^2 = 0$, where a and b are constants not equal to zero, taken from [5]. The purpose of using this curve is to create a new profile curve of the surface to add two more ends. The general shape of the Vaigant surface is largely determined by the discriminant portion of the equation after solving for z, given as: $\sqrt{1 + u + v - uv}$ in (u, v) coordinates. To add another end, we change the discriminant such that another piece of the surface becomes imaginary.

Rather than stacking two three-ended pieces together, we bridge two three-ended surfaces by a bridge in the center. Note that this does not have the same type of symmetry as the original Vaigant surface. The way in which we construct it admits two ends point in the downward direction, and four ends pointing in the upward direction. The two ends pointing down will have the same index because of the symmetry, and the ends going up will have the same index. In (u, v) coordinates, the piece looks like this:

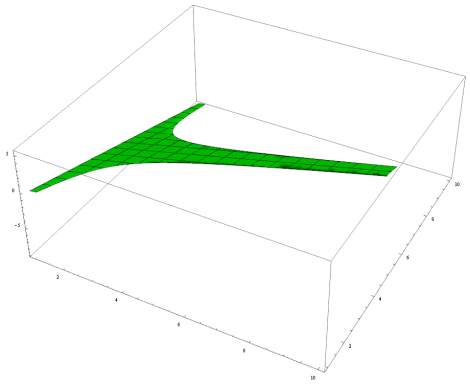

Thus, the index of the ends must satisfy the equation $2a + 4b = 4$, where a represents the index of the two ends going down, and b represents the index of the ends going up. While there are many finitely many solutions to this equation, mainly $a = 2 - 2b$, it is best to keep the index value of each end as low as possible, for these type of ends have simpler equations and planar slice curves.

The problem, however, with the cruciform curve, is that the ends do not taper like they do in Vaigant's surface. It is necessary for the ends to taper for this type of surface, because as stated by Efimov in [4], the curvature must tend to zero as one travels to infinity down at least one end of the surface. This led us to use hyperbolic curves instead. The general equation for this curve, taken from [5], is a lot simpler as well:

$$x^p y^q = a$$

For $a > 0$, $p \in \mathbb{N}$, $q \in \mathbb{N}$, G.C.D $(p, q) = 1$.

Using the same method of modifying the discriminant of the equation, we created a six-ended surface with cusp ends that tapered. After modifying the discriminant of the original Vaigant surface, we have the equation:

$$(z - u + v)^2(8 + u + v)^2 - \epsilon^2(1 + u + v - ((u - 1)^3(v - 5)^4)) = 0$$

Where u and v have the same replacements as they do in Vaigant's surface. The main difference is the original term uv in the discriminant being modified to $(u-1)^3(v-5)^4$ to create more ends on the surface. Furthermore, the translation is needed so that the center of the surface is not imaginary.

This yielded a surface that looked like this:

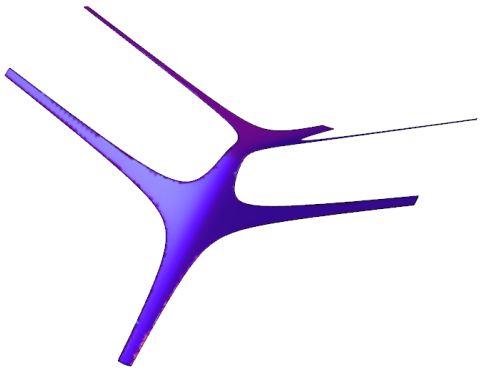

Its curvature was computed and graphed with a plane, and the surface showed some regions of positive curvature:

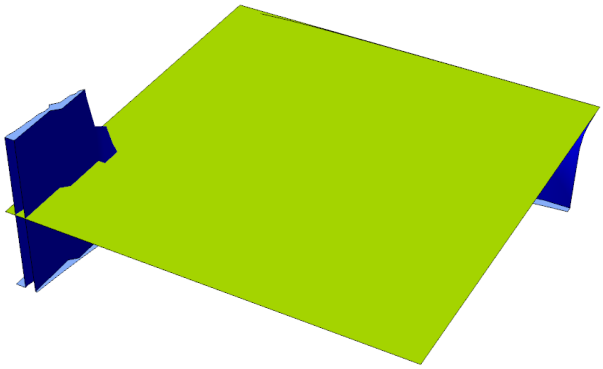

Now, we modify the surface in hope of changing the index of the ends in order to not violate the Poincaré-Hopf theorem under the assumption of negative curvature. While the Poincaré-Hopf theorem holds true no matter what the curvature is, if the sum of the indices for the ends does not account for the total index, then there must be points of zero curvature. Thus, at the very least, the ends must be modified. The main purpose of these modifications is to induce inflection points along the arms of the surface through scaling and bending.

We use the curve $f(x) = \frac{h}{\sqrt{1+x^2}} - \sqrt{1+x^2} - h$ for bending, for some $h > 0$. This is because its second derivative shows two inflection points. Incorporating

this curve into the equation of the surface will allow for more bending at certain points of the surface.

This is what this curve specifically looks for $f(x) = \frac{10}{\sqrt{1+x^2}} - \sqrt{1 + \frac{1}{10}x^2} - 10$.

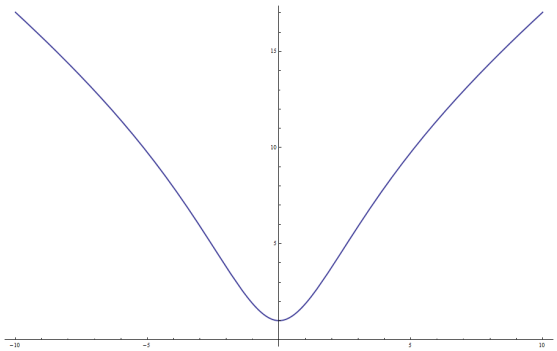

The next modification entails scaling the surface so that the inflection points are in the correct spot. This is important due to the tapering of the ends. Scaling can be done by holding v constant if we look at the equation in (u, v) coordinates. In (x, y) coordinates, this is done by multiplying the x term by $\sqrt{1+y^2}$ and dividing the entire expression by $\sqrt{1+y^2}$.

With that in mind, we have new replacements for the equation of the six-ended surface. We send $v \longrightarrow v$, and we send $u \longrightarrow u - \frac{h}{uv} + \frac{h}{\sqrt{v}}$. Note that u still equals $\sqrt{1+x^2}$ and v still equals $\sqrt{1+y^2}$. Thus, the new equation of the surface is the following:

$$\left(\frac{h}{uv} - \frac{h}{\sqrt{v}} - u + v + z\right)^2 \left(h\left(u\sqrt{v} - 1\right) + uv(8 + u + v)\right)^2 - \epsilon^2 u^2 v^2 \left(-\frac{(v-5)^4\left(h\left(u\sqrt{v}-1\right)+(u-1)uv\right)^3}{u^3 v^3} - \frac{h}{uv} + \frac{h}{\sqrt{v}} + u + v + 1\right) = 0.$$

It looks like this:

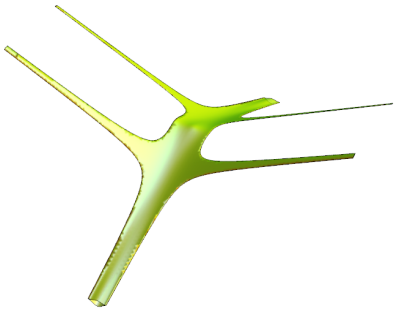

This, however, does not yield a surface with negative curvature, as seen by the following graph:

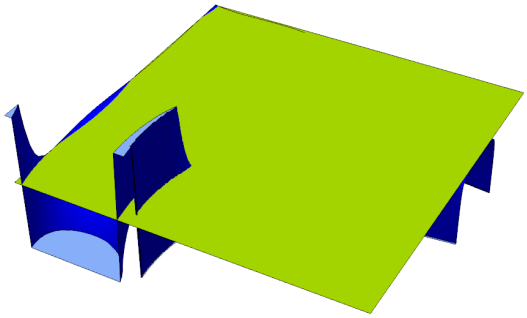

Here, the graph is the curvature function (in terms of sign) and the plane at 0.

What was realized, though, was that whether or not the ends have the correct index, the main issue with the six cuspidal ends is the center of the surface, the piece that bridge the ends together.

The following proposition, taken from [1], explains why this bridge is problematic:

Proposition 0.17. *Let $p \in S$ be an elliptic point of a surface S. Then there exists a neighborhood V of p in S such that all points in V belong to the same side of the tangent plane $T_p(S)$. Let $p \in S$ be a hyperbolic point. Then in each neighborhood of p there exist points of S in both sides of $T_p(S)$.*

If we take a tangent plane to this region of the surface, we can see a neighborhood of points to one side of the tangent plane. Thus, it cannot be negatively curved here.

IIc. Eight Ends.

In order to remove the positive curvature along the middle bend of the surface, we add two ends to the surface, to create a saddle-like shape in that region. The resulting surface has eight cuspidal ends.

Similar to the way we modified the original Vaigant surface, we strive to create a new profile curve to add more ends to the surface. This can be done by modifying the hyperbolic curves and creating more asymptotes. These asymptotes are created by adding more zeroes to the equation in the discriminant.

To give a better idea of this, we can look at the contour plot of the new piece:

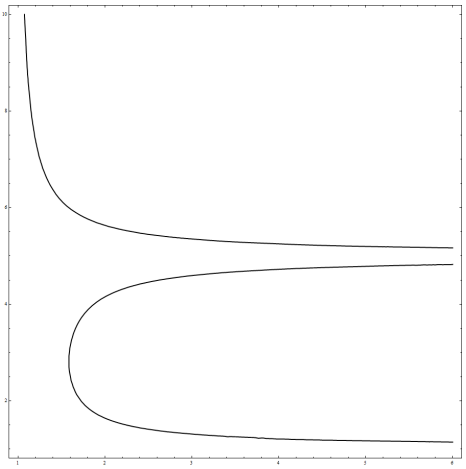

In order to get this shape, we change the original uv term in the discriminant to $(u-1)^2(v-1)^2(v-5)^2$. This looks like the following in (u,v) coordinates:

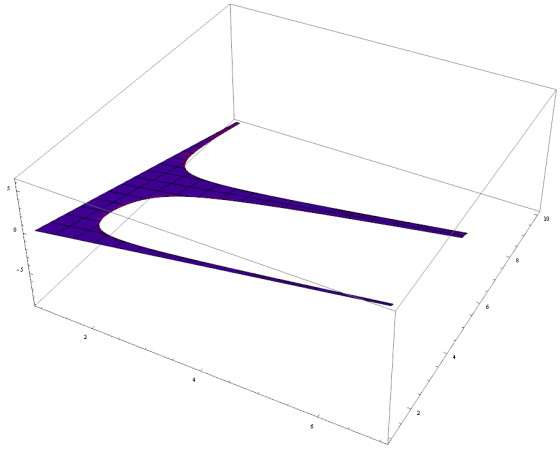

Our new equation is thus:

$(z-u+v)^2(8+u+v)^2 - \epsilon^2(1+u+v-((u-1)^2(v-1)^2(v-5)^2)) = 0$

The eight-ended surface looks like the following, for $\epsilon = \frac{1}{2}$:

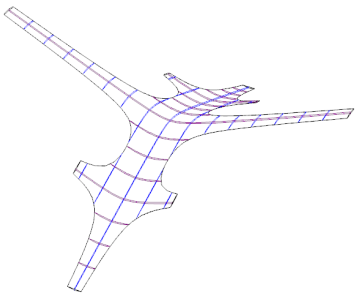

Note that the ends do go out to infinity here. Like the six-ended surface, however, we need to modify the ends so that the index is correct for each end. Without modifications, we have four cusp ends and four convex ends, leaving us with an index of 12. The sum of the indices for all the ends is $2a + 4b + 2c = 4$, because of the new symmetry of the surface. Here, a represents the ends that taper down, and b and c represent ends tapering up. We distinguish b from c because the center ends that taper up originally show a different planar slice curve. The four outside ends, which are represented by b, are the ends that are convex. Note that the Euler characteristic of the surface has not changed.

The following pictures show us the original slice curves:

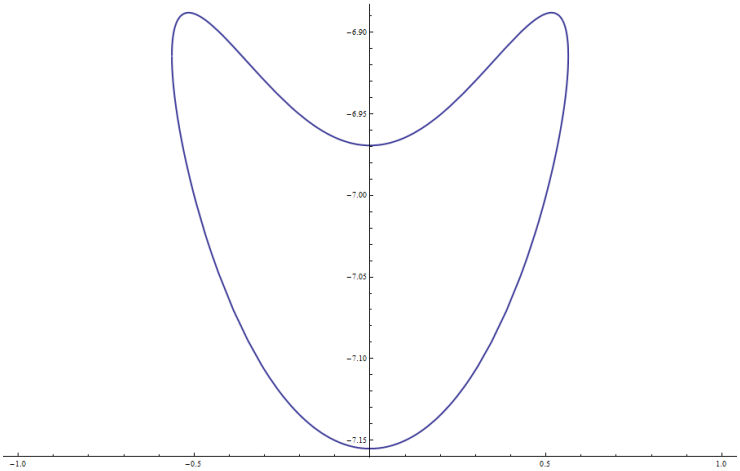

This is for the ends that go down, and the two center ends pointing up.

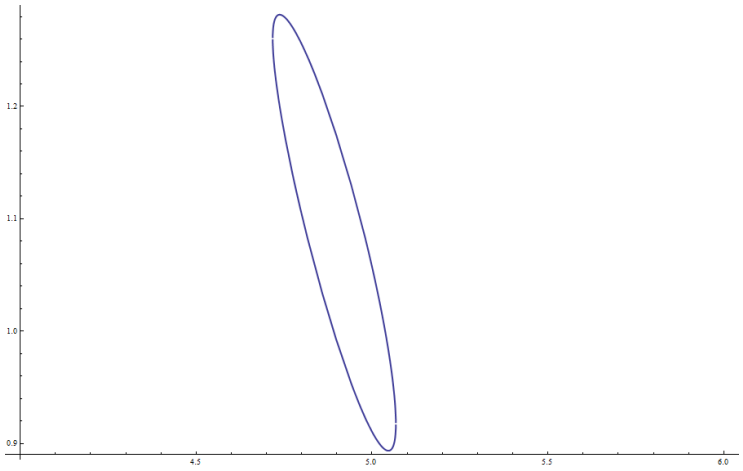

This is for the four outside ends pointing up.

It is important to note that we want our a ends to have an index of -1, and the b and c ends to each have an index of 1. This makes our index equation $2(-1) + 2(1) + 4(1) = 4$, which is two times the Euler characteristic, as desired. Our modification of the ends entails incorporating two different curves.

Bending the Surface Along the Spine.

We bend the surface along the spine to force the convex ends to become cuspidal.

We introduce two equations:

$$f(x) = h_2 + \sqrt{1+x^2} - \frac{h_2}{\sqrt{1+x^2}} \text{ and } f(y) = h_1 + \sqrt{1+y^2} - \frac{h_1}{\sqrt{1+y^2}},$$

For h_1 and h_2 not equal to zero.

These curves have two inflection points that are equal but opposite in sign. For the equation of $f(y)$ in particular, these inflection points are

$$\frac{\sqrt{1+h_1}}{\sqrt{-1+2h_1}}, \text{ and } -\frac{\sqrt{1+h_1}}{\sqrt{-1+2h_1}},$$

which are found by solving $f''(y) = 0$.

We find the value of h_1 by setting $f(y) = \sqrt{24}$, and letting y equal the inflection point. We choose $\sqrt{24}$ as our value because this is when v is equal to 5, and when v is equal to 5, the modified portion of the discriminant vanishes. Where this is on the surface, however, is the midpoint of the b ends, but in the place along the spine. This creates a bend that changes the index. On the other hand, h_2 does not have any constraints, because the surface is not subject to any limitations along the x direction.

This leads to new substitutions: $u \to h_2 + \sqrt{1+x^2} - \frac{h_2}{\sqrt{1+x^2}}$.

$v \to h_1 + \sqrt{1+y^2} - \frac{h_1}{\sqrt{1+y^2}}$

After solving for h_1, we get a value of approximately .540402.

Scaling the Bending of the Surface Along the Spine.

We also consider scaling the bending along the surface, by adding a constant in front of our substitution, such that $f(y)$ now equals:

$$f(y) = h_1 + \sqrt{1+y^2} - \frac{h_1}{\sqrt{1+sy^2}}$$

for some $s \in \mathbb{R}$, such that $s \neq 0$.

This modification controls how "sharp" the bending is. In general, this curve looks like the same curve that was used in modifying the surface with six ends. This time it is of interest, though, because this determines the shape of the bridge. For large s, the surface with eight ends will have a bridge that points more up.

Changing the a ends.

For our a ends to have an index of -1, we hope to induce a bending on the surface such that its planar slice curve has six inflection points, three for each asymptotic direction.

The curve for this modification is $f(x) = \sqrt{1+x^2} - \frac{13}{10}$. This function looks like this:

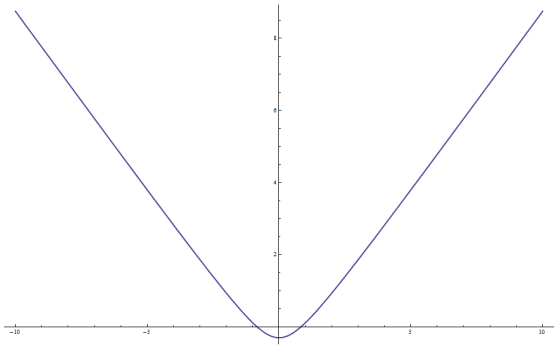

In our graph of the surface as a function of (x, y), we send $x \to \sqrt{1+x^2} - \frac{13}{10}$ to induce the bending. This creates six inflection points along the planar slice curve of the a ends, as desired. It can be seen as follows:

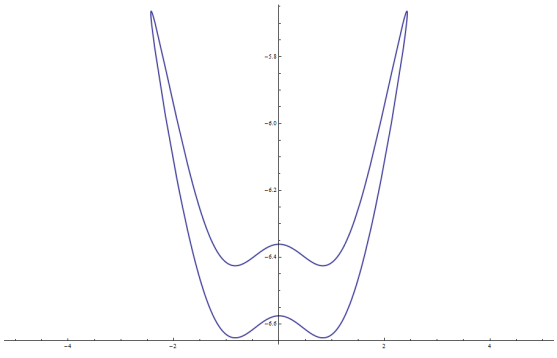

The problem that remains, however, is that in spite of the previous modifications, the b ends are convex, which means they have an index of 2. The c ends remain cuspidal. The slice curves of the other ends look like so:

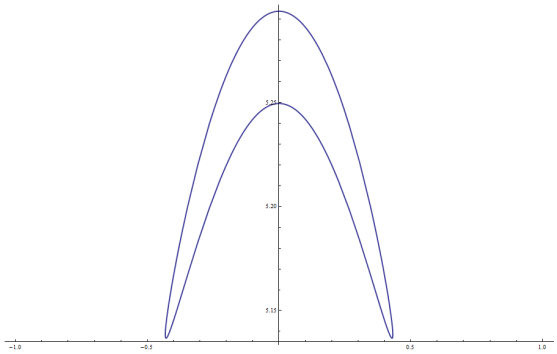

For the b ends, and

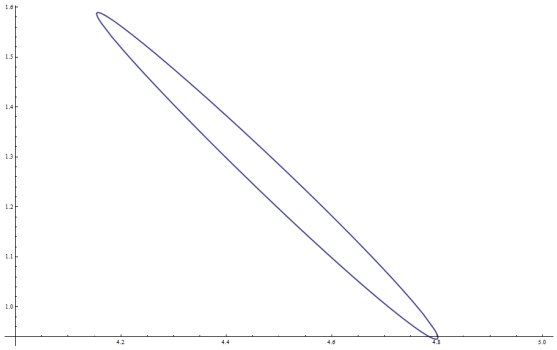

for the c ends.

Further work, in hopes of preserving negative curvature, would require more modification of the ends. This remains difficult because the surface becomes more insensitive to modifications as more ends are added.

III. Curvature of a Parametrized Tube.

We now begin an exploration of parametric surfaces. Suppose we have a parametrized tube, with parametric form

$$\vec{\phi}(t,z) = (x(t,z), y(t,z), z).$$

We show that in order for this tube to be negatively curved, then the following condition must be satisfied:

$$det\begin{pmatrix}\vec{V}_t\\ \vec{V}_{tt}\end{pmatrix} det\begin{pmatrix}\vec{V}_t\\ \vec{V}_{zz}\end{pmatrix} < \left(det\begin{pmatrix}\vec{V}_t\\ \vec{V}_{tz}\end{pmatrix}\right)^2$$

Where $\vec{V} = (x(t,z), y(t,z))$. We first compute the curvature of this tube in its general form and see what type of conditions must hold. We use the first

and second fundamental forms to find the curvature.

First fundamental form:

$$E = \langle \vec{V}_t, \vec{V}_t \rangle, F = \langle \vec{V}_t, \vec{V}_z \rangle, \text{ and } G = \langle \vec{V}_z, \vec{V}_z \rangle$$

And second fundamental form:

$$e = \langle N_t, \vec{V}_{tt} \rangle, f = \langle N_t, \vec{V}_{tz} \rangle, \text{ and } g = \langle N_t, \vec{V}_{zz} \rangle$$

And $K = \frac{eg-f^2}{EG-F^2}$.
After such computations, we have a general form for the curvature:

$$K = \frac{y_t^2(x_{zz}x_{tt}-x_{tz}^2)+x_t y_t(2x_{tz}y_{tz}-y_{zz}x_{tt}-x_{zz}y_{tt})+x_t^2(y_{zz}y_{tt}-y_{tz}^2)}{((1+y_z^2)x_t^2-2x_z y_z x_t y_t+(1+x_z^2)y_t^2)^2}$$

Since the denominator is always positive, we only consider the numerator in determining what conditions are necessary for negative curvature. After reducing the equation to when $y_t^2(x_{zz}x_{tt} - x_{tz}^2) + x_t y_t(2x_{tz}y_{tz} - y_{zz}x_{tt} - x_{zz}y_{tt}) + x_t^2(y_{zz}y_{tt} - y_{tz}^2) < 0$, we have some of the following cases:

(1)

$$x^{(0,2)}(t,z) > 0 \wedge y^{(2,0)}(t,z) > \frac{\frac{\left(x^{(1,1)}(t,z)y^{(1,0)}(t,z)-x^{(1,0)}(t,z)y^{(1,1)}(t,z)\right)^2}{x^{(1,0)}(t,z)y^{(0,2)}(t,z)-x^{(0,2)}(t,z)y^{(1,0)}(t,z)} + x^{(2,0)}(t,z)y^{(1,0)}(t,z)}{x^{(1,0)}(t,z)} \wedge x^{(1,0)}(t,z)$$
$$> 0 \wedge y^{(1,0)}(t,z) > \frac{x^{(1,0)}(t,z)y^{(0,2)}(t,z)}{x^{(0,2)}(t,z)}$$

(2)

$$x^{(0,2)}(t,z) > 0 \wedge y^{(2,0)}(t,z) > \frac{\frac{\left(x^{(1,1)}(t,z)y^{(1,0)}(t,z)-x^{(1,0)}(t,z)y^{(1,1)}(t,z)\right)^2}{x^{(1,0)}(t,z)y^{(0,2)}(t,z)-x^{(0,2)}(t,z)y^{(1,0)}(t,z)} + x^{(2,0)}(t,z)y^{(1,0)}(t,z)}{x^{(1,0)}(t,z)} \wedge x^{(1,0)}(t,z) <$$
$$0 \wedge y^{(1,0)}(t,z) < \frac{x^{(1,0)}(t,z)y^{(0,2)}(t,z)}{x^{(0,2)}(t,z)}$$

(3)

$$x^{(0,2)}(t,z) > 0 \wedge y^{(1,0)}(t,z) > \frac{x^{(1,0)}(t,z)y^{(0,2)}(t,z)}{x^{(0,2)}(t,z)} \wedge x^{(1,0)}(t,z) <$$
$$0 \wedge y^{(2,0)}(t,z) < \frac{\frac{\left(x^{(1,1)}(t,z)y^{(1,0)}(t,z)-x^{(1,0)}(t,z)y^{(1,1)}(t,z)\right)^2}{x^{(1,0)}(t,z)y^{(0,2)}(t,z)-x^{(0,2)}(t,z)y^{(1,0)}(t,z)} + x^{(2,0)}(t,z)y^{(1,0)}(t,z)}{x^{(1,0)}(t,z)}$$

(4)

$$x^{(0,2)}(t,z) > 0 \wedge x^{(1,0)}(t,z) > 0 \wedge y^{(1,0)}(t,z) < \frac{x^{(1,0)}(t,z)y^{(0,2)}(t,z)}{x^{(0,2)}(t,z)} \wedge y^{(2,0)}(t,z) <$$
$$\frac{\frac{\left(x^{(1,1)}(t,z)y^{(1,0)}(t,z)-x^{(1,0)}(t,z)y^{(1,1)}(t,z)\right)^2}{x^{(1,0)}(t,z)y^{(0,2)}(t,z)-x^{(0,2)}(t,z)y^{(1,0)}(t,z)} + x^{(2,0)}(t,z)y^{(1,0)}(t,z)}{x^{(1,0)}(t,z)}$$

(5)

$$x^{(0,2)}(t,z) < 0 \wedge y^{(2,0)}(t,z) > \frac{\frac{\left(x^{(1,1)}(t,z)y^{(1,0)}(t,z) - x^{(1,0)}(t,z)y^{(1,1)}(t,z)\right)^2}{x^{(1,0)}(t,z)y^{(0,2)}(t,z) - x^{(0,2)}(t,z)y^{(1,0)}(t,z)} + x^{(2,0)}(t,z)y^{(1,0)}(t,z)}{x^{(1,0)}(t,z)} \wedge y^{(1,0)}(t,z) > \frac{x^{(1,0)}(t,z)y^{(0,2)}(t,z)}{x^{(0,2)}(t,z)} \wedge x^{(1,0)}(t,z) < 0$$

(6)

$$x^{(0,2)}(t,z) < 0 \wedge y^{(2,0)}(t,z) > \frac{\frac{\left(x^{(1,1)}(t,z)y^{(1,0)}(t,z) - x^{(1,0)}(t,z)y^{(1,1)}(t,z)\right)^2}{x^{(1,0)}(t,z)y^{(0,2)}(t,z) - x^{(0,2)}(t,z)y^{(1,0)}(t,z)} + x^{(2,0)}(t,z)y^{(1,0)}(t,z)}{x^{(1,0)}(t,z)} \wedge x^{(1,0)}(t,z) > 0 \wedge y^{(1,0)}(t,z) < \frac{x^{(1,0)}(t,z)y^{(0,2)}(t,z)}{x^{(0,2)}(t,z)}$$

(7)

$$x^{(0,2)}(t,z) < 0 \wedge x^{(1,0)}(t,z) > 0 \wedge y^{(1,0)}(t,z) > \frac{x^{(1,0)}(t,z)y^{(0,2)}(t,z)}{x^{(0,2)}(t,z)} \wedge y^{(2,0)}(t,z) < \frac{\frac{\left(x^{(1,1)}(t,z)y^{(1,0)}(t,z) - x^{(1,0)}(t,z)y^{(1,1)}(t,z)\right)^2}{x^{(1,0)}(t,z)y^{(0,2)}(t,z) - x^{(0,2)}(t,z)y^{(1,0)}(t,z)} + x^{(2,0)}(t,z)y^{(1,0)}(t,z)}{x^{(1,0)}(t,z)}$$

(8)

$$x^{(0,2)}(t,z) < 0 \wedge x^{(1,0)}(t,z) < 0 \wedge y^{(1,0)}(t,z) < \frac{x^{(1,0)}(t,z)y^{(0,2)}(t,z)}{x^{(0,2)}(t,z)} \wedge y^{(2,0)}(t,z) < \frac{\frac{\left(x^{(1,1)}(t,z)y^{(1,0)}(t,z) - x^{(1,0)}(t,z)y^{(1,1)}(t,z)\right)^2}{x^{(1,0)}(t,z)y^{(0,2)}(t,z) - x^{(0,2)}(t,z)y^{(1,0)}(t,z)} + x^{(2,0)}(t,z)y^{(1,0)}(t,z)}{x^{(1,0)}(t,z)}$$

Note that there are other more general cases, such as when $x_t = 0$ or when $x_t \neq 0$.

Within these inequalities, we see determinant forms of the derivative of the vector form of the planar curve. This leads us to generalize with our original inequality statement containing the determinants. For instance, we can easily see that

$$\left(x^{(1,1)}(t,z)y^{(1,0)}(t,z) - x^{(1,0)}(t,z)y^{(1,1)}(t,z)\right)^2$$

is the determinant form of V_t and V_{tz}. We can summarize the above 8 cases into one condition because the inequality changes are consistent with changing x_{zz} to either positive or negative.

Now let us consider the following inequality:

$$det\begin{pmatrix}\vec{V}_t\\ \vec{V}_{tt}\end{pmatrix} det\begin{pmatrix}\vec{V}_t\\ \vec{V}_{zz}\end{pmatrix} - \left(det\begin{pmatrix}\vec{V}_t\\ \vec{V}_{tz}\end{pmatrix}\right)^2 < 0$$

Then the following holds for a curve parametrized by arclength:

$$-k\left\langle \vec{V}_{zz}, \hat{n} \right\rangle < \left\langle \vec{V}_{tz}, \hat{n} \right\rangle^2 = ||\vec{V}_{tz}||^2 \qquad (**)$$

Here, k is the signed curvature of the plane curve, $\hat{n}$ is the outward unit normal in the plane of the curve such that it is positively oriented. This equality follows from the fact that $\vec{V}_{tt} = k\hat{n}$, $\vec{V}_{tt}$ being orthogonal to $\vec{V}_t$, as well as $det\begin{pmatrix} \vec{V}_t \\ \hat{n} \end{pmatrix}$ equaling 1.

Note that $\vec{V}_{tz} = \pm||\vec{V}_{tz}||\hat{n}$. In terms of the curvature of the curve $\phi(t,z) = (x(t,z), y(t,z))$, we have the following cases:

Case 1. When $k = 0$, there is an inflection point on the curve. We need $\vec{V}_{tz} \neq \vec{0}$.

Case 2. For $k > 0$, the curve is convex, and what results is that $\left\langle \vec{V}_{zz}, \hat{n} \right\rangle > 0$. This essentially means that we need the radius deformation to be a convex function in the normal direction.

Case 3. For $k < 0$, the curvature is already negative.

Overall, these inequalities help us conclude what conditions are sufficient for a parametric tubular surface to have negative curvature. This can lead to new methods of gluing different ends to one another.

IV. Conclusion and Further Work

Although we were unable to construct negatively curved surfaces with more than four cuspidal ends, it is worthwhile to note that further work can be done on the surface with eight cuspidal ends, as well as the surface with genus. The latter surface would require careful consideration of changing the ends, while modifying the eight-ended one would require incorporating different types of curves into the original equation to change index. It would also be worthwhile to look at parametric tubular surfaces for specific forms of $x(t,z)$ and $y(t,z)$, such as when $x(t,z) = r_1(z)x(t)$ and $y(t,z) = r_2(z)x(t)$ for specific radius functions $r_1(z)$ and $r_2(z)$. The formula (**) provides a convenient necessary and sufficient set of conditions for tubing. This is an important step in a number of constructions of new negatively curved surfaces.

IV. Acknowledgments

I would really like to thank my advisor, Chris Connell, for being very helpful and encouraging throughout this project. I also extend my thanks to Indiana University and the faculty and staff of its mathematics department.

References

[1] M. do Carmo. Differential Geometry of Curves and Surfaces, Prentice Hall, Englewood Cliffs, NJ (1976).

[2] C. Connell and J. Thurman. The Construction of a Complete, Bounded, Negatively Curved Surface in $\mathbb{R}^3$, REU Report 2009.

[3] C. Connell and J. Ullman, *Ends of negatively curved surfaces in Euclidean space*, Manuscripta Math. **131** (2010), no. 3-4, 275–303.

[4] N. V. Efimov, *Surfaces with slowly varying negative curvature*, Uspehi Mat. Nauk **21** (1966), no. 5 (131), 3–58.

[5] E. Shikin. Handbook and Atlas of Curves, CRC Press, Boca Raton, FL (1995).

Negatively Curved Slab Surfaces

Clark Butler

Abstract

We study negatively curved slab surfaces, which are complete regular surfaces of negative curvature that are embedded between two parallel planes in Euclidean space. There are very few known examples of such surfaces, and all known examples are homeomorphic either to a plane or an annulus. We construct new examples of negatively curved slab surfaces of these known topological types, completely classify ruled negatively curved slab surfaces, and investigate the general properties of generic these surfaces with the goal of a classification of the possible topologies of these surfaces. Our primary tools are planar cross sections of the surface, Morse functions, and the behavior of the asymptotic line field of the surface at infinity.

1 Curvature of Regular Surfaces in $\mathbb{R}^3$

We begin with some background material (see Do Carmo [doCar76] for additional details.)

Definition 1.1. A regular surface S is a set $S \subset \mathbb{R}^3$ such that for each point $p \in S$, there are open sets $U \subset \mathbb{R}^2$, $V \subset \mathbb{R}^3$, with $p \in V$, and a differentiable map $\phi\colon U \to V$, such that

1. $\phi\colon U \to V \cap S$ is a homeomorphism.
2. $d\phi_q$ has rank 2, for $q = \phi^{-1}(p)$.

The function ϕ is called a *local parametrization* at p.

Write ϕ as $\phi(u, v)$. The vectors $\phi_u(q)$, $\phi_v(q)$ span a two-dimensional linear subspace of $\mathbb{R}^3$, called the *tangent space* to S at p, which is denoted $T_p(S)$. $T_p(S)$ is independent of the local parametrization used at p.

The Gauss map $N\colon \phi(U) \to S^2$ is defined by

$$N(p) = \frac{\phi_u \wedge \phi_v}{\|\phi_u \wedge \phi_v\|}(q)$$

The Gauss map gives the normal to $T_p(S)$. It is well-defined in a neighborhood of p up to a change in orientation. Since the Gauss map is a differentiable map between two surfaces, we may take its differential dN. The *Gaussian curvature* of S at p is, by definition,

$$K(p) = \det(dN_p)$$

K is defined independently of the orientation.

We can give an equivalent formulation of the Gaussian curvature in terms of second-order approximations to S. In a sufficiently small neighborhood of p, S is the graph of a function f over its tangent space $T_p(S)$. We may identify $T_p(S)$ with $\mathbb{R}^2$, and let the origin correspond to p. Write f as $f(x, y)$. By translation we may assume that $f(0, 0) = 0$. Since the normal at p is parallel to the plane of the graph, we have that $f_x(0, 0) = f_y(0, 0) = 0$. The second-order Taylor series approximation to f at $(0, 0)$ is thus,

$$f_{xx}(0,0)x^2 + f_{yy}(0,0)y^2 + 2f_{xy}(0,0)xy$$

The Gaussian curvature at p is the determinant of this quadratic form,

$$K(p) = (f_{xx}f_{yy} - f_{xy}^2)(0,0)$$

We are interested in negatively curved surfaces, i.e. those which satisfy $K < 0$ everywhere. We will also assume that S is *complete*, that is S is complete as a metric space in its intrinsic metric that is derived from the Euclidean metric on $\mathbb{R}^3$

2 Slab Surfaces

A slab surface is a complete regular surface S which lies between two parallel planes. We will suppose these two planes to always be parallel to the xy-plane. We are interested in the possible topological type of S when we assume that S is negatively curved. In particular, we are concerned with surfaces of finite topological type.

Definition 2.1. A complete regular surface M is of finite topological type if $M \cong \Sigma_g - \{p_1, \ldots, p_n\}$, where Σ_g is the compact orientable surface of genus g, a sphere with g handles attached.

The points $p_1, \ldots, p_n$ are the ends of S.We can then define the Euler characteristic χ for any surface of finite topological type,

Definition 2.2.

$$\chi(M) = 2 - 2g - n$$

Note that if a surface is negatively curved, then it must have at least one end, as otherwise the surface is compact, and thus contains a point of positive curvature. All known examples of negatively curved slab surfaces are homeomorphic to a plane or an annulus, i.e. they have either one or two ends and no genus. If we do not restrict ourselves to a slab, then a result due to Connell and Ullman[CU10] states that all finite topological types with at least one end are possible for negatively curved surfaces. Their constructions are done by joining together hyperboloids. We will show that an analagous construction inside of a slab is impossible due to the presence of inflection points on planar slices of the surface.

It should be noted as well that examples are known of slab surfaces of nonpositive curvature ($K \leq 0$) with any genus and with one end. These are due to Chan and Treibergs[CT01].

As just one example of the difference between negative and nonpositive curvature, however, we have the following proposition.

Proposition 2.3. *A negatively curved slab surface S cannot contact its bounding planes.*

Proof. At any such point of contact, S lies to one side of a plane it touches, and so must have nonnegative curvature at that point. □

3 Topological Restrictions

Let S be a complete, negatively curved surface of finite topological type, so that $S \cong \Sigma_g - \{p_1, \ldots, p_n\}$.We will formulate two restrictions on the topology of S. The first is based on the fields of asymptotic lines on S. At each point p in S, the differential of the Gauss map gives a self-adjoint linear map,

$$dN_p \colon T_p(S) \to T_{N(p)}(S^2)$$

Since $T_p(S) = T_{N(p)}(S^2)$, we may regard this as a linear map from $T_p(S)$ to itself. For $v \in T_p(S)$, we may then define a quadratic form,

$$II_p(v) = \langle v, dN_p(v) \rangle$$

This is the *second fundamental form* of S at p. Since $\det(dN_p) < 0$, there will be two linear subspaces in $T_p(S)$ on which $II_p(v) = 0$. We may choose one of these two subspaces at each point p in such a way that the assignment is continuous. The resulting association of a linear subspace of $T_p(S)$ to each point $p \in S$ is an asymptotic line field on S.

We note other properties of II_p that will be used later. There are two other distinguished subspaces of $T_p(S)$, given by the eigenvectors of the second fundamental form. These subspaces will be orthogonal, and are called the *principal curvature directions* at p. The principal curvature directions correspond to the maximal and minimal values of II_p on the unit circle in $T_p(S)$. These values are the eigenvalues κ_1 and κ_2 of dN_p. Note that,

$$K = \det(dN_p) = \kappa_1 \kappa_2$$

If $K < 0$, the eigenvalues thus have opposite signs.

Secondly, an equivalent definition of II_p is given as follows: Take any parametrized curve $\alpha \colon (-\epsilon, \epsilon) \to S$ with $\alpha(0) = p$, $\alpha'(0) = v$. Then, II_p is the *normal curvature* of the curve α at p,

$$II_p(v) = \langle N(p), \alpha''(0) \rangle$$

Observe that this only depends on the point p and v, by equivalence with the previous definition of II_p. We will be particularly interested in the case where α is the curve resulting from slicing S by a plane.

Returning to the asymptotic line fields, in a neighborhood of each of its ends, S is homeomorphic to a punctured disk. Consider a positively oriented closed curve $\gamma\colon [0,l] \to S$ in this punctured disk which wraps once about the puncture. Let $\theta(s)$ be the positively oriented angle that the linear subspace at $\gamma(s)$ makes with that at $\gamma(0)$.

$$\int_0^l \frac{d\theta}{ds} ds = \pi I$$

for some integer I, since the linear subspace at $\gamma(0)$ is the same as that at $\gamma(l)$. I is the index of the asymptotic line field around the end.

Let I_j be the index of the end p_j, $j = 1, \ldots, n$. By the Poincare-Hopf theorem for line fields, we have

$$2\chi(\Sigma_g) = \sum_{j=1}^{n} I_j$$

Thus the index of the ends of S determines the topology of S.

The second restriction is due to Verner[Ver67]. We suppose that there exists $v \in S^2$ such that there is no sequence of points $u_m \in S$ with u_m tending to an end of S and $N(u_m) \to \pm v$. Colloquially, the normal to S is bounded away from the axis of v at infinity. Let P be the plane through the origin with normal v. Let $P(h) = P + hv$ for $h \in (-\infty, \infty)$. Verner proved,

Theorem 3.1. *$P(h) \cap S$ has a finite number of connected components.*

The curves of $P(h) \cap S$ may be pulled back to $\Sigma_g - \{p_1, \ldots, p_n\}$ by the homeomorphism. These curves may be closed in S, but those curves that are not closed must converge to the ends p_j. Then each end p_j will have a finite number of topological rays coming into it, each of which will be called an *exit to infinity*.

The number of exits to infinity is also finite and is even. Furthermore, the number of exits to infinity is the same for every value of h. Let m be half the number of exits to infinity, and let q be the number of points on S at which the normal to S is parallel to v. Then

Theorem 3.2. (Verner)

$$m - q = \chi(S)$$

We hope to, under reasonable assumptions on the slab surface S, prove the existence of such an axis v, in order to apply this formula to investigate the topology of S.

4 Plane Slices of Negatively Curved Surfaces

In this section we introduce new tools for analyzing planar cross sections of negatively curved surfaces.

Let S be a negatively curved surface embedded in $\mathbb{R}^3$. Let P be a plane through the origin with unit normal N_P. Let $P_h = P + hN_P$ be the parallel translation of P by a distance h. P_h slices S in a collection of curves with isolated, nondegenerate critical points. Observe that, by continuity, sufficiently small changes in h will preserve the sign of the curvature of the slice curves in a neighborhood of any point on a slice curve where the curvature is nonzero. Hence points of inflection where the sign of the curvature changes are preserved under small changes in h. More generally, if the slice curve inflects across a line segment, the endpoints of this line are stable, and we will also refer to these as points of inflection. By this stability, then, an inflection point $q \in P_{h_0}$ extends to a family of inflection points $q_h \in P_h$, $h \in (h_0 - \epsilon, h_0 + \epsilon)$ which form a curve in $\mathbb{R}^3$. Let $\theta(h)$ be the integral of the directed angle that the tangent line at q_h makes with the tangent line at q_{h_0}.

Lemma 4.1. *$\theta(h)$ is strictly monotone.*

Proof. Near q_{h_0}, S is a graph over the plane which contains N_P and the tangent line to the slice curve at q_{h_0}. We can thus parametrize S locally as

$$(t, h, f(t, h))$$

for some function f. Setting $h = \text{const.}$ gives a parametrization for the slice curve near q_h as a graph over the tangent line at q_{h_0}. Let q_h correspond to its t value in the parametrization. Then $f_{tt}(q_h, h) = 0$. The condition that S is negatively curved implies that $f_{tt}f_{hh} - f_{th}^2 < 0$ everywhere. This gives $f_{th}^2(q_h, h) \neq 0$. It follows that either $f_{th}(q_h, h) > 0$ or $< 0 \; \forall \; h$. The slope of the tangent line at q_h relative to that at q_{h_0} thus only strictly increases or strictly decreases with increasing h. □

Thus as h increases, each inflection point on the slice curves will rotate monotonically either clockwise or counterclockwise according to an orientation of the plane P. Since the slice curve has zero curvature at an inflection point, the second fundamental form of S at that point will evaluate to 0 on the tangent direction of the slice curve. Thus an asymptotic line field is tangent to the slice curve at each inflection point. However, we do not know a priori which of the two asymptotic line fields is tangent to each inflection point. Let us suppose we have two neighboring inflection points p and q (not connected by a straight line segment) on a slice curve with no critical points between them. Extend these inflection points to curves p_h, q_h. Then,

Lemma 4.2. *The slope of the slice curve at p_h and q_h rotates in the same direction as h increases $\Leftrightarrow$ the slice curve is tangent to the same asymptotic line field at both p and q.*

Proof. In the proof of Lemma 4.1, note that f_{th} will also be exclusively positive or negative near the inflection point, by continuity. Thus, locally, the rotation of the slice curve about the inflection point as h varies will be in the same direction as the rotation of the tangent to the inflection point. Further, if we maintain our orientation along the slice plane and mark the relative orientation of the slice curve when writing the surface locally as a graph, one rotational direction will always correspond to $f_{th} > 0$, the other to $f_{th} < 0$. It thus suffices to observe what happens when the slopes change from rotating in one direction to rotating in the other, that is, we must investigate points where $f_{th} = 0$.

Note that if $f_{th}(t, h) = 0$, then the coordinate axes are the principal curvature directions, and so a principal curvature direction is tangent to the slice curve at the point $(t, h, f(t, h))$. Further, noting that we are in the case of a graph, observe that the eigenvectors of the second fundamental form in the basis $\{(1, 0, f_t), (0, 1, f_h)\}$ of the tangent space are given by,

$$(f_{tt} - f_{hh} - \sqrt{(f_{tt} - f_{hh})^2 + 4f_{th}^2}, 2f_{th})$$
$$(2f_{th}, -f_{tt} + f_{hh} + \sqrt{(f_{tt} - f_{hh})^2 + 4f_{th}^2})$$

Thus when f_{th} changes sign, each eigenvector crosses a distinct coordinate axis. The lemma then follows from the fact that between the two asymptotic directions there is always a single principal curvature direction corresponding to one of these eigenvectors. Thus if p and q have tangencies belonging to distinct asymptotic line fields, this principal curvature direction must cross the $(1, 0, f_t)$ coordinate axis an odd number of times as the curve is traversed from p to q, and so p_h and q_h must have slopes rotating in opposite directions as h increases. □

This lemma allows us to distinguish which inflection points belong to which asymptotic line field on a curve. This lemma is particularly useful when we know that two inflection points are rotating in opposing directions, as then we know that there is a tangency to the slice curve of a principal curvature direction in between the two points.

Now consider a point r on a slice curve in P_{h_0} with tangent line T. By similar stability arguments as before, if r is not a point of zero curvature on the slice curve, then r extends to a family of points $r_h \in P_h$, $h \in (h_0 - \epsilon, h_0 + \epsilon)$ where each r_h has the same tangent line T. Along this curve r_h, S can be written as the graph of a function $f(t, h)$ over the plane containing T and N_P. The curve r_h projects down onto a graph over the axis of N_P in this plane; let g be the corresponding function. Let us reparametrize the curve $(g(h), h)$ by arclength; let $\gamma(s) = (x(s), y(s))$ be the arclength parametrization. Set $w(s) = f(x(s), y(s))$.

Lemma 4.3. *$w''(s)$ has the same sign whenever $w''(s) \neq 0$, and this sign is the opposite of the sign of $f_{tt}(\gamma(s))$.*

Proof. Fix s. First suppose $\gamma'(s)$ and T are not parallel. We then have two independent directions in the plane of the graph, one given by T, the other

given by $\gamma'(s)$. The partial derivative of f_t in the direction of $\gamma'(s)$ at $\gamma(s)$ is 0 since the tangent direction is fixed in that direction. Changing coordinates, we then have by the negative curvature of S that $f_{tt}(\gamma(s))w''(s) < 0$.

Now suppose $\gamma'(s)$ and T are parallel. The partial of f_t in the direction of $\gamma'(s)$ is still 0, so we have that $f_{tt}(\gamma(s)) = 0$. If this point is not a point of inflection, we may continue the fixed tangent curve past this slice, and f_{tt} will keep the same sign, so $w''(s)$ must also keep the same sign. If this is a point of inflection, then by Lemma 4.1, the slope of the tangent line at slice inflection points must be strictly monotone with increasing h. Since the fixed tangent direction traveled into the inflection point, the monotonicity of the slopes implies that the tangent direction must locally disappear when h increases so that the fixed tangent direction curve cannot be extended past this point. □

Thus $w''(s)$ never changes sign. $w''(s)$ can only be 0 when $\gamma'(s)$ and T are parallel, which happens only at a measure zero set of points. Hence we have the following corollary,

Corollary 4.4. *Suppose that the curve $\gamma(s)$ can be extended to $s \in (-\infty, \infty)$. Then $w(s)$ is unbounded.*

We hope to apply this corollary to show that certain arrangements of inflection points on the slice curves of a slab surface must lead to critical points. We will consider slicing the surface by planes transverse to the slab plane. Then the slice curves are always bounded between two parallel lines corresponding to the intersection of the slice plane with the bounding planes.

In particular, if we follow a fixed tangent direction as in Lemma 4.3, and suppose that this fixed tangent direction is not perpendicular to the bounding parallel lines, we can consider the surface along this fixed tangent direction curve to be locally a graph over the plane of the slab. Then, by the corollary, this curve cannot be extended to be defined for all values of an arclength parameter, since the function $w(s)$ must be bounded in this case. Thus the fixed tangent direction must eventually disappear. If it never encounters a point of inflection, then it must eventually vanish at a critical point.

5 New Examples

5.1 Pulled Annulus

The surface,

$$y^2 + x^2 = \frac{1}{1 - z^2}\ ,\ -1 < z < 1$$

is a known example of a negatively curved slab surface that is topologically an annulus. It is a surface of revolution; we note that similar examples may be obtained by rotating any plane curve which is bounded between two parallel lines, does not intersect the z-axis, has nonzero curvature, and tends to its

bounding lines as it tends to infinity, about the z-axis. These are the only possibilities.

We may pull the circles of this annulus out to infinity to construct a new negatively curved example,

$$x = y^2 - \frac{1}{1-z^2} \ , \ -1 < z < 1$$

This surface belongs to a more general class of slab surfaces. Let $\alpha(y)$ satisfy $\alpha''(y) > 0$, and $\beta(z)$ satisfy $\beta''(z) < 0$, $\beta(z) \to -\infty$ as $z \to \pm 1$. Set,

$$x = \alpha(y) + \beta(z) \ , \ -1 < z < 1$$

The Hessian of this graph over the yz-plane is $\alpha''(y)\beta''(z) < 0$, so this surface is negatively curved. As the z-slices move up through the surface, the convex plane curve α comes in from infinity, stops, and exits back to infinity in the direction from which it came.

One might hope to carry out a construction in analogy to Connell and Ullman, using the slab annulus and pulled annulus in place of the hyperboloid and ripped hyperboloid. However, such a construction is impossible, even if we do not glue along a plane. If we consider slices by parallel translations of the yz-plane, as the plane moves past the core of the annulus (or pulled annulus) the inflection points on the slice have slopes flattening to horizontal. However, if we glue another annulus onto this, the slopes of the inflection points must stop flattening out and rotate back in the opposite direction, contradicting Lemma 4.1.

5.2 Parabolic Helicoid

We first construct a negatively curved variation of the helicoid, using a rotating parabola instead of a line. We let z be the height parameter, and we let t parametrize the parabola. The equation is then,

$$\psi(t,z) = \left\{ t\cos(z) - t^2\sin(z), t^2\cos(z) + t\sin(z), z \right\}$$

In order to check the sign of the curvature, it suffices to check that the expression,

$$\tilde{K} = \langle \psi_{tt}, \psi_t \wedge \psi_z \rangle \langle \psi_{zz}, \psi_t \wedge \psi_z \rangle - \langle \psi_{tz}, \psi_t \wedge \psi_z \rangle^2$$

is always negative. A computation gives,

$$\tilde{K} = -16t^4 - 6t^2 - 1$$

which is easily checked to be negative for all t.

We now attempt to fit this parabolic helicoid into a slab. We replace z by $\arctan z$ so that the surface only reaches a finite height in each direction, and translate the basepoint of the parabola by $(z, 0)$ so it does not contact the bounding planes of the slab as $z \to \pm\infty$. The result is the parametrization,

$$\bar{\psi}(t,z) = \left\{ -\frac{t^2 z}{\sqrt{z^2+1}} + \frac{t}{\sqrt{z^2+1}} + z, \frac{t^2}{\sqrt{z^2+1}} + \frac{tz}{\sqrt{z^2+1}}, \arctan(z) \right\}$$

where the trigonometric functions have become algebraic. $\tilde{K}$ is then,

$$-\frac{16t^4 + 6t^2 + 8tz\sqrt{z^2+1} + 4z^2\sqrt{z^2+1} + 1}{(z^2+1)^4}$$

The sign of the curvature is determined by the sign of the numerator. As $(t,z) \to \pm\infty$, the t^4 term dominates, so the numerator is negative outside some compact ball about the origin. Another computation yields that the gradient of the numerator vanishes only at $t = 0, z = 0$, where the numerator has value -1. It follows that the numerator is always negative, and so the surface is negatively curved.

It is possible to add more turns to the surface inside a slab by replacing the argument of sin and cos by $n \arctan z$ instead of $\arctan z$, for $n \in \mathbb{N}$. The equation to determine the sign of the curvature will again be algebraic, but of increasingly higher degree as n increases, making verification of the negative curvature more difficult.

5.3 Classification of Ruled, Negatively Curved Slab Surfaces

The known examples of ruled slab surfaces are of the following form [CG08]:

$$y = xz + \frac{z^n}{1-z^2}\ ,\ -1 < z < 1$$

We generalize these examples and completely classify negatively curved ruled slab surfaces.

Theorem 5.1. *If S is a connected, ruled, negatively curved surface that lies minimally between the planes $z = -1$ and $z = 1$, then S admits a parametrization of the form*

$$F(v,z) = (v\cos a(z) + b(z), v\sin a(z) + c(z), z)\ ,\ -1 < z < 1$$

where $a'(z) \neq 0$.

Furthermore, S is intrinsically complete iff the lines $l_z(v) = v(\cos a(z), \sin a(z)) + (b(z), c(z))$ are such that as $z \to \pm 1$, there is no sequence of compact sets $K_m \subseteq \mathbb{R}^2$ with $\bigcap K_m$ a single point, such that a portion of the line l_z always lies in K_m for $z \in (\epsilon_m, 1)$ (or $z \in (-1, -\epsilon_m)$, for $z \to -1$) for $\epsilon_m \to 1$.

Conversely, if S is defined by such a parametrization, then S is intrinsically complete and negatively curved.

Proof. Suppose S is a connected, intrinsically complete, negatively curved, ruled surface that lies between the planes $z = -1$ and $z = 1$, with these bounding planes being minimal. Since S is ruled, there must be a line passing through each point of S. This line must lie in a parallel translation of the xy-plane, as otherwise it will escape the slab. A slice of S parallel to the xy-plane thus consists of a collection of lines. But there can only be one line, since if there were two, the two lines would have to meet as the slice moved upward with z, by the connectedness of S. The intersection of two nonparallel lines is stable under small perturbation, however, so the point at which the two lines meet must be a degenerate critical point, i.e. a point of zero curvature. Thus if the two lines meet, they must meet when they are parallel, but then the normal to S along the line along which they meet must be in the z-direction, so that S has zero curvature along this line.

The slice of S by a plane $z = \text{const.}$ is thus a single line. This line can be parametrized by

$$l_z(v) = v(\cos a(z), \sin a(z)) + (b(z), c(z))$$

where a, b, c are differentiable functions in z. This extends immediately to a full parametrization of the surface,

$$F(v, z) = (v \cos a(z) + b(z), v \sin a(z) + c(z), z) \ , \ -1 < z < 1$$

A straightfoward computation verifies that S is negatively curved iff $a' \neq 0$.

It is clear that if such a sequence of compact sets K_m exists, then S cannot be intrinsically complete: any sequence in S with z-coordinate converging to ± 1 and that remains within the sets K_m is Cauchy in the metric of S, but cannot converge in S since S cannot contact its bounding planes.

Conversely, if no such sequence K_m exists, then S is intrinsically complete: Let s_n be a Cauchy sequence in S. Then s_n is Cauchy in $\mathbb{R}^3$ as well, and thus converges to a point $s \in \mathbb{R}^3$. If the z-coordinate of s is in $(-1, 1)$, then the sequence s_n lies in the image of a compact portion of the parametrization F, and thus converges in S. Suppose the z-coordinate of s is 1 (the case for -1 is analagous). Since s_n is Cauchy in S, for a sequence $\epsilon_m \to 1$, we can find $\delta_m \in \mathbb{N}$ such that $n, k \geq \delta_m \Rightarrow d(s_n, s_k) \leq 1 - \epsilon_m$. Consider the sets,

$$K_m = \{p \in S \mid d(p, s_{\delta_m}) \leq 1 - \epsilon_m\}$$

Projecting these sets into the xy-plane (which we identify with $\mathbb{R}^2$) gives a sequence of compact sets whose intersection is a point. Such a sequence cannot contain a portion of the line l_z for every z sufficiently near ± 1, so there must be some sequence of lines l_{z_m}, defined for large enough m, such that l_{z_m} misses the projection of K_m. But then s_n cannot be Cauchy, as when such a missed line occurs, the points of the sequence before and after the missed line occurs in the z-height must cross out of the compact set to reach the line in S, and then back in, thus contradicting the distance bound defining the K_m.

□

Note that a useful sufficient condition for completeness is simply that for any compact subset K of $\mathbb{R}^2$, there is a sequence of lines l_{zm}, $z_m \to \pm 1$, such that l_{z_m} misses K.

If we let $a(z)$ increase from $-\infty$ to ∞ (for example, $a(z) = \tan \frac{\pi}{2} z$), while setting $b(z) = 0$, $c(z) = z$ we obtain a surface which is extrinsically incomplete but intrinsically complete, as infinitely many sheets of the helicoid approach the bounding planes as $z \to \pm 1$. Note as well that the Gauss map of this surface must be dense on a hemisphere of S^2 at infinity. Otherwise, by Theorem 3.1, we would be able to find a plane which slices the surface in a finite number of components, and for which each parallel translation of the plane has the same number of exits to infinity. It is clear that any plane not parallel to the xy-plane must slice the surface in an infinite number of components, as the slicing plane eventually misses the translated core of the helicoid. If we consider slices parallel to the xy-plane, then those slices with $-1 < z < 1$ have two exits to infinity, since the slice is a line, while those with $|z| \geq 1$ have no exits to infinity, since the plane misses the surface.

If instead we let $a(z)$ be bounded (for example, $a(z) = rz$, $b(z) = 0$, $c(z) = \frac{1}{1-z^2}$), we may obtain helicoidal slab surfaces with arbitrarily many twists that are extrinsically complete.

6 Future Research

We hope to resolve the following questions with future research.

1. Can a slab surface have more than two ends, or have genus? Closely related to this is,

2. Can a slab surface have a normal that is parallel to the z-direction? All of the examples constructed so far have z-slices consisting of a single curve at each height; there are no critical points as the height increases.

3. If we have a slab surface whose z-slices are a single curve, can this curve have points where the sign of the curvature changes?

4. Can a slab surface be a graph over the plane of the slab?

7 Acknowledgements

I would like to thank the NSF for making the Indiana University REU possible. I would also like to thank my faculty mentor Chris Connell for his guidance, and the program directors Kevin Pilgrim and Bruce Solomon for organizing this great experience.

References

[CG08] C. Connell and M. Ghomi, *Topology of negatively curved real affine algebraic surfaces*, J. Reine Angew. Math. **624** (2008), 1-26.

[CT01] H. Chan and A. Treibergs, *Nonpositively curved surfaces in* $\mathbb{R}^3$, J. Differential Geom. **57** (2001), 389-407.

[CU10] C. Connell and J. Ullman, *Ends of negatively curved surfaces in Euclidean space*, Manuscripta Math. **131** (2010), no. 3-4, 275-303.

[doCar76] M. do Carmo, *Differential Geometry of Curves and Surfaces*, (1976)

[Ver67] A. L. Verner, *On the extrinsic geometry of elementary complete surfaces with nonpositive curvature. I*, Mat. Sb. (N.S.) **74** (**116**) (1967), 205-224.

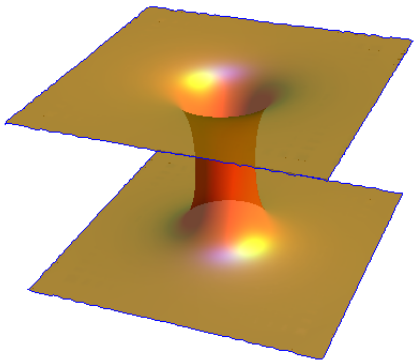

Figure 1: The slab annulus

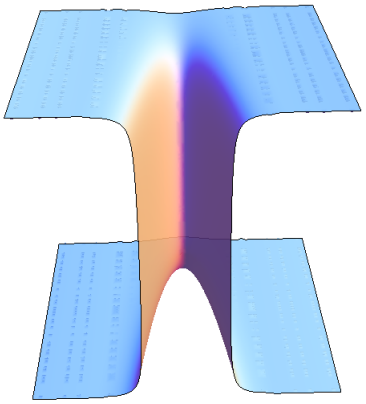

Figure 2: The pulled annulus

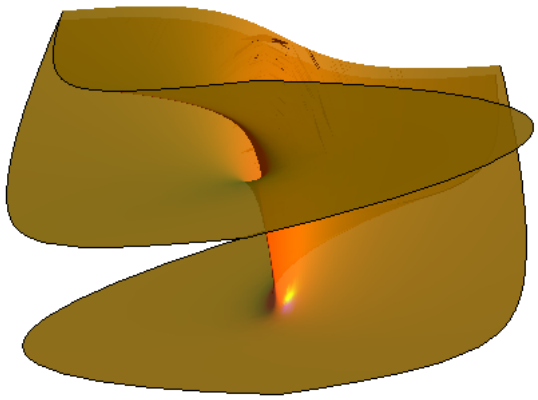

Figure 3: The slab parabolic helicoid

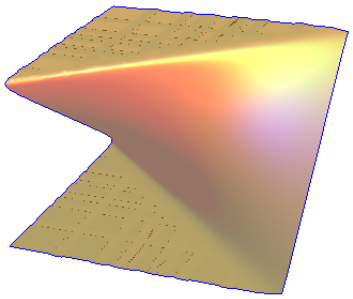

Figure 4: (a) $n = 1$

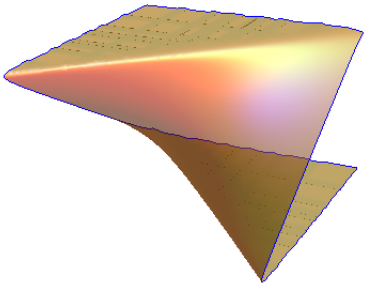

Figure 5: (b) $n = 0$

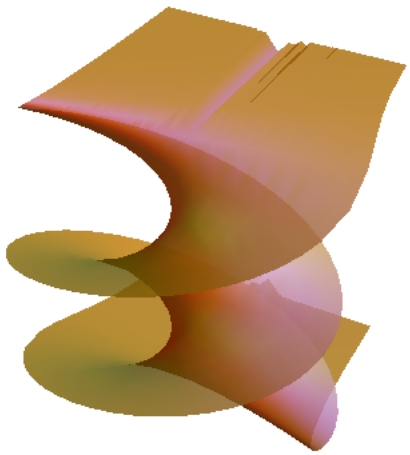

Figure 6: A ruled slab surface with $a(z) = \frac{5\pi}{4}z$, $b(z) = 0$, $c(z) = \frac{1}{1-z^2}$

Helicoidal Surfaces of Constant Mean Curvature in $\mathbb{R}^3$, $\mathbb{S}^3$ and $\mathbb{H}^3$

Nick Edelen

Abstract

We develop a conservation law for constant mean curvature (CMC) surfaces introduced by Korevaar, Kusner and Solomon [2], and provide a converse, so as to characterize CMC surfaces by a conservation law. We work with 'twizzler' construction, which applies a screw-motion to some base curve. We show that, excluding cylinders, CMC helicoidal surfaces can be completely determined by a first-order ODE of the base curve. Further, we demonstrate that in $\mathbb{R}^3$ this condition is equivelent to the treadmillsled characterization of helicoidal CMC surfaces given by Perdomo [3].

1 Introduction

We study immersed, constant mean curvature (CMC) surfaces which have screw-motion symmetry. Such surfaces can be described by the *twizzler* construction, which applies a screw-motion to some base curve γ. Recently Perdomo [3] characterized CMC twizzlers in $\mathbb{R}^3$ by giving, and geometrically interpreting, a first-order ODE on γ, using what he called the 'treadmillsled coordinates.'

In 1989 Korevaar, Kusner and Solomon [2] derived (later refined by Kusner [1]) a 'flux conservation' law of any CMC surface Σ immersed in a simply-connected spaceform. The law describes in essence a conserved quantity on any loop on Σ in a given homology class. When calculating this quantity for certain examples of surfaces, a stiking similarity with Perdomo's treadmillsled condition arises.

Here we will extend the result of [1] to the converse: given that a certain quantity is conserved over every loop in some homology class of Σ, then necessarily Σ has constant mean curvature. In each spaceform $\mathbb{R}^3$, $\mathbb{S}^3$ (the 3-sphere), $\mathbb{H}^3$ (3-dimensional hyperbolic space), we use the conservation law to derive a first-order ODE on γ for its twizzler to have constant mean curvature. Further, by considering γ parameterized by the angle of normal (the *support* parameterization), we show that the treadmillsled condition of [3] is identical to the conservation law on γ in $\mathbb{R}^3$.

This is helpful since the second-order ODE for constant mean curvature is quite difficult to understand. In $\mathbb{R}^3$ [3] classified geometrically the curves satisfying this first-order ODE, and we hope to find a similar analysis in $\mathbb{S}^3$ and $\mathbb{H}^3$.

I would like to extend my sincerest thanks to Professor Bruce Solomon for supervising, and to the NSF for funding this research as part of the 2011 Indiana University REU program.

1.1 Preliminaries

Consider an orientable surface Σ embedded in some 3-dimensional, simply-connected spaceform N. Pick ν to be the smooth unit normal of Σ in N. Let (g_1, g_2, g_3) be any local, orthonormal frame on N, and likewise (f_1, f_2, ν) a local, orthonormal adapted frame of Σ. For any vector field Y on Σ, we call $Y^\top = (Y \cdot \nu)\nu$ and $Y^\perp = Y - Y^\top$ the normal and tangential components of Y.

Denote covariant differentiation in N by D. For any smooth vector field Y, the divergence in N is given by $\mathrm{DIV}(Y) = \sum_1^3 (\mathrm{D}_{g_i} Y) \cdot g_i$, and the divergence on Σ by $\mathrm{div}(Y) = \mathrm{D}_{f_1} Y \cdot f_1 + \mathrm{D}_{f_2} \cdot f_2$. The gradient and Laplacian on Σ are given by $\nabla Y = (DY)^\perp$ and $\Delta Y = \mathrm{div}(\nabla Y)$.

All 3-dimensional integrals are taken with respect to the volume element of N; integrals of 2-dimensions are taken w.r.t. the surface element.

The mean curvature vector of Σ is $\mathbf{h} = h\nu = \Delta \mathbf{x}$, for $\mathbf{x}$ the inclusion mapping. The mean curvature h is, up to sign, the trace of the second fundamental form.

Let $(e_1, \cdots, e_n)$ denote the standard orthonormal frame of $\mathbb{R}^n$. In $\mathbb{R}^3$, we will often (implicitly) identify $\mathrm{span}(e_1, e_2)$ with $\mathbb{C}$ by $ae_1 + be_2 \leftrightarrow a + ib$. Likewise, we will identity $\mathbb{R}^4$ with $\mathbb{C} \times \mathbb{C}$.

2 Conservation Law

We loosely follow [2]. Let Σ be a connected, orientable surface embedded in a 3-dimensional, simply-connected spaceform N (i.e. effectively $\mathbb{R}^3$, $\mathbb{S}^3$ or $\mathbb{H}^3$). Identify the Killing fields on N with the Lie algebra $\mathfrak{g}$ of N's isometry group. Observe that the Killing vectors span each tangent space on N.

Let Γ_1 and Γ_2 be two smooth, homologous 1-cycles in Σ bounding a compact subset $S \subset \Sigma$. As $H_1(N) = 0$, we can take K_1 and K_2 to be any smooth 2-chains so that $\partial K_i = -\Gamma_i$. Then, since $H_2(N) = 0$, there is a 3-chain $U \subset N$ with piecewise smooth boundary $\partial U = S + K_1 + K_2$.

We write ν for the unit normal on any 2-chain in N; likewise, denote the unit cornomal on any 1-chain in Σ by η.

Pick a Killing field $Y \in \mathfrak{g}$. It is easily found that the variation of volume $|U|$ along Y is

$$\delta_Y(|U|) = \int_U \mathrm{div}(Y) = \int_{K_1 - K_2} Y \cdot \nu + \int_S Y \cdot \nu$$

Similarly, the variation of area $|S|$ along Y is known to be [4]:

$$\begin{aligned}\delta_Y(|S|) = \int_S \operatorname{div}(Y) &= \int_S \operatorname{div}(Y^\top) + \operatorname{div}(Y^\perp) \\ &= \int_{\partial S} Y \cdot \eta + \int_S Y \cdot \nu \operatorname{div}(\nu) \\ &= \int_{\Gamma_1 - \Gamma_2} Y \cdot \eta + \int_S Y \cdot h\nu\end{aligned}$$

having used Stoke's theorem, and observing that $\operatorname{div}(\nu) = \operatorname{trace}(\nabla \nu) = h$.

Combining these two calculations, we obtain the *first variation formula*:

$$\begin{aligned}0 &= \delta_Y(|S| - H|U|) \\ &= \int_{\Gamma_1 - \Gamma_2} Y \cdot \eta - H \int_{K_1 - K_2} Y \cdot \nu + \int_S (h - H) Y \cdot \nu \end{aligned} \tag{2.1}$$

The first equality is a direct consequence of Y being a Killing field.

Our main theorem arises naturally from relation (2.1).

Theorem 2.1. *Using the above notation, if Σ has constant mean curvature H then there is a linear function $\omega : H_1(\Sigma) \to \mathfrak{g}^*$ defined by*

$$\omega([\Gamma])(Y) = \oint_\Gamma Y \cdot \eta - H \iint_K Y \cdot \nu \tag{2.2}$$

where K is any smooth 2-chain with $\partial K = -\Gamma$.

Conversely, if for any homology class $[\Gamma] \in H_1(\Sigma)$, $\omega([\Gamma])$ as given by (2.2) is well-defined, then Σ has constant mean curvature.

Proof. If $h = H$ everywhere on Σ, then the first variation formula (2.1) reduces to

$$0 = \oint_{\Gamma_1 - \Gamma_2} Y \cdot \eta - H \iint_{K_1 - K_2} Y \cdot \nu$$

and as our choice of Γ_i is arbitrary, we can fix Γ_1, and immediately observe that for any Γ_2,

$$\oint_{\Gamma_2} Y \cdot \eta - H \iint_{K_2} Y \cdot \nu = \oint_{\Gamma_1} Y \cdot \eta - H \iint_{K_1} Y \cdot \nu = \text{constant}$$

Conversely, suppose that ω is well-defined for the null homology class $[0] \in H_1(\Sigma)$. Then by the first variation formula,

$$0 = \iint_S (h - H) Y \cdot \nu \tag{2.3}$$

for any compact $S \subset \Sigma$ with smooth boundary.

Suppose, towards a contradiction, there is a $p \in \Sigma$ with $h(p) \neq H$; wlog suppose $h(p) > H$, and hence $h(p) > H$ in some open neighboord S_1 of p. Then

we can choose a Y so that $\nu(p) \cdot Y(p) > 0$, an $\epsilon > 0$, and a neighborhood S_2 of p so that $\nu \cdot Y > \varepsilon$ on S_p. Then for any sufficiently small ball B centered at p, with $B \cap \Sigma \subset S_1 \cap S_2$,

$$0 = \iint_{B \cap \Sigma} (h - H) Y \cdot \nu > 0$$

This contradiction shows that $h \equiv H$ on Σ.

More generally, if ω is well-defined for an arbitrary homology class $[\Gamma] \in H_1(\Sigma)$, we have that $\omega([\Gamma + \Gamma_0]) = \omega([\Gamma])$ for any null-homologous Γ_0. Thus, by linearity of ω, $\omega([\Gamma_0]) = 0$, and we have already shown this forces Σ to have constant mean curvature. □

Remark 2.2. Embedding of Σ is not essential in the theorem above, which can be readily generalized to immersed surfaces.

Remark. By considering 3-currents instead of 3-chains, the above theorem can be readily generalized to immersed surfaces.

A further generalization can relax the conditions on N to allow non-trivial first and second homologies. Given the inclusion map $\mathcal{I} : H_1(\Sigma) \to H_1(N)$, we would then have for each smooth 1-cycle β in N a function $\omega_\beta : \mathcal{I}^{-1}([\beta]) \times \mathfrak{g} \to \mathbb{R}$. ω_β would satisfy (2.2), except the 2-chain K would have boundary $\partial K = -\Gamma - \beta$. To by-pass $H_2(N) \neq 0$, we would consider the 3-current $U \subset N$ to have boundary $\partial U = S + K_1 + K_2 + C$, where C is some fixed 2-cycle homologous to $S + K_1 + K_2$.

3 Twizzlers in $\mathbb{R}^3$, $\mathbb{S}^3$ and $\mathbb{H}^3$

In this section we introduce twizzlers to explicitly parameterize helicoidal surfaces in terms of a base curve. Using the ideas presented by theorem 2.1, we then derive a first-order ODE on the base curve to characterize CMC twizzlers.

We will only lay out in full the proof of twizzlers in $\mathbb{R}^3$, as it readily generalizes to $\mathbb{S}^3$ and $\mathbb{H}^3$.

3.1 Case: $\mathbb{R}^3$

Definition 3.1. Let $\gamma : I \to \mathbb{C}$ be an immersed C^2 curve on the interval $I \subset \mathbb{R}$, and $m \in \mathbb{R}_+$. Then the *twizzler of γ with pitch m* in $\mathbb{R}^3$ is the surface T parameterized by

$$\mathbf{T}(u, v) = e^{iv}\gamma(u) + mv\mathbf{e_3} \quad (u, v) \in I \times \mathbb{R}$$

which we may also reference with the pair $\langle \gamma, m \rangle$.

T is always immersed, orientable, and connected. Holding $u = u_0$ constant, we call the curve $\mathbf{T}(u_0, v)$ a *helix* of T. T has discrete translational symmetry along the z-axis, described by the group G with action $g \cdot \mathbf{r} = \mathbf{r} + 2\pi m\mathbf{e_3}$. Denote

the quotient surface T/G by $\hat{T}$, and observe that the helices of T are smooth loops in $\hat{T}$.

Using the language of section 2, we would like to take Γ as a helix of T, and N as $\mathbb{R}^3/G$. Complications arise, however, since helices are not null-homologous in $\mathbb{R}^3/G$. We bypass this issue by using the z-axis as a 'reference' 1-cycle, homologous to the helices in $\mathbb{R}^3/G$, to construct 2-chains with a common boundary.

As suggested by our remark 2.2, we will explicitly prove that theorem 2.1 applies although T is not embedded.

Definition 3.2. The *shaving of* $\hat{T}$ *at* u_0 is the surface $\mathcal{T}[u_0]$ parameterized by

$$\mathcal{T}[u_0](v,t) = te^{iv}\gamma(u_0) + mve_3 \quad (v,t) \in [0,2\pi] \times [0,1]$$

we can consider $\mathcal{T}[-]$ a bijection between I and shavings on $\hat{T}$.

Theorem 3.3. *The twizzler* $T \equiv \langle \gamma, r \rangle$ *in* $\mathbb{R}^3$ *has constant mean curvature iff there are constants* H *and* C *so that*

$$C = \frac{2\pi}{\sqrt{g}} m\gamma' \cdot i\gamma - H\pi|\gamma|^2 \tag{3.1}$$

where $\sqrt{g} = \sqrt{(\mathbf{T}_u \cdot \mathbf{T}_u)(\mathbf{T}_v \cdot \mathbf{T}_v) - (\mathbf{T}_u \cdot \mathbf{T}_v)^2}$ *is the are density on* T.

Further, if T *is not a cylinder,* H *is the mean curvature of* T.

Proof. Take $\mathbf{Y} = \mathbf{e_3}$, generating translation along the z-axis; $\mathbf{Y}$ then descends to $\mathbb{R}^3/G$. Assume T has constant mean curvature H, and pick an interval $J \subset I$ so that $S = \mathbf{T}(J \times [0,2\pi])$ is embedded. For $i = 1,2$, let $\Gamma_i \subset S$ be the helix at any point $u_i \in J$, and $K_i \equiv \mathcal{T}[u_i]$. Then $K_1 + K_2 + S$ bounds a compact volume in $\mathbb{R}^3/G$, and the first variation formula (2.1) holds. As in the proof of theorem 2.1, we deduce the existence of a constant C so that, for any shaving $\mathcal{T}[u]$, $u \in J$,

$$C = \oint_{\partial \mathcal{T}[u]} \mathbf{Y} \cdot \eta - H \iint_{\mathcal{T}[u]} \mathbf{Y} \cdot \nu \tag{3.2}$$

Note that if T is a cylinder, $\iint_S \nu$ vanishes for any $S \subset \Sigma$ bounded by helices, so for any H we can find a C so that (3.2) holds. We then evaluate (3.2) explicitly to give relation (3.1).

Using Gram-Schmidt, we calculate that

$$\begin{aligned} \eta \cdot Y &= \frac{\sqrt{T_v \cdot T_v}}{\sqrt{(T_u \cdot T_u)(T_v \cdot T_v) - (T_u \cdot T_v)^2}} \left(T_u - \frac{T_u \cdot T_v}{T_v \cdot T_v} T_v \right) \cdot \eta \\ &= -\frac{\sqrt{|\gamma|^2 + m^2}}{\sqrt{g}} \frac{\gamma' \cdot i\gamma}{|\gamma|^2 + m^2} m \end{aligned}$$

so that

$$\begin{aligned} \oint_{\partial S} \mathbf{e_3} \cdot \eta &= \frac{1}{\sqrt{g}} \int_0^{2\pi} -\frac{m\gamma' \cdot i\gamma}{|\gamma|^2 + m^2} (|\gamma|^2 + m^2) dv \\ &= -\frac{2\pi}{\sqrt{g}} m\gamma' \cdot i\gamma \end{aligned}$$

.

On the shaving,

$$\nu dS = S_v \wedge S_t = i\gamma e^{iv} - t|\gamma|^2 \mathbf{e_3}$$

Note order of cross product: we must be consistent with the requirement $\partial K = -\Gamma$. The second integral becomes

$$\iint_S \mathbf{e_3} \cdot \nu = -\int_0^{2\pi} \int_0^1 t|\gamma|^2 dt dv = -\pi|\gamma|^2$$

For each point u we can find a neighborhood $u \in J_u \subset J$ so that $\mathbf{T}(J_u \times [0, 2\pi])$ is embedded, and hence a constant C_u satisfying (3.1) on $\mathbf{T}(J_u \times [0, 2\pi])$. By compactness, any closed interval $[a, b] \subset I$ is covered by finitely many J_u, implying that $C_a = C_b$. We deduce that $C = C_a = C_b$ satisfies (3.1) everywhere on T.

Conversely, given that (3.1) – and hence the conservation formula (2.2) – holds for every shaving, the first variation formula (2.1) gives

$$\begin{aligned} 0 &= \iint_{\mathbf{T}(J\times[0,2\pi])} (h - H)\mathbf{Y} \cdot \nu \\ &= 2\pi \int_{\gamma(J)} (h - H)\mathbf{Y} \cdot \nu \sqrt{|\gamma|^2 + m^2} \end{aligned} \tag{3.3}$$

whenever $J \subset I$ is sufficiently small for $\mathbf{T}(J \times [0, 2\pi])$ to be embedded.

The subet $I^* \subset I$ defined by $\mathbf{Y} \cdot \nu \neq 0$ is open in I. Suppose $h(p) \neq H$ at some point $p \in I^*$, then there is a ball $B_\varepsilon \ni p$ in I^* on which $h - H$ has a fixed sign. But likewise $\mathbf{Y} \cdot \nu \neq 0$ in B_ε, so the integral (3.3) cannot vanish, a contradiction. It follows that $h \equiv H$ on I^*.

If I^* is also dense in I, then $h = H$ everywhere. If I^* is not dense, there is a maximal interval $I_0 \subset I - I^*$ on which $\mathbf{Y} \cdot \nu = 0$. Then necessarily, $\gamma' \perp \gamma$ on I_0, and hence $\mathbf{T}(I_0 \times [0, 2\pi])$ is a segment of a cylinder having some constant mean curvature H_0.

If $I_0 = I$ then T is entirely a cylinder, with mean curvature H_0. Otherwise there is a sequence of points in I^* approaching an end-point of I_0, implying by continuity of h that $H = H_0$. □

3.2 Case: $\mathbb{S}^3$

Embed $\mathbb{S}^3$ in $\mathbb{R}^4$ by equipping the submanifold $\{\mathbf{x} \in \mathbb{R}^4 | \mathbf{x} \cdot \mathbf{x} = 1\}$ with the induced metric.

Definition 3.4. Let $(\gamma, f) : I \to \mathbb{C} \times \mathbb{R} \subset \mathbb{S}^3$ be a curve on the interval $I \subset \mathbb{R}$, so that $|\gamma|^2 + f^2 = 1$. Pick an $m \in \mathbb{R}_+$. Define the twizzler $T : I \times \mathbb{R} \to \mathbb{C} \times \mathbb{C} \cong \mathbb{R}^4$ in $\mathbb{S}^3$ to be the surface parameterized by

$$\mathbf{T}(u, v) = (e^{iv}\gamma(u), e^{imv} f(u))$$

Definition 3.5. For a twizzler T in $\mathbb{S}^3$, define the shaving at $u_0 \in I$ to be the surface parameterized by

$$\mathcal{T}[u_0](v,t) = (e^{iv}\frac{\gamma(u_0)}{|\gamma(u_0)|}\sin t, e^{imv}\cos t) \quad (v,t) \in [0,2\pi] \times [0, \cos^{-1} f(u_0)]$$

Theorem 3.6. *The twizzler T in $\mathbb{S}^3$ has constant mean curvature iff there are constants H and C so that, for all values of γ*

$$C = \frac{2\pi}{\sqrt{g}} m f^2(\gamma' \cdot i\gamma) - H\pi|\gamma|^2 \tag{3.4}$$

Further, if T is not a torus, H is the mean curvature of T.

Proof. Pick $\mathbf{Y}(z,w) = (0, iw)$. Then the proof is precisely the same as in $\mathbb{R}^3$, only considering the $\mathbb{S}^3$ equivelent of the cylinder to be the torus. Torii in $\mathbb{S}^3$ are defined by the parameterization $T(u,v) = (\cos e^{iu}, \sin te^{iv})$, for some constant $\xi \in \mathbb{R}$. All $\mathbb{S}^3$ torii have constant mean curvature, as every point $T(u,v)$ can be mapped to $T(0,0)$ by ambient isometries. □

3.3 Case: $\mathbb{H}^3$

We work with the Lorentz model of $\mathbb{H}^3$, as follows. Define the quadratic form $Q = diag(-1,-1,-1,1)$. Then $\mathbb{H}^3 \cong \{\mathbf{x} \in \mathbb{R}^4 | < \mathbf{x}, \mathbf{x} >= 1\}$ with inner product $< \mathbf{x}, \mathbf{y} >= \mathbf{x}^\top Q\mathbf{y}$. Further, for some non-zero real m, define the mapping $B_m : \mathbb{R} \to SO(1,1)$ by

$$B_m(v) = \begin{pmatrix} \cosh mv & \sinh mv \\ \sinh mv & \cosh mv \end{pmatrix}$$

Definition 3.7. Let $(\gamma, f) : I \to \mathbb{C} \times \mathbb{R}$ be a curve on the interval $I \subset \mathbb{R}$, so that $f^2 - |\gamma|^2 = 1$. Pick $m \in \mathbb{R}_+$. Define the twizzler $T : I \times [-\infty, \infty] \to \mathbb{C} \times \mathbb{C}$ in $\mathbb{H}^3$ by the parameterization

$$\mathbf{T}(u,v) = (e^{iv}\gamma(u), B_m(v) i f(u))$$

Define a cylinder in hyperbolic space to be the twizzler of $(\gamma(u), f(u)) = (ae^{iu}, b)$, for $a, b \in \mathbb{R}$ satisfying $b^2 - a^2 = 1$.

Definition 3.8. For a twizzler T in $\mathbb{H}^3$, define the shaving at $u_0 \in I$ to be the surface S parameterized by

$$\mathcal{T}[u_0](v,t) = (e^{iv}\frac{\gamma(u_0)}{|\gamma(u_0)|}\sinh t, B_m(v) i \cosh t) \quad (v,t) \in [0,2\pi] \times [0, \cosh^{-1} f(u_0)]$$

Theorem 3.9. *The twizzler T in $\mathbb{H}^3$ has constant mean curvature iff there are constants H and C so that, for all values of γ*

$$C = \frac{2\pi}{\sqrt{g}} m f^2 < \gamma', i\gamma > + H\pi|\gamma|^2 \tag{3.5}$$

where $g =< \mathbf{T}_u, \mathbf{T}_u >< \mathbf{T}_v, \mathbf{T}_v > + < \mathbf{T}_u, \mathbf{T}_v >^2$.

Further, if T is not a cylinder, then H is the mean curvature of T.

Proof. Take $\mathbf{Y}(z,w) = (0, \begin{pmatrix} 0 & 1 \\ 1 & 0 \end{pmatrix} w)$. The proof now follows as in the $\mathbb{R}^3$ case. □

4 Perdomo's Characterization

An alternate characterization of helicoidal, constant mean curvature surfaces in $\mathbb{R}^3$ is given by Perdomo [3]. A first integral for the second-order constant mean curvature ODE is interpreted by a kinetic condition called the *treadmillsled*. We shall use a special parameterization (by angle of normal) to better relate his condition with our conservation law.

4.1 The treadmillsled

Intuitively, the treadmillsled is a variation of a roulette – imagine rolling a curve along a line, while simultaneously moving the line in the opposite direction, so that the curve's point of contact stays in one place. By tracing out the path of a point fixed relative to the curve, one obtains the treadmillsled. We shall consider a slight generalization, allowing for any proportion ℓ of movement of the line: when $\ell = 0$, the line doesn't move, and we have a roulette; when $\ell = 1$, the line matches the curve's speed, yielding the treadmillsled.

Definition 4.1. The *ℓ-treadmill* of a C^2 curve $\gamma : I \to \mathbb{C}$ is defined by $\sigma_\ell[\gamma] = (1-l)s - \frac{1}{v}\gamma'\bar{\gamma}$, where s is the arc-length of γ, and v the speed.

By construction, σ_ℓ is independent of parameterization of γ. We write τ for Perdomo's treadmillsled, which is the same as our σ_1.

Remark. Observe that σ satisfies

$$\frac{1}{v}\sigma' = ik(1-\ell)s - (\ell + ik\sigma)$$

Proposition 4.2. *A curve $(x,y) : I \to \mathbb{C}$ is the ℓ-treadmill of a curve γ iff it satisfies the differential equations*

$$\begin{aligned} \frac{1}{s'}x' &= -\ell + ky \\ \frac{1}{s'}y' &= (1-\ell)ks - kx \end{aligned} \tag{4.1}$$

with $s : I \to \mathbb{R}_+$ is strictly increasing, and $k : I \to \mathbb{R}$.

Further, up to rotations, σ_ℓ maps C^2 curves injectively to C^1 curves.

Proof. Given γ, verifying (4.1) if $(x,y) = \sigma_\ell[\gamma]$ is a simple calculation. k is then the curvature of γ, and s the arc-length.

Conversely, given equation (4.1), then by the fundamental theorem of curves, there is a planar curve $\gamma(t)$ having curvature k and arc-length s. The further condition that $\sigma_\ell[\gamma](0) = (x,y)(0)$ fixes the orientation of γ with respect to the origin, i.e. up to rotation. The curve γ is well-defined in the sense that, if $(x_1, y_1) = (x,y) \circ f$ is a reparameterization of (x,y), then $\sigma_\ell[\gamma \circ f] = (x_1, y_1)$. □

Observe that shifting the 'starting position' of γ will effectively translate $\sigma_\ell[\gamma]$. Formally, if $I = (a, b] \cup (b, c)$, then $\sigma_\ell[\gamma]|_{(b,c)} = (1 - \ell)s(b) + \sigma_\ell[\gamma|_{(b,c)}]$. This is true except for the special case τ (i.e. $\ell = 1$); since no s term is present, τ is determined without the ambiguity of 'starting position'. Further, $\tau[\gamma](p)$ is determined by only $\gamma(p)$ and $\gamma'(p)$. This fact, and that τ is continuous, immediately gives the following lemma.

Lemma 4.3. *Given a smooth curve $\gamma : I \to \mathbb{C}$, knowing the values of γ and γ' on some dense subset of I is sufficient to completely determine $\tau[\gamma]$.*

4.2 Support parameterization

Our key angle of attack in relating the ODE's of [3] and the conservation law lies in our choice of parameterization. We will parameterize in the (culmulative) angle of normal, called the *support parameterization*. We shall lay out the relavant machinery below.

Definition 4.4. A curve is *strictly convex* if the curvature never vanishes.

Lemma 4.5. *Every strictly convex curve can be support-parameterized.*

Proof. Consider a curve $\gamma : I = (a, b) \to \mathbb{C}$ with curvature k and speed v. Without loss of generality suppose $k < 0\ \forall t \in I$. Let n be the normal of the curve γ, and $\theta = \arg(n)$ be the normal angle. Then $n := \frac{i}{v}\gamma'$.

Define the culmulative normal angle by $\Theta : I \to \mathbb{R}$ by $\Theta(t) = \int_a^t \mathrm{d}\theta$. Since $\theta' = -vk > 0$, Θ is strictly increasing. Therefore there is a an inverse $\Theta^{-1} : \Theta(I) \to I$. □

There is a nice form for the support parameterization. Let θ be the normal angle of γ. We can then write $\gamma(\theta) = (q+ir)e^{i\theta}$, for some functions $q, r : \Theta(I) \to \mathbb{R}$.

So that θ is indeed the angle of the normal, we require that $\theta = \arg(n) = \arg(i\gamma')$, imposing the condition $q' = r$. We have then $\gamma = (q + iq')e^{i\theta}$, and $\gamma'' = (q+q'')ie^{i\theta}$. As long as $q+q'' > 0$, this is a valid param of γ, by the above lemma. (Conversely, every q satisfying $q + q'' > 0$ is the support function for some convex curve.)

The function $q : \Theta(I) \to \mathbb{R}$ is called the *support function of* γ. The advantage in this choice of parameterization becomes clear from the following.

Proposition 4.6. *If strictly convex curve γ has support function q, then*

$$\tau[\gamma] = -q' - iq$$

Proof. From the definition of $\sigma_1 \equiv \tau$, and the above comments, we have

$$\begin{aligned}\tau[\gamma](\theta) &= -\frac{1}{q+q''}(q+q'')ie^{i\theta}(q-iq')e^{-i\theta} \\ &= -q' - iq\end{aligned}$$

□

4.3 Twizzlers of constant mean curvature

In the interest of focus, we will quote Perdomo's theorem without proof, but will provide a sketch of its origin.

Theorem 4.7. *(Perdomo) The twizzler $T \equiv \langle \gamma, m \rangle$ has constant mean curvature H iff: T is a cylinder of radius $-\frac{1}{2H}$, or $\tau[\gamma]$ satisfies*

$$H(x^2 + y^2) - \frac{2my}{\sqrt{m^2 + x^2}} = M \tag{4.2}$$

for some constant $M \geq -\frac{1}{H}$.

Remark 4.8. The above theorem arises directly as a first-integral of the second-order ODE condition for CMC twizzlers. Explicitly, suppose γ has a support parameterization. Then express $\tau[\gamma]$ in terms of the support function q of γ, and differentiate (4.2). We obtain

$$\frac{H}{2m}(2q'q + 2q''q') = \frac{-q'}{(m^2 + q'^2)^{1/2}} + \frac{q''q'q}{(m^2 + q'^2)^{3/2}}$$

which, if $q' \neq 0$ (i.e. T is not a cylinder), simplifies to the canonical expression for mean curvature H of a twizzler, expressed in terms of a support function q:

$$H = \frac{-m}{v(m^2 + q'^2)^{3/2}}(m^2 + q'^2 - qq'')$$

4.4 Equivalence

An equivelance can be directly established between the two treadmillsled and conservation law characterizations. This equivalence is clear if T is the helicoid, as both relations (3.1) and (4.2) reduce to 0. Otherwise we need the following lemma.

Lemma 4.9. *An xy-slice of a CMC twizzler contains a line segment iff it is a line.*

Proof. Immediate from the fact the only ruled, non-planar CMC surface is the helicoid, and the well-known property that CMC surfaces are real analytic. □

Then if T is not a helicoid, using lemmas 4.9 and 4.3, we can (piecewise) support parameterize γ of the twizzler $\langle \gamma, m \rangle$, using support function q. The conservation law (3.1), written in terms of q, is precisely equation (4.2):

$$\begin{aligned} C &= \frac{2\pi}{\sqrt{g}} m\gamma' \cdot i\gamma - H\pi|\gamma|^2 \\ &= \frac{2\pi mq(q + q'')}{\sqrt{(q + q'')^2(q^2 + q'^2 + m^2) - (q + q'')^2 q^2}} - H\pi(q^2 + q'^2) \\ &= \frac{2\pi}{\sqrt{m^2 + q'^2}} mq - H\pi(q^2 + q'^2) \\ &= -\pi M \end{aligned}$$

Thus, our theorem 2.1 can be expressed in the language of Perdomo's treadmillsled, and conversely Perdomo's theorem 4.7 can be rewritten as a conservation law.

Theorem 4.10. *If C is the constant from theorem 2.1, and M the constant from theorem 4.7, then $C = -\pi M$.*

References

[1] R. Kusner, *Bubbles, conservation laws and balanced diagrams*, Geometric Analysis and Computer Graphics, P. Concus, R. Finn and D. Hoffman, Springer-Verlage (1990).

[2] N. Korevaar and R. Kusner and B. Solomon, *The structure of complete embedded surfaces with constant mean curvature*, Journal of Differential Geometry, vol 30 (1989), pp 465–503.

[3] O. Perdomo, *A dynamical interpretation of the profile curve of CMC twizzler surfaces*, ArXiv preprint #1001.5198.

[4] L. Simon, *Lectures on Geometric Measure Theory*, Proc. Centre Math. Anal. Austral. Nat. Univ. 1983.

The Poisson Integral Formula and Representations of SU(1,1)

Ewain Gwynne

Abstract

We present a new proof of the Poisson integral formula for harmonic functions using the methods of representation theory. In doing so, we exhibit the irreducible subspaces and unitary structure of a representation of the group $SU(1,1)$ of 2×2 complex generalized special unitary matrices. Our arguments illustrate a technique that can be used to prove similar reproducing formulas in higher dimensions and for other classes of functions. Our paper should be accessible to readers with minimal knowledge of complex analysis.

Keywords: Poisson integral formula, harmonic functions, representations of SU(1,1), fractional linear transformations, conformal transformations

1 Introduction

Recall that a function f of two variables x and y is *harmonic* if it is twice continuously differentiable and satisfies $\frac{\partial^2 f}{\partial x^2} + \frac{\partial^2 f}{\partial y^2} = 0$. Such functions are exactly the solutions to *Laplace's equation*, $\Delta f = 0$. This equation has numerous physical applications. For various interpretations of the function f, it can represent Fick's Law of diffusion, Fourier's law of heat conduction, or Ohm's law of electrical conduction. Moreover, harmonic functions play a role in probabalistic models of Brownian motion [2].

By identifying $z = x + iy \in \mathbb{C}$ with $(x, y) \in \mathbb{R}^2$, a function of a complex variable can be viewed as a function of two real variables and can thus be defined as harmonic in a natural manner. The Poisson integral formula is a fundamental result that enables one to recover all of the values of a harmonic function defined on a disk in the complex plane given only its values on the boundary of the disk:

Theorem 1.1 (The Poisson Integral Formula)**.** *Let f be a complex-valued harmonic function defined on a neighborhood of a closed disk $D(p, R)$ of radius R and center p in the complex plane. Then*

$$f(re^{i\theta} + p) = \frac{1}{2\pi} \int_0^{2\pi} f(Re^{i\phi} + p) \frac{R^2 - r^2}{R^2 + r^2 - 2r\cos(\theta - \phi)} d\phi,$$

where $re^{i\theta}$ is an element of the interior of $D(p, R)$.

By translating and scaling the disk, it is no loss of generality to assume that $R = 1$ and $p = 0$, in which case $D(p, R)$ is the closed unit disk, which we henceforth denote simply by D. In this case, the formula reduces to

$$f(re^{i\theta}) = \frac{1}{2\pi} \int_0^{2\pi} f(e^{i\phi}) \frac{1 - r^2}{1 + r^2 - 2r\cos(\theta - \phi)} d\phi.$$

In this paper, we give a new proof of the Poisson integral formula. Our method makes use of a representation (essentially a group action on a vector space by linear transformations) of the group $SU(1, 1)$ of 2×2 generalized special unitary matrices with complex entries (isomorphic to $SL(2, \mathbb{R})$) over the vector space of harmonic functions on D. The interested reader can find more information on matrix Lie groups like $SU(1, 1)$ and their representations in [1]. We show that as a representation, the space of harmonic functions is generated by the identity function $z \mapsto z$ and its conjugate $z \mapsto \overline{z}$. We then use this fact to reduce the proof of the Poisson integral formula to a few elementary computations, in much the same way that one reduces the study of a linear transformation to the study of its effect on a basis. Along the way, we describe the irreducible subspaces and unitary structure of our representation, properties which the reader may find of independent interest.

Our proof is inspired by a paper by Igor Frenkel and Matvei Libine [3] which uses representation theory to develop analysis over the quaternions. In particular, the authors make use of the theory of the conformal group $SL(2, \mathbb{H})$, the group of 2×2 matrices with quaternion entries and determinant 1. Many of the parallels between complex and quaternionic analysis are made apparent by restating results in complex analysis from the perspective of representations of the complex analogue of $SL(2, \mathbb{H})$, $SL(2, \mathbb{C})$. This lends importance to the question of which results in complex analysis can, in fact, be restated and proven in terms of representations of $SL(2, \mathbb{C})$ and its subgroups, including $SU(1, 1)$, for these are the results which can likely be extended to quaternionic analysis.

Although the classical proof of the Poisson integral formula is short and elementary, our proof illustrates a technique which has been successfully used to prove reproducing formulas for other kinds of functions (as is done in [3] and [4]), and which is likely to be used again in the future. For example, methods similar to ours might be used to prove higher dimensional analogues of the Poisson formula in $\mathbb{R}^n$, which are discussed in [11]. The matrix group $SO(n + 1, 1)$ acts on the vector space of harmonic functions on $\mathbb{R}^n$ and its subgroup $SO(n, 1)$ preserves the unit ball, as is explained in [6]. Plausibly, $SO(n, 1)$ group and its own subgroup $SO(n)$ could play roles similar to those that the groups $SU(1, 1)$ and $SO(2)$ play in our paper to engender a proof of the higher dimensional formulas.[1] As another example, in Section 5.4 of [3], the authors conjecture that the Feynman diagrams, which describe the interactions of subatomic particles, correspond to projections onto irreducible components

[1] To complete the analogy, we note that, as real Lie groups, $SL(2, \mathbb{C})/\{\pm 1\}$ is isomorphic to the connected component of the identity of $SO(3, 1)$ and $SU(1, 1)/\{\pm 1\}$ is isomorphic to the connected component of the identity of $SO(2, 1)$.

of certain representations of the group $SU(2,2)$. It is quite possible that the technique we illustrate here could be used to prove this conjecture.

We begin with a preliminary section in which we introduce the definitions and concepts we shall use in the remainder of the paper and construct our representation of $SU(1,1)$. This is followed by Section 3, which contains the proof that certain subrepresentations of our representation are in fact irreducible. The only fact from this section that is needed for the proof of the Poisson integral formula is that z and $\overline{z}$ generate the entire vector space, but we give a more detailed exposition of the invariant subspace structure of our representations which the reader might find of independent interest. Section 4 consists of the elementary computations needed to finish the proof of the Poisson integral formula. To complete the description of our representations, we conclude with Section 5, in which we define an $SU(1,1)$-invariant inner product on a modified version of our vector space.

2 Preliminaries

An action of a group G on a set S is a function from $G \times S \to S$, denoted by $(g,x) \mapsto gx$, such that for all $x \in S$ and all $g,h \in G$, $(gh)x = g(hx)$ and $1x = x$, where 1 is the identity in G.

Definition 2.1. A *representation* of a group G over a vector space V is a group homomorphism $\rho : G \to GL(V)$, where $GL(V)$ is the group of invertible linear transformations from V to V.

In effect, a representation is an action of a group on a vector space by linear transformations. Oftentimes, when there is no danger of ambiguity, one refers to the vector space itself, rather than the function ρ, as a representation. A group G that acts on a set U possesses a natural representation over a vector space of functions defined on U given by composition on the right: for $g \in G$, $\rho(g) : f \mapsto f \circ g^{-1}$. The inverse of g is needed so that the representation preserves group multiplication. Representations arise frequently in this context, and it is this sort of representation that we study here. Let us first define our group.

Definition 2.2. The group $SU(1,1)$ is the set of matrices

$$SU(1,1) = \left\{ \gamma = \begin{pmatrix} a & b \\ \overline{b} & \overline{a} \end{pmatrix} : a,b \in \mathbb{C},\ |a|^2 - |b|^2 = 1 \right\},$$

with group multiplication given by matrix multiplication.

The group $SU(1,1)$ is isomorphic to the group $SL(2,\mathbb{R})$ of 2×2 real matrices with determinant 1.

We let $\mathbb{C}P^1$ denote complex projective space, the set of pairs of complex numbers which are not both equal to zero modulo the equivalence relation of being scalar multiples of one another: $(z,w) \sim (z',w')$ provided $z/w = z'/w'$

or $w = w' = 0$. The group $SL(2,\mathbb{C})$ of 2×2 invertible matrices with complex entries and determinant 1, and hence also its subgroup $SU(1,1)$, acts on $\mathbb{C}P^1$ by matrix-vector multiplication. If we associate with each $z \in \mathbb{C}$ the equivalence class of the tuple $(z,1) \in \mathbb{C}P^1$ and with ∞ the equivalence class of the tuple $(1,0) \in \mathbb{C}P^1$, we may think of this as an action of $SL(2,\mathbb{C})$ on the extended complex plane $\mathbb{C} \cup \{\infty\}$. Under this action, $\gamma = \begin{pmatrix} a & b \\ c & d \end{pmatrix} \in SL(2,\mathbb{C})$ sends $z \in \mathbb{C} \cup \{\infty\}$ to $\frac{az+b}{cz+d}$.

A function from $\mathbb{C} \cup \{\infty\}$ to itself of the form $z \mapsto \frac{az+b}{cz+d}$ is called a *Möbius transformation*. Thus, we see that each element of $SL(2,\mathbb{C})$ defines a Möbius transformation on $\mathbb{C}$. We shall henceforth denote the Möbius transformation associated with $\gamma \in SL(2,\mathbb{C})$ by $\tilde{\gamma}$.

Of particular interest for our purposes are those matrices whose Möbius transformations preserve the closed unit disk D. It is easily checked that for each matrix $\gamma \in SU(1,1)$, the Möbius transformation

$$\tilde{\gamma}(z) = \frac{az+b}{cz+d}$$

associated with γ maps each element $z \in D$ to another element of D and does so in a bijective manner[2]. Via these Möbius transformations, the group $SU(1,1)$ acts on D.

We identify the circle group $SO(2)$ with the subgroup of $SU(1,1)$ given by

$$SO(2) = \left\{ k_\theta = \begin{pmatrix} e^{i\theta} & 0 \\ 0 & e^{-i\theta} \end{pmatrix} : \theta \in [0, 2\pi) \right\}.$$

The group $SO(2)$ is thereby associated with Möbius transformations that merely rotate D, i.e. those of the form $\tilde{k_\theta}(z) = e^{2i\theta} z$.

We next define our vector space.

Definition 2.3. We denote by $\mathcal{V}$ the vector space of complex-valued functions which are continuous on D and harmonic on the interior of D,

$$\mathcal{V} = \left\{ f : D \to \mathbb{C} : \ f \textit{ continuous}, \ \frac{\partial^2 f}{\partial x^2}(z) + \frac{\partial^2 f}{\partial y^2}(z) = 0 \ \forall z \in \mathrm{int}(D) \right\}.$$

A complex valued function is harmonic if and only if both its real and imaginary parts are harmonic. Recall that for U an open subset of $\mathbb{C}$, a complex valued function $f = u + iv : U \to \mathbb{C}$ is called *holomorphic* if f is complex differentiable. A complex-valued function $f = u + iv : U \to \mathbb{C}$ is *anti-holomorphic* if its complex conjugate $\overline{f} = u - iv$ is holomorphic.

The partial derivatives of a holomorphic function satisfy the Cauchy-Riemann Equations, $\frac{\partial u}{\partial x} = \frac{\partial v}{\partial y}$ and $\frac{\partial u}{\partial y} = -\frac{\partial v}{\partial x}$. Given these equations, it follows from a

[2]In fact, these Möbius transformations are the *only* complex diffeomorphisms of D [7], but we will not need this fact for our paper.

simple computation of derivatives that every holomorphic function and every anti-holomorphic function is harmonic. Thus, every function which is either holomorphic or anti-holomorphic on the interior of D and continuous on its boundary is an element of $\mathcal{V}$.

Definition 2.4. We denote by $\mathcal{V}_h$ the subspace of $\mathcal{V}$ consisting of functions which are holomorphic on $\text{int}(D)$, by $\mathcal{V}_{ah}$ the subspace of $\mathcal{V}$ consisting of functions which are anti-homomorphic on $\text{int}(D)$, and by $\mathcal{V}_c$ the subspace of $\mathcal{V}$ consisting of constant functions.

Proposition 2.5. $\mathcal{V} = \mathcal{V}_h + \mathcal{V}_{ah}$.

Proof. Let $f = u + iv : D \to \mathbb{C}$ be in $\mathcal{V}$. We seek to show that f can be expressed as the sum of a holomorphic function and an anti-holomorphic function in $\mathcal{V}$. The real and imaginary parts of f, u and v, are harmonic on $\text{int}(D)$ and continuous on ∂D. So, there exist harmonic conjugates $\tilde{u}$ and $\tilde{v}$ for u and v, respectively, such that the functions $g = u + i\tilde{u}$ and $h = v + i\tilde{v}$ are holomorphic on the interior of D and continuous on its boundary [7]. Then $u = \frac{1}{2}(g + \overline{g})$ and $v = \frac{1}{2}(h + \overline{h})$, so $f = \frac{1}{2}(g + \overline{g}) + \frac{i}{2}(h + \overline{h})$ expresses f as the sum of holomorphic and antiholomorphic functions $f_1 = \frac{1}{2}(g + ih)$ and $f_2 = \frac{1}{2}(\overline{g} + i\overline{h})$. □

This is almost, but not quite a direct sum: harmonic functions cannot be expressed as a sum of holomorphic and antiholomorphic functions in a unique way, since constant functions are both holomorphic and anti-holomorphic: $\mathcal{V}_h \cap \mathcal{V}_{ah} = \mathcal{V}_c$.

It can be shown that every holomorphic function is analytic in the sense of being equal to a convergent power series in any open disk contained in its domain. Typically this fact is proven using the Cauchy integral formula [7], but it can also be proven using elliptic operator theory [5]. As is always the case for analytic functions, the series representation centered at any given point is unique. From the fact that any holomorphic function can be expressed as a convergent series in powers of $z - p$ on any open disc with center p contained in its domain, it follows immediately that any anti-holomorphic function can be expressed as a convergent series in powers of $\overline{z - p}$ on any open disk with center p contained in its domain.

Since the interior of D is an open disk centered at the origin, Proposition 2.5 implies that each function in $f \in \mathcal{V}$ can be expressed as $f(z) = \sum_{n=0}^{\infty} a_n z^n + \sum_{n=1}^{\infty} b_n \overline{z}^n$ on $\text{int}(D)$. We thus have the following alternative characterization of $\mathcal{V}$:

$$\mathcal{V} = \left\{ f : D \to \mathbb{C} : f \textit{ continuous},\ f(z) = \sum_{n=0}^{\infty} a_n z^n + \sum_{n=1}^{\infty} b_n \overline{z}^n \textit{ on } \text{int}(D) \right\}.$$

When there is no danger of ambiguity, we sometimes write $f(z) = \sum_{n=0}^{\infty} a_n z^n + \sum_{n=1}^{\infty} b_n \overline{z}^n$ for functions $f \in \mathcal{V}$, keeping in mind that this series representation is only valid on the interior of D.

Define a norm on $\mathcal{V}$ by

$$\|f\| = \max\{|f(z)| : z \in D\}.$$

Like any norm, $\|.\|$ induces a topology on $\mathcal{V}$. Henceforth when we speak of subspaces of $\mathcal{V}$ being closed or open, we mean with respect to this topology.

Recall that a sequence of functions $\{f_n\}$ on a common domain X converges uniformly to a function f on a set $S \subset X$ if for each $\epsilon > 0$, there exists $N \in \mathbb{N}$ such that for all $n \geq N$, $|f_n(x) - f(x)| < \epsilon$ for all $x \in S$. This is contrasted with pointwise convergence, under which N may vary for different choices of x. If the domain X is open, one often replaces uniform convergence on X with the requirement that $\{f_n\}$ converge uniformly on any compact subset K of X, as we do in Section 4. It is easily seen that convergence with respect to the maximum norm we defined above is equivalent to uniform convergence on D. In introductory analysis texts, it is proven that the integrals of a uniformly convergent sequence of functions converge to the integral of the limit function [9].

A metric space M is said to be *complete* if every Cauchy sequence in M converges to an element of M, and a normed linear space is said to be a *Banach space* if it is complete with respect to its norm. Once the Poisson formula is established, it is easy to show that $\mathcal{V}$ is complete, and is hence a Banach space. This fact is, of course, not needed in our proof.

We are now ready to define our representation.

Definition 2.6. Define a map $\rho : SU(1,1) \to GL(\mathcal{V})$ by $\rho(\gamma)f = (f \circ \tilde{\gamma}^{-1})$, where $\tilde{\gamma}$ is the Möbius transformation induced by γ by its action on D.

Before we prove that this is indeed a representation of $SU(1,1)$, we note that for a representation over an infinite-dimensional vector space, most authors require that the representation function ρ be continuous. There are a variety of notions of continuity, discussed, for example, in [10]. It can be shown that our representation satisfies this requirement under most standard definitions.

Proposition 2.7. *ρ is a representation of $SU(1,1)$.*

Proof. In light of the discussion after Definition 2.1, we need only show that for all $f \in \mathcal{V}$, for all $\gamma \in SU(1,1)$, $\rho(\gamma)f \in \mathcal{V}$. The Möbius transformation $\tilde{\gamma}^{-1}$ associated with γ^{-1} is holomorphic on D, and the composition of holomorphic functions is holomorphic. Since the composition of continuous functions is continuous, if $f_1 \in \mathcal{V}_h$, then $\rho(\gamma)f_1 \in \mathcal{V}_h$. If $c : z \mapsto \overline{z}$ denotes the conjugate function, then $f_2 \in \mathcal{V}_{ah}$ if and only if $(c \circ f_2)$ is holomorhpic on $\text{int}(D)$, in which case $\rho(\gamma)(c \circ f_2) = (c \circ f_2 \circ \tilde{\gamma}^{-1})$ is holomorphic on $\text{int}(D)$. So, $(f_2 \circ \tilde{\gamma}^{-1})$ is anti-holomorphic on $\text{int}(D)$ and $\rho(\gamma)f_2 \in \mathcal{V}_{ah}$. A function is in $\mathcal{V}$ if and only if it is the sum of a function in $\mathcal{V}_h$ and a function in $\mathcal{V}_{ah}$. Therefore $\rho(\gamma)f \in \mathcal{V}$ for all $f \in \mathcal{V}$. □

This representation of $SU(1,1)$ induces a representation of the subgroup $SO(2)$ of $SU(1,1)$ in the obvious way: by restricting ρ to $SO(2)$.

The question of which subspaces of a vector space are preserved under the action of a group is of great importance in representation theory. We devote the remainder of this section and most of the next to exploring which subspaces of $\mathcal{V}$ are preserved under the action of $SU(1,1)$.

Definition 2.8. Let ρ be a representation of a group G over a vector space V. We say that a subspace W of V is *G-invariant* if $\rho(g)w \in W$ for all $g \in G$ and all $w \in W$. A G-invariant subspace W of V is a *subrepresentation* if W is closed, and is a *proper subrepresentation* if W is neither the zero subspace nor all of V. A subrepresentation W of V is *irreducible* if W itself has no proper subrepresentations.

Note here the requirement that a subrepresentation W be closed, in the topological sense. This is important in the context of infinite dimensional representations in that it implies that W must contain the limit of any convergent series of its elements, as well as any finite linear combination of them. For example, although the set of rational functions with no singularities on D is an $SU(1,1)$-invariant subspace of $\mathcal{V}$, it is not closed because there exist sequences of rational functions (even polynomials) which converge uniformly to elements of $\mathcal{V}$ which are not themselves rational functions, such as the exponential function e^z. So, this subspace is not a subrepresentation.

Proposition 2.9. *$\mathcal{V}_c$, $\mathcal{V}_h$, and $\mathcal{V}_{ah}$ are $SU(1,1)$ subrepresentations of $\mathcal{V}$.*

Proof. We have established that these subspaces are $SU(1,1)$-invariant in the proof of Proposition 2.7. It remains to show that they are closed. Let $\{f_n\}$ be a sequence in $\mathcal{V}_h$ which converges uniformly on D to $f \in \mathcal{V}$. For each n, express f_n as a power series on $\text{int}(D)$ as $f_n(z) = \sum_{k=0}^{\infty} a_{nk} z^k$. Write $f(z) = \sum_{k=0}^{\infty} c_k z^k + \sum_{k=1}^{\infty} d_k \overline{z}^k$ for $z \in \text{int}(D)$. To show that $f \in \mathcal{V}_h$, we must show that $d_m = 0$ for all $m = 1, 2, 3, ...$

Fix $r \in (0,1)$. Since the series for f is valid on $\text{int}(D)$ and $r < 1$, $f_r(z) = f(rz)$ is equal to a power series on all of D, including its boundary. Because power series converge uniformly on compact subsets of their domain [9], they can be integrated term by term. For each positive integer m, we thus have

$$\begin{aligned}\frac{1}{2\pi}\int_0^{2\pi} f_r(e^{i\theta})e^{im\theta}d\theta &= \frac{1}{2\pi}\sum_{k=0}^{\infty} c_k \int_0^{2\pi} e^{im\theta}(re^{i\theta})^k d\theta + \frac{1}{2\pi}\sum_{k=1}^{\infty} d_k \int_0^{2\pi} e^{im\theta}\overline{(re^{i\theta})}^k d\theta \\ &= \frac{1}{2\pi}\sum_{k=0}^{\infty} r^k c_k \int_0^{2\pi} e^{i(m+k)\theta}d\theta + \frac{1}{2\pi}\sum_{k=1}^{\infty} r^k d_k \int_0^{2\pi} e^{i(m-k)\theta}d\theta.\end{aligned}$$

We evaluate the terms of this sum individually. For each non-negative integer k,

$$\int_0^{2\pi} e^{i(m+k)\theta}d\theta = -i(m+k)^{-1}e^{i(m+k)\theta}\Big|_0^{2\pi} = 0,$$

since the period of $e^{i(m+k)\theta}$ is an integer fraction of 2π. Similarly, for each $k \neq m$, $\int_0^{2\pi} e^{i(m-k)\theta} d\theta = 0$. Therefore

$$\frac{1}{2\pi}\int_0^{2\pi} f_r(e^{i\theta})e^{im\theta}d\theta = \frac{r^m d_m}{2\pi}\int_0^{2\pi} e^{i(m-m)\theta}d\theta = r^m d_m.$$

Because $\{f_n(rz)\} \longrightarrow f(rz)$ uniformly as $n \longrightarrow \infty$ and integrals commute with uniform limits, we can integrate the series for $f_n(rz)$ on ∂D term by term to obtain

$$r^m d_m = \frac{1}{2\pi}\int_0^{2\pi} f(re^{i\theta})e^{im\theta}d\theta = \lim_{n\to\infty}\frac{1}{2\pi}\int_0^{2\pi} f_n(re^{i\theta})e^{im\theta}d\theta = 0,$$

by the same computations as above and the fact that the series for the holomorphic functions f_n contain no $\overline{z}^m$ term. Therefore $d_m = 0$ for every m, so $f \in \mathcal{V}_h$ and $\mathcal{V}_h$ is closed. By an identical argument, $\mathcal{V}_{ah}$ is closed. As a consequence, $\mathcal{V}_c = \mathcal{V}_h \cap \mathcal{V}_{ah}$, as the intersection of closed sets, is also closed. Thus, these three $SU(1,1)$-invariant subspaces are indeed subrepresentations. □

We end this section with a lemma about $\mathcal{V}$ which we shall need in Section 3.

Lemma 2.10. *Let $f \in \mathcal{V}$ be expressed as a convergent series on* $\mathrm{int}(D)$ *as $f(z) = \sum_{k=0}^{\infty} a_n z^k + \sum_{m=1}^{\infty} b_m \overline{z}^m$. Then there exists a sequence of polynomials in z^k and $\overline{z}^m$ (finite linear combinations of powers of z and $\overline{z}$) which converges uniformly to f. We may choose this sequence so that for each k with $a_k = 0$ and each m with $b_m = 0$, the coefficients on z^k and $\overline{z}^m$ for the polynomials in the sequence are zero.*

Proof. For each $r \in (0,1)$, define $f_r(z) = f(rz)$. Since f is uniformly continuous on D, f_r converges uniformly to f on D as $r \longrightarrow 1$ from the left. As in the proof of Proposition 2.9, the series representation of f is valid on the interior of D, so since each r is less than 1, f_r is equal to a series on all of D. Since power series converge uniformly on compact subsets of their domain,

$$f_r(z) = \lim_{n\to\infty}\sum_{k=0}^{n} r^k a_k z^k + \sum_{m=1}^{n} r^m b_m \overline{z}^m \equiv \lim_{n\to\infty} g_{r,n}(z),$$

and this limit is uniform on all of D. Each $g_{r,n}$ is a polynomial in z^k and $\overline{z}^m$, and for each k or m with a_k or b_m equal to zero, the coefficients on z^k and $\overline{z}^m$ in the formula for $g_{r,n}$ are zero. Moreover, for a suitable choice of $\{r_j\} \longrightarrow 1^-$ and $\{n_j\} \longrightarrow \infty$, a diagonal subsequence $\{g_{r_j,n_j}\}$ converges uniformly to f, as desired. □

In particular, this lemma, along with Proposition 2.9, implies that $\mathcal{V}_h = \overline{\mathrm{span}\{1, z, z^2, ...\}}$ and $\mathcal{V}_{ah} = \overline{\mathrm{span}\{1, \overline{z}, \overline{z}^2, ...\}}$, where the bar denotes the closure.

3 Invariant Subspaces

Our aim in this section is to show that $\mathcal{V}_h$, $\mathcal{V}_{ah}$, and $\mathcal{V}_c$ are in fact the *only* proper $SU(1,1)$ subrepresentations of $\mathcal{V}$. In particular, this will imply that the identity function and its conjugate *generate* $\mathcal{V}$ as a representation of $SU(1,1)$, in the sense that the smallest subrepresentation of $\mathcal{V}$ which contains these two functions is is all of $\mathcal{V}$. This fact will play a key role in our proof of the Poisson integral formula in Section 4. We shall first consider subspaces of $\mathcal{V}$ which are invariant under the action of the subgroup $SO(2)$ of $SU(1,1)$.

Lemma 3.1. *Let $\alpha \in \mathbb{R}$ and define an operator $A_\alpha : \mathcal{V} \to \mathcal{V}$ by*

$$A_\alpha(f)(z) = \frac{1}{\pi}\int_0^\pi e^{i\alpha\theta}\rho(k_\theta)f(z)d\theta = \frac{1}{\pi}\int_0^\pi e^{i\alpha\theta}f(e^{-2i\theta}z)d\theta,$$

where each $k_\theta \in SO(2)$. If W is a closed $SO(2)$-invariant subspace of $\mathcal{V}$ and $f \in W$, then $A_\alpha(f) \in W$.

Proof. It is clear that $A_\alpha(f)$ is continuous on D, and it follows from differentiation under the integral sign that $A_\alpha(f)$ is harmonic on $\mathrm{int}(D)$, so $A_\alpha(f)$ is an element of $\mathcal{V}$. It remains to show that $A_\alpha(f) \in W$. The integral expression for $A_\alpha(f)$ is given by a limit of Riemann sums: for each $z \in D$,

$$A_\alpha(f)(z) = \lim_{n\to\infty}\frac{1}{n}\sum_{j=1}^{n} e^{i\alpha\theta_j}f(e^{-2i\theta_j}z),$$

where for each n, $0 \le \theta_1 < ... < \theta_n \le \pi$ are test points in a partition of the interval $[0,\pi]$ which becomes arbitrarily fine as $n \longrightarrow \infty$. Since W is $SO(2)$-invariant, the function

$$f_n(z) \equiv \frac{1}{n}\sum_{j=1}^{n} e^{i\alpha\theta_j}f(e^{-2i\theta_j}z)$$

is in W for each n. By definition, $\{f_n\} \longrightarrow A_\alpha(f)$ pointwise. We claim that this convergence is uniform.

By the Arzelá-Ascoli Theorem [8], it suffices to show that $\{f_n\}$ is *equicontinuous*[3]. That is, given $\epsilon > 0$, there is a single $\delta > 0$ such that for all n, for all $z, w \in D$ with $|z - w| < \delta$, we have $|f_n(z) - f_n(w)| < \epsilon$. The function f is uniformly continuous, so we can choose $\delta > 0$ such that $|f(z) - f(w)| < \epsilon$ for all $z, w \in D$ with $|z - w| < \delta$. Since $|e^{-2i\theta_j}| = 1$ for all j, $|z - w| < \delta$ implies

[3]The Arzelá-Ascoli Theorem states that any bounded sequence of equicontinuous functions on a compact set has a uniformly convergent subsequence. It is an immediate consequence (and indeed is usually proven in the course of proving the theorem itself) that an equicontinuous sequence which converges poitwise on a compact set also converges uniformly.

that $|e^{-2i\theta_j}z - e^{-2i\theta_j}w| < \delta$. For all n we thus have

$$\begin{aligned} |f_n(z) - f_n(w)| &= \left| \frac{1}{n}\sum_{j=1}^{n} e^{i\alpha\theta_j} f(e^{-2i\theta_j}z) - \frac{1}{n}\sum_{j=1}^{n} e^{i\alpha\theta_j} f(e^{-2i\theta_j}w) \right| \\ &\leq \frac{1}{n}\sum_{j=1}^{n} |f(e^{-2i\theta_j}z) - f(e^{-2i\theta_j}w)| < \frac{n\epsilon}{n} = \epsilon. \end{aligned}$$

So, δ satisfies the ϵ requirement for equicontinuity of $\{f_n\}$. Thus, $\{f_n\} \longrightarrow A_\alpha(f)$ uniformly, so since W is closed, $A_\alpha(f) \in W$. □

Lemma 3.2. *Let W be a closed $SO(2)$-invariant subspace of $\mathcal{V}$ and let $f \in W$, $f(z) = \sum_{k=0}^{\infty} a_k z^k + \sum_{k=1}^{\infty} b_k \overline{z}^k$ on $\mathrm{int}(D)$. For each n, if $a_n \neq 0$ then $z^n \in W$, and if $b_n \neq 0$ then $\overline{z}^n \in W$.*

Proof. We consider only z^n. The case for its conjugate is identical. By the Lemma 3.1, the function $A_{2n}(f)$ is in W. We claim that this function is a constant multiple of z^n. Indeed, let $z \in \mathrm{int}(D)$. Then since power series can be integrated term by term,

$$\begin{aligned} A_{2n}(f)(z) &= \frac{1}{\pi}\sum_{k=0}^{\infty} \int_0^\pi a_k e^{2ni\theta}(e^{-2i\theta}z)^k d\theta + \frac{1}{\pi}\sum_{k=1}^{\infty} \int_0^\pi b_k e^{2ni\theta}\overline{(e^{-2i\theta}z)}^k d\theta \\ &= \frac{1}{\pi}\sum_{k=0}^{\infty} a_k \int_0^\pi e^{2(n-k)i\theta} d\theta z^k + \frac{1}{\pi}\sum_{k=1}^{\infty} b_k \int_0^\pi e^{2(n+k)i} d\theta \overline{z}^k. \end{aligned}$$

As in the proof of Proposition 2.9, for each non-negative integer $k \neq n$,

$$\int_0^\pi e^{2(n-k)i\theta} d\theta = (2(n-k)i)^{-1} e^{2(n-k)i\theta}|_0^\pi = 0,$$

and if $k > 0$, $\int_0^\pi e^{2(n+k)i\theta} d\theta = 0$. Therefore

$$A_{2n}(f)(z) = \frac{a_n}{\pi}\int_0^\pi e^{2(n-n)i\theta} d\theta z^n = a_n z^n.$$

By continuity, $A_{2n}(f)(z) = a_n z^n$ on ∂D as well. So, since $a_n \neq 0$, W contains z^n. □

We can use these two lemmas to completely characterize the closed $SO(2)$-invariant subspaces of $\mathcal{V}$.

Proposition 3.3. *Let W be a closed $SO(2)$-invariant subspace of $\mathcal{V}$. Then*

$$W = \overline{\mathrm{span}\{z^{n_1}, \overline{z}^{m_1}, z^{n_2}, \overline{z}^{m_2} ...\}},$$

where the n_j are the non-negative integers such that $z^{n_j} \in W$, the m_j are the positive integers such that $\overline{z}^{m_j} \in W$, and the bar denotes the closure.

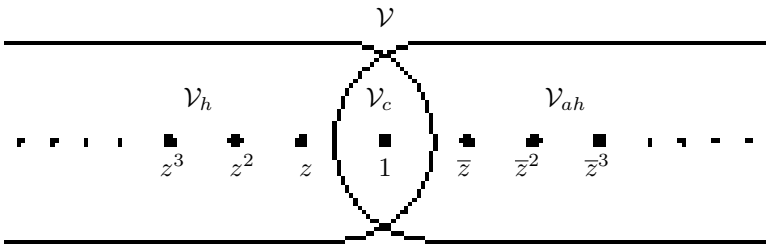

Figure 1: Subrepresentations of $\mathcal{V}$.

Proof. Let $f(z) = \sum_{n=0}^{\infty} a_n z^n + \sum_{m=1}^{\infty} b_m \overline{z}^m \in W$ be expressed as a power series valid on $\text{int}(D)$. By Lemma 3.2, for each n such that $a_n \neq 0$, $z^n \in W$ and for each m such that $b_m \neq 0$, $\overline{z}^m \in W$. By Lemma 2.10, f is equal to the uniform limit of a sequence of polynomials in only those z^n and $\overline{z}^m$ that occur with non-zero coefficients in the power series for f, i.e. only a subset of the z^{n_j} and the $\overline{z}^{m_j}$. Thus, $W = \overline{\text{span}}\{z^{n_1}, \overline{z}^{m_1}, z^{n_2}, \overline{z}^{m_2}\}$, as required. □

Before we prove the climactic theorem of this section, we take a moment to think about our representation visually, and, perhaps, to reflect on why we decided to study mathematics rather than, say, art. The subrepresentation structure of our representation is shown in Figure 1. The subspaces $\mathcal{V}_h$ and $\mathcal{V}_{ah}$ of functions which are holomorphic or anti-holomorphic on the interior of D are subrepresentations, and intersect in a third subrepresentation: the constant functions, $\mathcal{V}_c$. We are about to prove that $\mathcal{V}$ cannot be decomposed any further than shown in the diagram. Note that our claim is only the quotient spaces $\mathcal{V}_h/\mathcal{V}_c$ and $\mathcal{V}_{ah}/\mathcal{V}_c$, not $\mathcal{V}_h$ and $\mathcal{V}_{ah}$ themselves, are irreducible[4]. Indeed, this is the best that could be hoped for, given that the space of constant functions $\mathcal{V}_c$ is an $SU(1,1)$-invariant subspace of both $\mathcal{V}_h$ and $\mathcal{V}_{ah}$.

Theorem 3.4. *The only proper $SU(1,1)$ subrepresentations of $\mathcal{V}$ are $\mathcal{V}_h$, $\mathcal{V}_{ah}$, and $\mathcal{V}_c$. In particular, $\mathcal{V}_h/\mathcal{V}_c$ and $\mathcal{V}_{ah}/\mathcal{V}_c$ are irreducible.*

Proof. Let W be a proper $SU(1,1)$ subrepresentation of $\mathcal{V}$, i.e. a closed $SU(1,1)$-invariant subspace not equal to $\mathcal{V}$ or $\{0\}$. Assume that W does not consist solely of constant functions. Since W is invariant under the action of $SU(1,1)$, W is also invariant under the action of its subgroup $SO(2)$. Because W contains a non-constant function, Lemma 3.2 implies that W must contain either z^n or $\overline{z}^n$ for some $n > 0$.

Suppose first that W contains z^n. Because W is $SU(1,1)$-invariant, for each Möbius transformation $\tilde{\gamma}(z) = \frac{az+b}{\overline{b}z+\overline{a}}$ corresponding to an element of $SU(1,1)$, W contains the function $\tilde{\gamma}(z)^n$. Choose one such $\tilde{\gamma}$ with a and b non-zero. Since $\tilde{\gamma}(z)^n$ is holomorphic on D, it equals its Taylor series about the origin. The linear coefficient of this series is the derivative of $\tilde{\gamma}(z)^n$ evaluated at $z = 0$,

$$n\tilde{\gamma}(0)^{n-1}\tilde{\gamma}'(0) = n\left(\frac{b}{\overline{a}}\right)^{n-1}\left(\frac{1}{\overline{a}^2}\right) = \frac{b^{n-1}}{\overline{a}^{n+1}} \neq 0.$$

[4]Since $\mathcal{V}_c$ is $SU(1,1)$-invariant, the representation ρ gives rise to a well-defined representation of $SU(1,1)$ on the quotient space $\mathcal{V}/\mathcal{V}_c$.

Thus, by Lemma 3.2, the identity function z must be in W. Therefore, again by invariance, W contains the function $\tilde{\gamma}$ itself. Using partial fractions and the properties of geometric series, we find that for all $z \in D$,

$$\tilde{\gamma}(z) = \frac{az+b}{\overline{b}z+\overline{a}} = \frac{b}{\overline{a}} + \frac{z}{\overline{a}^2}\left(\frac{1}{1+(\overline{b}/\overline{a})z}\right) = \frac{b}{\overline{a}} + \frac{1}{\overline{a}^2}\sum_{k=1}^{\infty}(-\overline{b}/\overline{a})^{k-1}z^k.$$

In particular, for each non-negative integer k, the coefficient on z^k in this series is non-zero. Thus, again by Lemma 3.2, W contains z^k for every non-negative integer k. Since W is closed, the comment following Lemma 2.10 implies that W must contain all of $\mathcal{V}_h$. This same argument works for a subspace of $\mathcal{V}_h$ that contains a non-constant function. Hence, $\mathcal{V}_h/\mathcal{V}_c$ is irreducible.

By an identical argument, if $\overline{z}^n \in W$ for some n, then W contains $\overline{z}$, and hence $\overline{z}^k$ for all k. Therefore $\mathcal{V}_{ah} \subset W$ and $\mathcal{V}_{ah}/\mathcal{V}$ is irreducible. Likewise, if W contains both z^n and $\overline{z}^m$ for some m and n, then W contains both $\mathcal{V}_h$ and $\mathcal{V}_{ah}$, and since $\mathcal{V} = \mathcal{V}_h + \mathcal{V}_{ah}$, W is all of $\mathcal{V}$, contrary to the assumption that W is proper. We are thus left with only two possibilities: W must be either $\mathcal{V}_h$ or $\mathcal{V}_{ah}$. This completes the proof. □

Let W be a closed $SU(1,1)$-invariant subspace of $\mathcal{V}$ which contains h and $\overline{h}$. Theorem 3.4 implies that W must be all of $\mathcal{V}$. In other words,

Corollary 3.5. *The identity function $h : z \mapsto z$ and its conjugate $\overline{h} : z \mapsto \overline{z}$ generate $\mathcal{V}$ as a representation of $SU(1,1)$.*

In particular, each $f \in \mathcal{V}$ must be the uniform limit of a sequence of finite linear combinations of the images of h and $\overline{h}$ under the action of elements of $SU(1,1)$.

4 The Poisson Integral Formula

Having established the necessary representation theoretic background for our proof of the Poisson integral formula (Theorem 1.1 in the introduction), we are almost ready to prove the formula itself. We start with a definition.

Definition 4.1. Let ρ be a representation of a group G over a vector space V. An operator T on V is *G-equivariant* or *G-invariant* if $\rho(g)T(v) = T(\rho(g)v)$ for all $g \in G$ and all $v \in V$.

The proof we finish in this section is based on the following general result:

Proposition 4.2. *Let ρ be a representation of a group G over a topological vector space V. Suppose that the set $S \subset V$ generates V as a representation of V (in the terminology given at the beginning of Section 3). Then a continuous, linear G-equivariant operator T on V is completely determined by its values on S.*

Proof. Since S generates V, any $v \in V$ can be expressed as $v = \lim_{n\to\infty} v_n$, where each $v_n = \sum_{k=1}^{N_n} a_{nk}\rho(g_{nk})s_{nk}$ for scalars a_{nk} and for some $s_{nk} \in S$ and $g_{nk} \in G$. Since T is continuous and linear, it commutes with limits and sums. Thus, G-invariance gives

$$T(v) = \lim_{n\to\infty} T(v_n) = \lim_{n\to\infty} \sum_{k=1}^{N_n} a_{nk}\rho(g_{nk})T(s_{nk}).$$

In particular, $T(v)$ depends only on the values of T on the s_{nk}. □

The idea of Proposition 4.1 is similar to that of a linear transformation being completely determined by its values on a basis for a vector space, or a group homomorphism being completely determined by the images of a set of generators. In our case, we have already shown that our generating set consists of the identity function h and its conjugate $\overline{h}$ (Corollary 3.5). We must now show that the Poisson integral operator is in fact continuous and equivariant under the action of the group $SU(1,1)$, then evaluate the operator at the identity function and its conjugate. The necessary computations require no more analysis than is typically encountered in introductory courses.

Before we define the Poisson integral operator, we need to define its target space. The formula is only defined for z on the interior of the disk D, so properly speaking it does not output an element of $\mathcal{V}$, which consists of functions defined on the boundary of D as well. However, since the integrand in the formula is continuous, by the properties of the integral we do know that the output function is continuous as well. We therefore define $\mathcal{V}'$ to be the vector space of all continuous complex-valued functions defined on the interior of D, with topology such that convergence in $\mathcal{V}'$ is equivalent to uniform convergence on compact subsets of the interior of D. We note that by restricting elements of $\mathcal{V}$ to the interior of D, $\mathcal{V}$ can be viewed as a subspace of $\mathcal{V}'$. Since convergence in $\mathcal{V}$ is uniform convergence, convergence in $\mathcal{V}$ implies convergence in $\mathcal{V}'$. Consequently, this inclusion of $\mathcal{V}$ in $\mathcal{V}'$ is continuous.

Definition 4.3. Let $P : \mathcal{V} \to \mathcal{V}'$ be the Poisson integral operator,

$$P(f)(re^{i\theta}) = \frac{1}{2\pi}\int_0^{2\pi} f(e^{i\phi})\frac{1-r^2}{1+r^2-2r\cos(\theta-\phi)}d\phi$$

for $z = re^{i\theta} \in \text{int}(D)$.

The term multiplied by f in the integrand is called the *Poisson Kernel*. Routine computation shows that for $z = re^{i\theta}$, this term equals

$$\frac{1-r^2}{r^2+1-2r\cos(\theta-\phi)} = \frac{1-|z|^2}{|z-e^{i\phi}|^2} = \frac{e^{i\phi}}{e^{i\phi}-z} + \frac{e^{-i\phi}}{e^{-i\phi}-\overline{z}} - 1. \tag{4.1}$$

Proposition 4.4. *P is a continuous operator on $\mathcal{V}$.*

Proof. Let $K \subset \text{int}(D)$ be compact. Then since the Poisson kernel is continuous on the compact set $K \times [0, 2\pi]$, there exists $B > 0$ such that for all $re^{i\theta} \in K$, for all $\phi \in [0, 2\pi]$,

$$\left| \frac{1 - r^2}{1 + r^2 - 2r\cos(\theta - \phi)} \right| < B.$$

Now, suppose that $\{f_n\} \longrightarrow f$ in $\mathcal{V}$. Then $\{f_n - f\} \longrightarrow 0$ uniformly. So by the properties of integration under uniform limits,

$$\begin{aligned} |P(f_n)(re^{i\theta}) - P(f)(re^{i\theta})| &= \left| \frac{1}{2\pi} \int_0^{2\pi} (f_n(e^{i\phi}) - f(e^{i\phi})) \frac{1 - r^2}{1 + r^2 - 2r\cos(\theta - \phi)} d\phi \right| \\ &\leq \frac{B}{2\pi} \int_0^{2\pi} \left| f_n(e^{i\phi}) - f(e^{i\phi}) \right| d\phi \longrightarrow 0. \end{aligned}$$

Since the term tending to zero does not depend on $re^{i\theta} \in K$, this convergence is uniform on all compact subsets K of D. □

To show the $SU(1,1)$-equivariance of P, we shall need two simple lemmas.

Lemma 4.5. *The operator P is $SO(2)$-equivariant, i.e. if $\psi \in [0, 2\pi)$ and $k_\psi \in SO(2)$, then for all $f \in \mathcal{V}$, $\rho(k_\psi)P(f) = P(\rho(k_\psi)f)$.*

Proof. Writing $z = re^{i\theta} \in \text{int}(D)$, we have

$$\begin{aligned} \rho(k_\psi)P(f)(re^{i\theta}) &= P(f \circ \tilde{k}_{-\psi})(re^{i\theta}) \\ &= \frac{1}{2\pi} \int_0^{2\pi} f(e^{i(\phi - 2\psi)}) \frac{1 - r^2}{r^2 + 1 - 2r\cos(\theta - \phi)} d\phi. \end{aligned}$$

Substituting $\sigma = \phi - 2\psi$ and $d\sigma = d\phi$ gives

$$\begin{aligned} \frac{1}{2\pi} \int_0^{2\pi} f(e^{i(\sigma)}) \frac{1 - r^2}{r^2 + 1 - 2r\cos(\theta - 2\psi - \sigma)} d\sigma &= P(f)(re^{i(\theta - 2\psi)}) \\ &= P(\rho(k_\psi)f)(re^{i\theta}). \end{aligned}$$

□

Lemma 4.6. *Each $\gamma \in SU(1,1)$ can be decomposed as $\gamma = k_s \gamma_r k_t$, where*

$$k_s = \begin{pmatrix} e^{is} & 0 \\ 0 & e^{-is} \end{pmatrix}, \quad \gamma_r = \begin{pmatrix} \cosh(r) & \sinh(r) \\ \sinh(r) & \cosh(r) \end{pmatrix}, \quad \textit{and} \quad k_t = \begin{pmatrix} e^{it} & 0 \\ 0 & e^{-it} \end{pmatrix}$$

for $s, r, t \in \mathbb{R}$.

Proof. For $a, b \in \mathbb{R}$, we may write

$$\gamma = \begin{pmatrix} ae^{i\psi} & be^{i\theta} \\ be^{-i\theta} & ae^{-i\psi} \end{pmatrix} = \begin{pmatrix} e^{is} & 0 \\ 0 & e^{-is} \end{pmatrix} \begin{pmatrix} a & b \\ b & a \end{pmatrix} \begin{pmatrix} e^{it} & 0 \\ 0 & e^{-it} \end{pmatrix},$$

where $s = \frac{\psi + \theta}{2}$ and $t = \frac{\psi - \theta}{2}$. Since $\det(\gamma) = a^2 - b^2 = 1$, $a = \cosh(r)$ and $b = \sinh(r)$ for some $r \in \mathbb{R}$. □

Proposition 4.7. *The operator P is $SU(1,1)$-equivariant, i.e. if $\gamma \in SU(1,1)$, then for all $f \in \mathcal{V}$, $P(\rho(\gamma)f) = \rho(\gamma)P(f)$.*

Proof. It suffices to check this fact only for the generators of $SU(1,1)$. The matrices shown to generate $SU(1,1)$ in Lemma 4.6 correspond to Möbius transformations of the forms

$$\tilde{k}_t(z) = e^{2it}z \qquad \text{and} \qquad \tilde{\gamma}_r(z) = \frac{\cosh(r)z + \sinh(r)}{\sinh(r)z + \cosh(r)}.$$

The verification that $P(\rho(k_t)f) = \rho(k_t)P(f)$ for $k_t \in SO(2)$ was completed in Lemma 4.5. Therefore we can restrict our attention to Möbius transformations of the latter form. Moreover, by rotating the unit disk so that the point in question lies on the real axis, we may assume that $z \in \text{int}(D) \cap \mathbb{R}$. Applying equation (1), for all $f \in \mathcal{V}$, we have

$$\begin{aligned}
\rho(\gamma_r^{-1})(P(\rho(\gamma_r)f)(z) &= P(f \circ \tilde{\gamma}_r^{-1})(\tilde{\gamma}_r(z)) \\
&= \frac{1}{2\pi}\int_0^{2\pi} f(\tilde{\gamma}_r^{-1}(e^{i\phi}))\frac{1-|\tilde{\gamma}_r(z)|^2}{|\tilde{\gamma}_r(z)-e^{i\phi}|^2}d\phi \\
&= \frac{1}{2\pi}\int_0^{2\pi} f(\tilde{\gamma}_r^{-1}(e^{i\phi}))\frac{1-\tilde{\gamma}_r(z)^2}{|\tilde{\gamma}_r(z)-e^{i\phi}|^2}d\phi,
\end{aligned}$$

where the last equality follows from the fact that z is real. We must show that this quantity equals $P(f)(z)$. Let $e^{i\sigma} = \tilde{\gamma}_r^{-1}(e^{i\phi}) = \frac{\cosh(r)e^{i\phi}-\sinh(r)}{-\sinh(r)e^{i\phi}+\cosh(r)}$. Then $e^{i\phi} = \tilde{\gamma}_r(e^{i\sigma})$. Differentiating gives

$$ie^{i\sigma}d\sigma = \frac{ie^{i\phi}d\phi}{(-\sinh(r)e^{i\phi}+\cosh(r))^2} = \frac{i\tilde{\gamma}_r(e^{i\sigma})d\phi}{(-\sinh(r)\tilde{\gamma}_r(e^{i\sigma})+\cosh(r))^2}.$$

Plugging in the expression for γ_r, solving for $d\phi$ and simplifying yields

$$\begin{aligned}
d\phi &= e^{i\sigma}\left(\frac{\cosh(r)e^{i\sigma}+\sinh(r)}{\sinh(r)e^{i\sigma}+\cosh(r)}\right)^{-1} \\
&\quad\times\left(-\sinh(r)\left(\frac{\cosh(r)e^{i\sigma}+\sinh(r)}{\sinh(r)e^{i\sigma}+\cosh(r)}\right)+\cosh(r)\right)^2 d\sigma \\
&= \left(\sinh(r)^2+\cosh(r)^2+\sinh(r)\cosh(r)(e^{i\sigma}+e^{-i\sigma})\right)^{-1}d\sigma.
\end{aligned}$$

Substitute $e^{i\sigma} = \tilde{\gamma}_r^{-1}(e^{i\phi})$ and $d\phi = ((\sinh(r)^2+\cosh(r)^2+\sinh(r)\cosh(r)(e^{i\sigma}+e^{-i\sigma}))^{-1}d\sigma$. Since $\gamma_r(1) = 1$, the limits of integration remain unchanged and we obtain

$$\begin{aligned}
\frac{1}{2\pi}\int_0^{2\pi} f(e^{i\sigma})&\left(\frac{1-\tilde{\gamma}_r(z)^2}{|\tilde{\gamma}_r(z)-\tilde{\gamma}_r(e^{i\sigma})|^2}\right) \\
&\times\left(\sinh(r)^2+\cosh(r)^2+\sinh(r)\cosh(r)(e^{i\sigma}+e^{-i\sigma})\right)^{-1}d\sigma.
\end{aligned} \tag{4.2}$$

For the numerator of the middle term, we have

$$\begin{aligned} 1-\tilde{\gamma}_r(z)^2 &= 1-\left(\frac{\cosh(r)z+\sinh(r)}{\sinh(r)z+\cosh(r)}\right)^2 \\ &= \frac{(\sinh(r)z+\cosh(r))^2-(\cosh(r)z+\sinh(r))^2}{(\sinh(r)z+\cosh(r))^2} \\ &= \frac{1-z^2}{(\sinh(r)z+\cosh(r))^2}. \end{aligned}$$

The denominator equals

$$\begin{aligned} |\tilde{\gamma}_r(z)-\tilde{\gamma}_r(e^{i\sigma})|^2 &= \left|\left(\frac{\cosh(r)z+\sinh(r)}{\sinh(r)z+\cosh(r)}\right)-\left(\frac{\cosh(r)e^{i\sigma}+\sinh(r)}{\sinh(r)e^{i\sigma}+\cosh(r)}\right)\right|^2 \\ &= \left|\frac{(\cosh(r)z+\sinh(r))(\sinh(r)e^{i\sigma}+\cosh(r))-(\cosh(r)e^{i\sigma}+\sinh(r))(\sinh(r)z+\cosh(r))}{(\sinh(r)z+\cosh(r))(\sinh(r)e^{i\sigma}+\cosh(r))}\right|^2 \\ &= \frac{|z-e^{i\sigma}|^2}{(\sinh(r)z+\cosh(r))^2\,(\sinh(r)^2+\cosh(r)^2+\sinh(r)\cosh(r)(e^{i\sigma}+e^{-i\sigma}))}, \end{aligned}$$

where we can drop the absolute value on the denominator since z is real. Substituting into equation (2) and cancelling terms gives

$$(\tilde{\gamma}_r \circ P(f) \circ \tilde{\gamma}_r^{-1})(z) = \frac{1}{2\pi}\int_0^{2\pi} f(e^{i\sigma})\frac{1-z^2}{|z-e^{i\sigma}|^2}d\sigma = P(f)(z),$$

as required. We thus see that P is an $SU(1,1)$-equivariant operator. □

Proposition 4.8. *Let $h(z)=z$ be the identity function on D and let $\overline{h}(z)=\overline{z}$ be its conjugate. Then $P(h)=h$ and $P(\overline{h})=\overline{h}$.*

Proof. By Lemma 4.5, P is invariant under rotations of D, so once again it suffices to consider only the case where z is positive and real. Equation (1) and partial fraction decomposition give

$$\begin{aligned} P(h)(z) &= \frac{1}{2\pi}\int_0^{2\pi} e^{i\phi}\left(\frac{e^{i\phi}}{e^{i\phi}-z}+\frac{e^{-i\phi}}{e^{-i\phi}-\overline{z}}-1\right)d\phi \\ &= \frac{1}{2\pi}\int_0^{2\pi} \frac{e^{2i\phi}}{e^{i\phi}-z}+\frac{1}{e^{-i\phi}-z}-e^{i\phi}d\phi \\ &= \frac{1}{2\pi}\int_0^{2\pi} z+\frac{z^2}{e^{i\phi}-z}+\frac{1}{e^{-i\phi}-z}d\phi \\ &= z+\frac{1}{2\pi}\int_0^{2\pi} \frac{z^2}{e^{i\phi}-z}+\frac{1}{e^{-i\phi}-z}d\phi. \end{aligned}$$

To show that the remaining term of this integral equals 0, substitute $u=e^{i\phi}$ and $du=ie^{i\phi}d\phi=iud\phi$. Letting a circled integral sign indicate integration

once counter-clockwise around the unit circle, this gives

$$\begin{aligned}\frac{1}{2\pi}\int_0^{2\pi}\frac{z^2}{e^{i\phi}-z}+\frac{1}{e^{-i\phi}-z}d\phi &= \frac{1}{2\pi i}\oint\frac{z^2}{u(u-z)}+\frac{1}{1-zu}du\\ &= \frac{1}{2\pi i}\oint\frac{(1/z)}{u-z}-\frac{(1/z)}{u}+\frac{1}{1-zu}du\\ &= \frac{1}{2\pi zi}\left(\log(e^{i\phi}-z)-\log(e^{i\phi})-\log(1-ze^{i\phi})\right)\Big|_0^{2\pi}\\ &= 0,\end{aligned}$$

since $e^{0i}=e^{2\pi i}$. Thus, the entire integral equals z, as desired.

For $\overline{h}$, equation (1) again gives

$$P(\overline{h})(z)=\frac{1}{2\pi}\int_0^{2\pi}e^{-i\phi}\left(\frac{e^{i\phi}}{e^{i\phi}-z}+\frac{e^{-i\phi}}{e^{-i\phi}-z}-1\right)d\phi.$$

Substitute $\sigma=-\phi$ and $d\sigma=-d\phi$ and use the periodicity of $e^{i\phi}$ to obtain

$$P(\overline{h})(z)=-\frac{1}{2\pi}\int_{-2\pi}^{0}e^{i\sigma}\left(\frac{e^{-i\sigma}}{e^{-i\sigma}-z}+\frac{e^{i\sigma}}{e^{i\sigma}-z}-1\right)d\phi=P(h)(z)=z=\overline{z},$$

since z is assumed real. □

We are now ready to prove the Poisson integral formula.

Proof of Theorem 1.1. We must show that for any function $f\in\mathcal{V}$, $P(f)=f$ on $\mathrm{int}(D)$. But, for h the identity function and $\bar{h}$ its conjugate, $P(h)=h$ and $P(\overline{h})=\overline{h}$. Since h and $\overline{h}$ generate $\mathcal{V}$ as a representation of $SU(1,1)$ and P is continuous, linear, and $SU(1,1)$-equivariant, Proposition 4.1 implies that $P(f)$ does indeed equal f for all $f\in\mathcal{V}$. □

The astute reader will have noticed that we did not invoke the full force of Theorem 3.4 in our proof. We used only the implication that h and $\overline{h}$ generate all of $\mathcal{V}$, rather than the stronger assertion, which we proved, that $\mathcal{V}_c$, $\mathcal{V}_h$ and $\mathcal{V}_{ah}$ are the only proper subrepresentations of $\mathcal{V}$. The stronger result was proven to shed more light on the structure of our representations.

5 An SU(1,1)-Invariant Inner Product

Although it is not a necessary part of our proof of the Poisson integral formula, for the sake of completeness of our description of our representations of $SU(1,1)$, we end this paper by constructing an inner product which is invariant under the action of $SU(1,1)$: that is, one satisfying $\langle\rho(\gamma)f,\rho(\gamma)g\rangle=\langle f,g\rangle$ for all $\gamma\in SU(1,1)$. However, $\mathcal{V}$ itself cannot possess an $SU(1,1)$-invariant inner product, for if it did, the orthogonal complement of a subrepresentation would also be a subrepresentation. But, as we proved in Section 3, the only subrepresentations of

$\mathcal{V}$ are $\mathcal{V}_h$, $\mathcal{V}_{ah}$ and their intersection $\mathcal{V}_c$. In particular, every subrepresentation intersects the proper subrepresentation $\mathcal{V}_h$ non-trivially, so $\mathcal{V}_h$ cannot have a closed $SU(1,1)$-invariant orthogonal complement. Consequently, we must define a slightly modified version of our vector space for use in this section.

Definition 5.1. We denote by $\tilde{\mathcal{V}}$ the vector space of complex-valued functions f which are harmonic on some neighborhood U_f of the closed unit disk $D \subset \mathbb{C}$ modulo the equivalence relation of differing by a constant:

$$\tilde{\mathcal{V}} = \left\{ f : U_f \to \mathbb{C} : D \subset U_f,\ \frac{\partial^2 f}{\partial x^2}(z) + \frac{\partial^2 f}{\partial y^2}(z) = 0 \ \forall z \in U_f \right\} /\{\text{constant functions}\}.$$

For each $\gamma \in SU(1,1)$, $\rho(\gamma)$ preserves the subspace of constant functions in $\mathcal{V}$, and the set of functions which are harmonic on a neighborhood of D is a subset of $\mathcal{V}$. Therefore our representation restricts to a well defined representation of $SU(1,1)$ on $\tilde{\mathcal{V}}$.

Define the degree operator from $\tilde{\mathcal{V}}$ to $\tilde{\mathcal{V}}$ by

$$\deg(f)(x+iy) = \left(x\frac{\partial f}{\partial x}(x+iy) + y\frac{\partial f}{\partial y}(x+iy) \right).$$

Since the partial derivatives of a constant are zero, deg is well-defined on $\tilde{\mathcal{V}}$. Moreover, if p_n is the equivalence class of $z \mapsto z^n$ in $\tilde{\mathcal{V}}$, for each $n = 1, 2, 3, ...$ we have

$$\deg(p_n)(x+iy) = nx(x+iy)^{n-1} + niy(x+iy)^{n-1} = n(x+iy)^n = np_n$$

and, similarly,

$$\deg(\overline{p}_n)(x+iy) = n\overline{p}_n.$$

Proposition 5.2. *Define an operator $\langle ., . \rangle$ on $\tilde{\mathcal{V}} \times \tilde{\mathcal{V}}$ by*

$$\langle f, g \rangle = \frac{1}{2\pi} \int_0^{2\pi} \deg(f)(e^{i\phi})\overline{g(e^{i\phi})} d\phi.$$

Then $\langle ., . \rangle$ is a hermitian inner product on $\tilde{\mathcal{V}}$, and $\{p_1, \overline{p}_1, p_2, \overline{p}_2, ...\}$ is orthogonal with respect to $\langle ., . \rangle$.

Proof. Linearity in the first argument and anti-linearity in the second are obvious. To show that $\langle ., . \rangle$ is an inner product, we must show that it is well defined on $\tilde{\mathcal{V}}$ (i.e. adding a constant to one or the other input function doesn't change the operator's value), and we must check positive definiteness and symmetry. Since any element of $\tilde{\mathcal{V}}$ can be written as a power series in z^n and $\overline{z}^n$, $n = 1, 2, ...$, valid on all of D, it suffices to verify these properties only for elements of $\{p_1, \overline{p}_1, p_2, \overline{p}_2, ...\}$. The relevant properties can then be generalized to arbitrary elements of $\tilde{\mathcal{V}}$ using the fact that power series can be integrated term by term.

From the computations given after the definition of the degree operator, we obtain that if $f(z) = c$ is constant, then for any positive integer n,

$$\langle p_n, f\rangle = \frac{1}{2\pi}\int_0^{2\pi} ne^{ni\phi}\overline{c}d\phi = -i\overline{c}e^{ni\phi}\ |_0^{2\pi} = 0,$$

since the period of $e^{i\phi}$ is an integer fraction of 2π. Similarly, $\langle \overline{p}_n, f\rangle = 0$. Since $\deg(f) = 0$, $\langle f, g\rangle = 0$ for any $g \in \tilde{\mathcal{V}}$. Therefore $\langle ., .\rangle$ is well defined on $\tilde{\mathcal{V}}$: it does not matter which representatives of the equivalence classes of functions which differ by a constant we choose in computing the inner product.

Moreover, for any positive integers n and m,

$$\langle p_n, p_m\rangle = \frac{1}{2\pi}\int_0^{2\pi} ne^{ni\phi}e^{-mi\phi}d\phi = \frac{n}{2\pi}\int_0^{2\pi} e^{i(n-m)\phi}d\phi = \begin{cases} n & \text{if } m = n; \\ 0 & \text{if } m \neq n. \end{cases}$$

Similar computations show that $\langle \overline{p}_n, \overline{p}_m\rangle = n\delta_{n,m}$ and $\langle p_n, \overline{p}_m\rangle = \langle \overline{p}_n, p_m\rangle = 0$. This implies that $\{p_1, \overline{p}_1, p_2, \overline{p}_2, ...\}$ is orthogonal with respect to $\langle ., .\rangle$, and that $\langle ., .\rangle$ is both symmetric and positive definite on powers of z and $\overline{z}$.

Thus, if $f = \sum_{n=1}^{\infty} a_n p_n + \sum_{n=1}^{\infty} b_n \overline{p}_n$ and $g(z) = \sum_{n=1}^{\infty} c_n p_n + \sum_{n=1}^{\infty} d_n \overline{p}_n$ are elements of $\tilde{\mathcal{V}}$,

$$\begin{aligned}
\langle f, g\rangle &= \langle \sum_{n=1}^{\infty} a_n p_n, \sum_{n=1}^{\infty} c_n p_n\rangle + \langle \sum_{n=1}^{\infty} a_n p_n, \sum_{n=1}^{\infty} d_n \overline{p}_n\rangle \\
&\quad + \langle \sum_{n=1}^{\infty} b_n \overline{p}_n, \sum_{n=1}^{\infty} c_n p_n\rangle + \langle \sum_{n=1}^{\infty} b_n \overline{p}_n, \sum_{n=1}^{\infty} d_n \overline{p}_n\rangle \\
&= \sum_{n=1}^{\infty} a_n \overline{c}_n \langle p_n, p_n\rangle + \sum_{n=1}^{\infty} b_n \overline{d}_n \langle p_n, p_n\rangle \\
&= \sum_{n=1}^{\infty} n a_n \overline{c}_n + \sum_{n=1}^{\infty} n b_n \overline{d}_n = \overline{\langle g, f\rangle}
\end{aligned}$$

and

$$\langle f, f\rangle = \sum_{n=1}^{\infty} n|a_n|^2 + \sum_{n=1}^{\infty} n|b_n|^2 \geq 0,$$

so $\langle ., .\rangle$ is an inner product. The fact that $\{p_1, \overline{p}_1, p_2, \overline{p}_2, ...\}$ is orthogonal was established above. □

Unlike $\mathcal{V}$ under the maximum norm, $\tilde{\mathcal{V}}$ is not complete with respect to the norm induced by this inner product. However, $\tilde{\mathcal{V}}$ can be completed to a *Hilbert space,* or a complete inner product space with Hilbert basis $\{p_1, \overline{p}_1, p_2, \overline{p}_2, ...\}$.

Proposition 5.3. *The inner product $\langle ., .\rangle$ is $SU(1,1)$-invariant, i.e. for all $f, g \in \tilde{\mathcal{V}}$, for all $\gamma \in SU(1,1)$, $\langle f, g\rangle = \langle \rho(\gamma)f, \rho(\gamma)g\rangle$.*

Proof. Let $\tilde{\gamma} = \frac{az+b}{\overline{b}z+\overline{a}}$ be the Möbius transformation associated with $\gamma \in SU(1,1)$. We must show that $\langle f \circ \tilde{\gamma}, g \circ \tilde{\gamma} \rangle = \langle f, g \rangle$ for all $f, g \in \tilde{\mathcal{V}}$. By linearity and term-by-term integration of power series, it suffices to show this only for the cases where $f(z) = z^n$ and $f(z) = \overline{z}^n$, $n \in \mathbb{N}$. Define $f(z) = z^n$. We first compute $\deg(f \circ \tilde{\gamma})$. Writing $z = x + iy$,

$$\frac{\partial}{\partial x}\left(\frac{a(x+iy)+b}{\overline{b}(x+iy)+\overline{a}}\right)^n = n\left(\frac{a(x+iy)+b}{\overline{b}(x+iy)+\overline{a}}\right)^{n-1}\left(\frac{1}{(\overline{b}(x+iy)+\overline{a})^2}\right)$$

and

$$\frac{\partial}{\partial y}\left(\frac{a(x+iy)+b}{\overline{b}(x+iy)+\overline{a}}\right)^n = n\left(\frac{a(x+iy)+b}{\overline{b}(x+iy)+\overline{a}}\right)^{n-1}\left(\frac{i}{(\overline{b}(x+iy)+\overline{a})^2}\right).$$

Thus,

$$\begin{aligned}\deg(f \circ \tilde{\gamma})(z) &= n\left(\frac{a(x+iy)+b}{\overline{b}(x+iy)+\overline{a}}\right)^{n-1}\left(\frac{x}{(\overline{b}(x+iy)+\overline{a})^2} + \frac{iy}{(\overline{b}(x+iy)+\overline{a})^2}\right) \\ &= \frac{n\tilde{\gamma}(z)^{n-1}z}{(\overline{b}z+\overline{a})^2}.\end{aligned}$$

For all $g \in \tilde{\mathcal{V}}$, we therefore have

$$\langle f \circ \tilde{\gamma}, g \circ \tilde{\gamma} \rangle = \frac{1}{2\pi}\int_0^{2\pi} n\tilde{\gamma}(e^{i\phi})^{n-1}\left(\frac{e^{i\phi}}{(\overline{b}e^{i\phi}+\overline{a})^2}\right)\overline{g(\tilde{\gamma}(e^{i\phi}))}d\phi.$$

Let $e^{i\sigma} = \tilde{\gamma}(e^{i\phi})$. Then $e^{i\sigma}d\sigma = \left(\frac{e^{i\phi}}{(\overline{b}e^{i\phi}+\overline{a})^2}\right)d\phi$, so substitution gives

$$\langle f \circ \tilde{\gamma}, g \circ \tilde{\gamma} \rangle = \frac{1}{2\pi}\int_{\psi}^{2\pi+\psi} n(e^{i\sigma})^n\overline{g(e^{i\sigma})}d\sigma = \frac{1}{2\pi}\int_0^{2\pi} \deg(f)(e^{i\sigma})\overline{g(e^{i\sigma})}d\sigma = \langle f, g \rangle,$$

where $e^{i\psi} = \tilde{\gamma}(1)$ and the equivalence of the different limits of integration follows because both correspond to integrating exactly once around the unit circle in the same direction. A similar computation shows that $\langle f \circ \tilde{\gamma}, g \circ \tilde{\gamma} \rangle = \langle f, g \rangle$ for $f(z) = \overline{z}^n$, and we thus conclude that $\langle f \circ \tilde{\gamma}, g \circ \tilde{\gamma} \rangle = \langle f, g \rangle$ for all $f, g \in \tilde{\mathcal{V}}$. $\square$

6 Acknowledgements

I would like to thank Professor Matvei Libine for his support and mentorship during my work on this paper. I would also like to thank Professors Kevin Pilgrim and Bruce Solomon, and the National Science Foundation for providing the organization and funding for the REU program at Indiana University that made this project possible. This REU program was supported by the NSF grant DMS-0851852.

References

[1] C. Chevalley. *Theory of Lie Groups.* Princeton University Press, 1999.

[2] L. C. Evans. *Partial Differential Equations.* American Mathematical Society, 1998.

[3] I. Frenkel, M. Libine. *Quaternionic analysis, representation theory and physics*. Advances in Math 218 (2008), 1806-1877.

[4] I. Frenkel and M. Libine. *Split Quaternionic Analysis and Separation of the Series for* $SL(2,\mathbb{R})$ *and* $SL(2,\mathbb{C})/SL(2,\mathbb{R})$. To appear in Adv. Math., 2011.

[5] L. Hörmander. *The Analysis of Linear Partial Differential Operators I: Distribution Theory and Fourier Analysis*. Springer, 2nd edition, 2004.

[6] T. Kobayashi and B. Ørsted. *Analysis on the Minimal Representation of* $O(p,q)$*, I.* Adv. Math. 180 (2002), no. 2, 486-512.

[7] S. Lang. *Complex Analysis.* Springer. 4th edition, 1998.

[8] H.L. Royden and P.M. Fitzpatrick. *Real Analysis*. Prentice Hall, 4th edition, 2010.

[9] W. Rudin. *Principles of Mathematical Analysis.* McGraw-Hill Science/Engineering/Math, 3rd edition, 1976.

[10] W.Schmid and M.Libine. *Geometric methods in representation theory (lecture notes from a minicourse at the PQR2003 Euro school in Brussels).* Proceedings of the International Euroschool and Euroconference PQR2003, also math.RT/0402306.

[11] E. M. Stein and G. Weiss. *Introduction to Fourier analysis on Euclidean spaces*. Princeton Mathematical Series, Vol. 32, Princeton University Press, Princeton, NJ, 1971.

Properties and Applications of the Ising Model

Rebecca McCarthy

Abstract

The Ising Model arises in the study of classical statistical mechanics. Using this model, we can determine the macroscopic properties based on its microscopic constituents. Through the use of Linear Algebra techniques, the problem can be simplified for further analysis and application to particle behavior in quantum mechanics. Using these techniques we can look at the behavior of the system as the temperature goes to zero, infinity, and a critical point in between. Additionally, we look at the quantum particle interpretation at each of these temperatures and a possible mapping among the three.

1 Background

The physicist Wilhelm Lenz developed the Ising model as a problem for his student Ernest Ising. This model uses a configuration of particles with either a positive or negative spin to describe a ferromagnetic system as a whole. Only interactions between neighboring particles and the external magnetic field on individual particles are considered. We assume periodic boundary conditions, so that in a system of N particles, the $N+1$ term is equivalent to the first term, creating translational invariance within the model. The energy of each configuration can be calculated as follows.

$$E(\sigma) = -J \sum_{i=1}^{N} \sigma_i \, \sigma_{i+1} - H \sum_{i=1}^{N} \sigma_i \tag{1.1}$$

We can use this information to calculate the probability that the system is in a particular state.

$$P(\sigma) = \frac{e^{-(\frac{E(\sigma)}{T\,k})}}{Z_N} \tag{1.2}$$

In these equation, T is the temperature of the system, k is Boltzmann's constant, J is the strength of the interaction between particles, and H is the strength of the external magnetic field. The normalizing factor in the equation for the Boltzman distribution (1), called the partition function and labeled as Z_N, is the central equation within the Ising model. Z_N is the sum of all the Boltzman factors, the numerator in (1), of all possible spin configurations. This partition function is of interest because from it we can derive many different properties of the system, such as free energy [1].

2 The One-Dimensional Model

The one-dimensional Ising model consist of a string of N particles. The image below shows a representation in terms of positive and negative spins for a chain of length four.

$$++-+$$

There are two possible states for each particle, positive or negative, and there are N particles. The result is 2^N possible spin configurations for a given system.

$$Z_N = \sum_{\sigma} e^{K \sum_{i=1}^{N} \sigma_i \sigma_{i+1} + h \sum_{i=1}^{N} \sigma_i} \tag{2.1}$$

In equation (2) $K = \frac{J}{kT}$ and $h = \frac{H}{kT}$, with J as the strength of the magnetic interaction between neighboring particles and H the strength of the external magnetic field. This model has been solved using transfer matrices. Define $V(\sigma_j, \sigma_{j+1})$ to be the following.

$$V(\sigma_j, \sigma_{j+1}) = e^{K \sigma_j \sigma_{j+1} + \frac{1}{2}(\sigma j + \sigma_{j+1})} \tag{2.2}$$

Using the fact that and exponent raised to a sum is equivalent to a product of exponents, we can rewrite (2).

$$Z_N = \sum_{\sigma} \prod_{j=1}^{N} V(\sigma_j, \sigma_{j+1}) \tag{2.3}$$

Since there are only two possible values for each σ_j, there are only four possible values for (3). We can place all of these values within a matrix, called the transfer matrix. The resulting matrix is shown in (5).

$$\begin{pmatrix} V(+,+) & V(+,-) \\ V(-,+) & V(-,-) \end{pmatrix} = \begin{pmatrix} e^{K+h} & e^{-K} \\ e^{-K} & e^{K-h} \end{pmatrix} \tag{2.4}$$

N multiplications of this matrix give all possible values for string of length $N+1$. The top left value of the resulting matrix is the partition function over all strings starting with σ_j and ending with σ_{j+1}. Due to the assumption the $N+1$ term is the first term, only strings starting and ending with the same value are valid. Thus, only the diagonal values are valid strings of length N, making the diagonal of the resulting matrix the quantity we are interested in. Additionally the transfer matrix can be diagonalized, allowing for further simplification of the equation.

$$Z_N = \text{Trace} \begin{pmatrix} e^{K+h} & e^{-K} \\ e^{-K} & e^{K-h} \end{pmatrix} \tag{2.5}$$

$$= \text{Trace} \left(\left(P \begin{pmatrix} \lambda_1 & 0 \\ 0 & \lambda_2 \end{pmatrix} P^{-1} \right)^N \right) \tag{2.6}$$

A final simplification can be made using the fact that for matrices A and B, the Trace(AB)=Trace(BA).

$$Z_N = \text{Trace}\left(\begin{pmatrix}\lambda_1 & 0\\ 0 & \lambda_2\end{pmatrix}^N\right) = \lambda_1^N + \lambda_2^N \tag{2.7}$$

This new form of Z_N is much more readily analyzed and lends itself to calculating the physical qualities of the system [1].

3 The Two-Dimensional Model

The two dimensional model consists of a square lattice of particles. We will only consider the case where there is no external magnetic field present, so temperature is the only variable changing within a given system. Below is an example of a possible configuration of a system of size three.

$$\begin{array}{c} + + - \\ - - - \\ + - - \end{array}$$

In the two-Dimensional model, equation (10) is the partition function, where K is the strength of the horizontal particle interaction and J is the strength of the vertical interactions. Both K and J are dependent upon temperature.

$$Z_N = \sum_{\sigma} e^{K \sum_{(i,j)} \sigma_i \sigma_j + L \sum_{(i,k)} \sigma_i \sigma_k} \tag{3.1}$$

As in the one-dimensional case, a transfer matrix can be made to create all possible states. Unlike the one dimensional case, successive multiplication of this matrix adds rows of particles rather than individual particles. There 2^N possible chains of length N, so the transfer matrix is now 2^N by 2^N with chains of particles denoted by ϕ. This formula can then be rearranged as a product of exponential terms [1].

$$\begin{aligned} V(\phi, \phi^{'}) &= e^{\sum_{j=1}^{N} K \sigma_{j+1} \sigma_j^{'} + L \sigma_j \sigma_j^{'}} \\ &= \prod_{j=1}^{N} e^{K \sigma_{j+1} \sigma_j^{'}} e^{L \sigma_j \sigma_j^{'}} \end{aligned} \tag{3.2}$$

Look at each exponential term separately. Because each σ can only take on values of positive or negative one, each individual exponential term can only take on two values, differing only by a sign. Using the delta function, as defined below, we can rewrite both $e^{K \sigma_{j+1} \sigma_j^{'}}$ and $e^{L \sigma_j \sigma_j^{'}}$.

$$\delta(a,b) = \begin{cases} 1 & \text{if } a = b \\ 0 & \text{if } a \neq b \end{cases} \tag{3.3}$$

$$
\begin{aligned}
e^{L\,\sigma_j\,\sigma_j^{'}} &= e^{L}\,\delta(\sigma_j\,,\sigma_j^{'}) + e^{-L}\,(1-\delta(\sigma_j\,,\sigma_j^{'})) \\
&= e^{L}\,[(1-e^{-2L})\delta(\sigma_j\,,\sigma_j^{'}) + e^{-2L}] \qquad (3.4)
\end{aligned}
$$

This allows us to factor out e^{L} as part of a normalizing factor that will not affect the structure of our matrix. A similar process can be done with the other exponential term yielding the following result.

$$
e^{K\,\sigma_{j+1}\,\sigma_j^{'}} = e^{K}\,[\delta(\sigma_{j+1}\,,\sigma_j^{'})\,(1-e^{-2\,K}) + e^{-2\,K}] \qquad (3.5)
$$

We can then rewrite the equation for both exponentials and the transfer matrix with the normalizing factors.

$$
f_{L,j} = (1-e^{-2L})\delta(\sigma_j\,,\sigma_j^{'}) + e^{-2L}
$$

$$
f_{K,j} = \delta(\sigma_{j+1}\,,\sigma_j^{'})\,(1-e^{-2\,K}) + e^{-2\,K}
$$

$$
\begin{aligned}
P(\phi,\phi^{'}) &= \prod_{j=1}^{N}[\delta(\sigma_{j+1}\,,\sigma_j^{'})\,(1-e^{-2\,K}) + e^{-2\,K}]\,[\delta(\sigma_j\,,\sigma_j^{'}) + e^{-2L}\,(1-\delta(\sigma_j\,,\sigma_j^{'}))] \\
&= \prod_{j=1}^{N} f_{K,j}\,f_{L,j} \qquad (3.6)
\end{aligned}
$$

Using Baxter's reparameterization of K and L we can then rewrite the equation for the transfer matrix in terms of u and k where $k = \sinh 2K \sinh 2L$. This function is analytic and can thus be written as a Taylor expansion as a function of u. For any fixed k, the terms of the Taylor expansion commute with one another. If two matrices commute, then they can be simultaneously diagonalized, which means that they can be diagonalized using the same set of eigenvectors. If all the eigenvalues of both matrices are distinct, then the eigenvectors are automatically identical. Using this fact, we can then restrict our attention to only one term within this expansion and derive information about the eigenvalues and eigenvectors of the system from this simplified model. The first term in the expansion is too simple to glean any useful information, so we turn our attention to the second term, which is complicated enough to be useful without being too difficult to analyze. After several manipulations we will call this matrix H. We will write out reparameterization of K and L in terms of u at the critical temperature, which can be done in terms of trigonometric functions and then written as a Taylor series. At other temperatures elliptic functions are necessary for this transformation, but the process of parameterizing and manipulating the system works in an analogous way.

$$
\begin{aligned}
e^{-2K} &= \frac{1-\sin u}{\cos u} \\
&= 1 - u + \frac{1}{2}u^2 - \frac{1}{3}u^3 + O(u^4) \qquad (3.7)
\end{aligned}
$$

$$e^{-2L} = \frac{1-\cos u}{\sin u}$$
$$= \frac{1}{2}u + \frac{1}{24}u^3 + O(u^5) \tag{3.8}$$

Because we want to look at the second term of the Taylor series, we need to calculate $\frac{dP}{du}$.

$$\frac{dP}{du} = P\sum_{j=1}^{N}\left[\frac{f_{L,j}^{'}}{f_{L,j}} + \frac{f_{K,j}^{'}}{f_{K,j}}\right] \tag{3.9}$$

Now we can evaluate $f_{L,j}^{'}$ and $f_{K,j}^{'}$ separately. First look at the Taylor expansion of e^{-2K} and e^{-2L} in terms of u evaluated at 0.

$$\frac{d}{du}\left(\frac{1-\sin u}{\cos u}\right)(0) = -1$$
$$\frac{d}{du}\left(\frac{1-\cos u}{\sin u}\right)(0) = \frac{1}{2} \tag{3.10}$$

Then we can substitute these values directly into the exponential product terms.

$$f_{L,j}^{'} = -\frac{1}{2}\delta(\sigma_j, \sigma_j^{'}) + \frac{1}{2}$$
$$f_{K,j}^{'} = \delta(\sigma_{j+1}, \sigma_j^{'}) - 1 \tag{3.11}$$

Substituting the above results into $\frac{dP}{du}$ we get equation (21).

$$P(\phi, \phi^{'}) = P\sum_{j=1}^{N}\left[\frac{-\frac{1}{2}\delta(\sigma_j, \sigma_j^{'}) + \frac{1}{2}}{\delta(\sigma_j, \sigma_j^{'})} + \frac{\delta(\sigma_{j+1}, \sigma_j^{'}) - 1}{1}\right] \tag{3.12}$$

Expanding out the $j = 1$ as follows allows us to make more generalizations.

$$\left(-\frac{1}{2}\delta(\sigma_1, \sigma_1^{'}) + \frac{1}{2}\right)(\delta(\sigma_2, \sigma_2^{'})(\delta(\sigma_3, \sigma_3^{'})...(\delta(\sigma_N, \sigma_N^{'})$$
$$-(\delta(\sigma_2, \sigma_1^{'}) + 1)(\delta(\sigma_1, \sigma_1^{'})(\delta(\sigma_2, \sigma_2^{'})...(\delta(\sigma_N, \sigma_N^{'}) \tag{3.13}$$

Let us denote the first portion of the sum as p_1 and the second portion as p_2. For each $j = i$, p_1 can be rewritten.

$$p_1 = \begin{cases} 0 & \text{if all } (\delta(\sigma_j, \sigma_j^{'}) = 1 \text{ or } \exists j \neq i \text{ such that } (\delta(\sigma_j, \sigma_j^{'}) = 0 \\ \frac{1}{2} & \text{otherwise} \end{cases} \tag{3.14}$$

Let us denote the following matrix as σ_x.

$$\sigma_x = \begin{pmatrix} 0 & 1 \\ 1 & 0 \end{pmatrix} \tag{3.15}$$

Each term in p_1 can be written as a Kronecker product of $N-1$ 2 by 2 identity matrices with the matrix σ_x as the jth term in this product. We will refer to each of these individual terms as σ_j^x Next we turn our attention to p_2. This term can also be formulated into a Kronecker product of $N-2$ identity matrices with the matrix below in the jth position, denoted by $\sigma_j^z \otimes \sigma_j^z$.

$$\begin{pmatrix} 2 & 0 & 0 & 0 \\ 0 & 1 & 0 & 0 \\ 0 & 0 & 1 & 0 \\ 0 & 0 & 0 & 2 \end{pmatrix} \tag{3.16}$$

Next we define a new matrix σ_z and rewrite the above matrix in terms of it.

$$\sigma_z = \begin{pmatrix} 1 & 0 \\ 0 & -1 \end{pmatrix} \tag{3.17}$$

$$\begin{pmatrix} 2 & 0 & 0 & 0 \\ 0 & 1 & 0 & 0 \\ 0 & 0 & 1 & 0 \\ 0 & 0 & 0 & 2 \end{pmatrix} = \left(\tfrac{3}{2}I + \tfrac{1}{2}(\sigma_z \otimes \sigma_z)\right) \tag{3.18}$$

Finally we can rewrite the entire sum as follows.

$$\frac{dP}{du} = -\frac{3}{2}N\sum_{j=1}^{x}\frac{1}{2}\sigma_j^x - \frac{1}{2}\sigma_j^z \otimes \sigma_j^z \tag{3.19}$$

Now we can define H as $\frac{dP}{du}$ without the leading multiple of the sum, which simply functions as a shift in the energy.

$$H = \sum_{j=1}^{N}\frac{1}{2}\sigma_j^x - \frac{1}{2}\sigma_j^z \otimes \sigma_j^z \tag{3.20}$$

Note that this is only the equation at the critical temperature, but the general equation looks the same. As we continue our manipulation of this equation into a more manageable form, we will switch from the statistical mechanics to the realm of quantum mechanics.

4 H in Quantum Mechanics

The method we are using to solve the two-dimensional Ising model matches a separate problem in quantum mechanics. This model analyzes a string of quantum particles in the presence of a magnetic field. In quantum mechanics σ_x and σ_z are Pauli spin matrices, and they are used, along with an additional matrix σ_y, to describe the angular momentum of $\frac{1}{2}$ spin particles. We define the current form of H as being in the x-basis. We will change the basis of H from x to z using the similarity transform described in equation (31). We will switch

between the two bases often as both have different interpretations physically. Define matrix U as the Kronecker product of N of the matrix below.

$$\frac{1}{\sqrt{2}}\begin{pmatrix} 1 & 1 \\ -1 & 1 \end{pmatrix} \tag{4.1}$$

Equation (31) shows H in the z basis, where $U^\dagger$ is the adjoint of U.

$$\begin{aligned} H &= UHU^\dagger \\ &= \sum_{j=1}^{N} \frac{1}{2}\sigma_j^z - \frac{1}{2}\sigma_j^x \otimes \sigma_j^x \end{aligned} \tag{4.2}$$

Since we are interested in more than just the critical temperature, we will write out the general form of H. In this new formula, the variables have been reparameterized so that μ now represents temperature. μ ranges from -1 to 1, where -1 is the temperature as it goes to infinity, 0 is the critical temperature, and 1 is the temperature as it goes to 0. This new form of H is based largely upon a paper by Pfeuty, but with minor adjustments to include terms the paper discarded as irrelevant [4].

$$H = -\frac{1-\mu}{2}\sum_{j=0}^{N}\sigma_j^z - \frac{1+\mu}{2}\sum_{j=0}^{N}\sigma_j^x \otimes \sigma_{j+1}^x \tag{4.3}$$

At this point, we will start looking at the eigenvalues and eigenvectors of the system. In order to study this system as a whole, we numerically calculate the eigenvalues and eigenvectors as μ goes from -1 to 1. A plot of the eigenvalues of the system at $N = 3$ is displayed in figure 1. Because H is a 2^N by 2^N matrix, there are 2^N eigenvalues. As a result, while the graph for $N = 3$ appears simple, for higher system sizes the graph quickly becomes much more complicated. Now that we can solve for the eigenvalues, which we interpret as energy, we move our focus to the eigenvectors. Each eigenvector can be associated with different states or mixtures of states, and then the states can be linked to a specific energy by the vector's eigenvalue. For example, when we evaluate H at $\mu = 0$ we find a specific set of energies associated states. The vector below is the eigenvector rounded to four decimal places associated with $\lambda = 2.7079$. The labeling to the left is the order that the values associated with each state are ordered within H, and as a result, the order they appear in the eigenvector.

$$\begin{array}{cc} --- & 0.9990 \\ --+ & -0.0454 \\ -+- & 0 \\ -++ & 0 \\ +-- & 0 \\ +-+ & 0 \\ ++- & 0 \\ +++ & 0 \end{array} \tag{4.4}$$

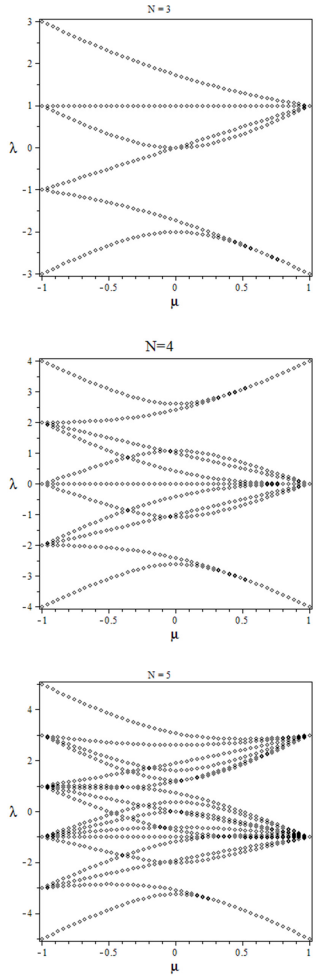

Figure 1: Eigenvalues

Clearly, the first entry of the vector has the highest magnitude, and therefore the state $---$ is associated with the energy 2.7079. We use this process with the rest of the eigenvalues and eigenvectors to associate all of the energies with one or more states. In the given example, the components of the vector clearly indicate just one state. However, in many cases, the results are not so clear. This hurdle in identifying the state in question largely follows from the degeneracy of H. As you can see from the graph, many eigenvalues converge at $\mu = -1$ and $\mu = 1$. Also, you may note that there are only 6 lines of eigenvalues represented on the graph when we expect there to be 2^N, which is 8 in this case. This discrepancy is due to the fact two sets of eigenvalues are identical for all values of μ, making it impossible to distinguish the them on the graph. In order to lessen the affects of the degeneracy and create a clearer image of the behavior of H, we break down H into more manageable pieces. Before we look at the process of breaking down H, there is still much to be gained from analyzing the behavior at the endpoints at this stage in our manipulation of H.

5 Behavior at the Endpoints

Different sides of the graph behave in different ways and have different particle interpretations. Our goal in this project is relating the endpoints to one another, so it is important to be familiar with the behavior on both sides.

5.1 $\mu = -1$

μ approaching -1 is equivalent to the temperature in the original system approaching infinity. When $\mu = -1$, H can be reduced to the following form:

$$H = -\frac{1-\mu}{2}\sum_{j=0}^{N}\sigma_j^z \tag{5.1}$$

When working on this side of the spectrum, we work within the z-basis, which refers to the fact that σ_z is a diagonal matrix within this basis. From the structure of H listed above, we can conclude that only the signs of the particles within a state effect H at this point. In fact, based on this information, we can calculate the eigenvalue of any given state at $\mu = -1$ as $-1\cdot$(the number of "$-$" signs within a state). The physical interpretation of this in the original Ising model is that at very high temperatures, interactions between particles become less of an influence upon the system, making this portion of the spectrum the disordered side. Now we can consider the quantum interpretation. On this side of the graph, minus signs within a state are considered particles. For example, in $N = 3$ $+-+$ would be a one particle state and $--+$ would be a two particle state. We can see from figure 1 that states with the same number of particles converge to the same eigenvalues, or equivalently, converge to the same energy, at $\mu = -1$.

5.2 $\mu = 1$

μ approaching 1 is equivalent to the temperature in the original system approaching 0. At this value of μ, we can simplify H like we did for $\mu = -1$.

$$H = -\frac{1+\mu}{2}\sum_{j=0}^{N}\sigma_j^x \otimes \sigma_{j+1}^x \tag{5.2}$$

Near values of $\mu = 1$, we will be working within the x-basis. In order to do this, we perform a change of basis upon H that diagonalizes σ_x. Define matrix A as the Kronecker product of the below matrix with itself N times.

$$-\frac{1}{\sqrt{2}}\begin{pmatrix}1 & 1\\ 1 & -1\end{pmatrix} \tag{5.3}$$

Now we can rewrite H in the appropriate basis as $AUA^\dagger$. The labeling of the eigenvectors stays the same, but now they take on a slightly different particle interpretation. First let us examine the new structure of H. As μ approaches 1, the temperature in the original model is approaching 0. The only factor that matters now is the inter-particle interactions, making this the ordered side. Particles are now defined as sign changes within the state. This means that $+-+$ is now a two particle state and $+++$ is a zero particle state. It follows that states with the same number of particles, and thus the same number of sign changes, converge to the same eigenvalue at $\mu = 1$ and therefore have the same energy at this point.

6 Block Diagonalization of H

By block diagonalizing H, we are able to look at the eigenvalues and eigenvectors of each block separately and lessen the effects of the degeneracy within H. In order to perform this diagonalization, we will break H down into different momentum sectors as well as even and odd sectors using the matrices T and F described in the next two sections.

6.1 Division into Momentum Sectors

In the beginning of this paper, we defined the model to be translationally invariant, which means that states that are translates of one another, such as $++-$ and $+-+$, will be numerically equivalent. Therefore, switching around states that are translates of one another has no effect on H. We construct a matrix T built from translation matrices that performs exactly that operation. Seeing as T does not effect H, T commutes with H. This commutation property allows for H and T to be simultaneously diagonalized, allowing us to gain information about H from T. T is composed of translation matrices, so its eigenvalues are Nth roots of unity, denoted by ω.

$$\omega = e^{\frac{2\pi i}{N}} \tag{6.1}$$

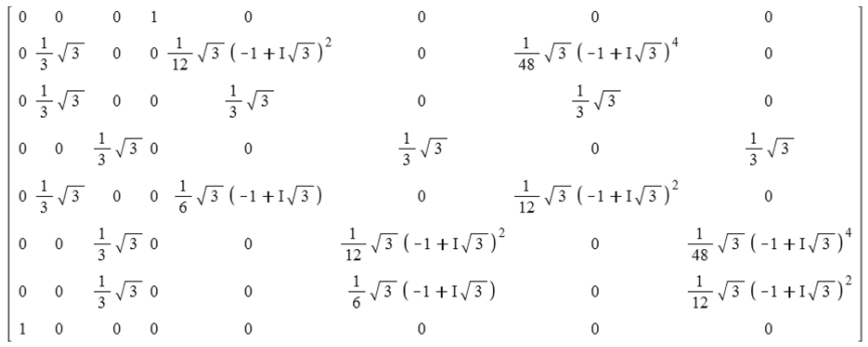

Figure 2: T Eigenvectors

We label each distinct eigenvalue of T as a momentum, p, that corresponds to the power ω is raised to. Using the eigenvectors of T grouped together by momentum, we form a unitary transformation matrix C. An example of C for $N = 3$ is listed below. In figure 2, the first four columns are eigenvectors with eigenvalue ω^0, so we label them momentum 0 vectors. The next two columns correspond to ω^1 and the final two match with ω^2, making them momentum 1 and 2 vectors respectively. Note that within this matrix, each vector only has nonzero entries in positions corresponding to translate of a particular state. The general format of each vector is $(\omega^p)^0 \, |state_1> + (\omega^p)^1 \, |state_1 \text{translated 1 position} > + ... + (\omega^p)^t \, |state_1 \text{translated } t \text{ positions} >$ where t is the number of translates of $state_1$ and p is the momentum. An eigenvector of this form exists in all momentums such that $\frac{p}{\frac{N}{t}}$ is an integer value. The following transformation separates H into blocks of momentum groups with all translates grouped together.

$$H = C^\dagger H C \tag{6.2}$$

Below is the structure of this matrix for $N = 3$. The labels for the top of the matrix are the same as those listed to the left of the matrix. All the blocks along the diagonal with the dimensions written inside are momentum sectors in increasing order as we move down the diagonal. All empty blocks are filled with 0s. We can extract each of the blocks along the diagonal and then analyze the eigenvalues and eigenvectors in the same manner as before, with the exception that each eigenvalue is now associated with a momentum eigenstate.

6.2 Division into Even and Odd Sectors

In order to further divide H, we use a unitary operator F. F commutes with H, and using it we block diagonalize each momentum sector into even and odd blocks. F is the matrix that flips the sign of the x-component of every spin. Doing this twice restores the original configuration, and therefore F must have eigenvalues 1 and -1. Once again, F behaves differently at opposite ends of the

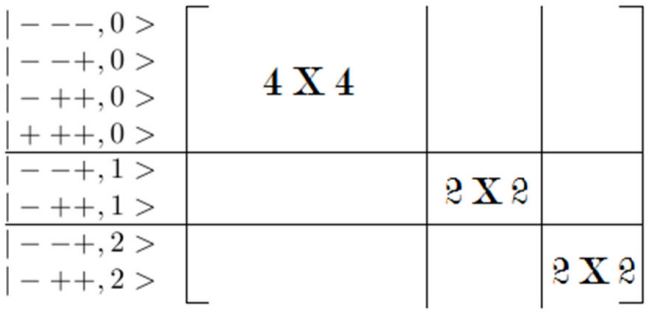

Figure 3: H after transformation to basis of T eigenstates

μ spectrum. Towards $\mu = -1$, a state is defined to be even if it has an even number of "$-$" signs and odd if it has an odd number of "$-$" signs. On the $\mu = 1$ side, a state is defined to be even if flipping the signs does not change the state and odd if flipping the signs does change the state. For example, $(+++) + (---)$ becomes $(---) + (+++)$ with the signs flipped, and therefore is even whereas $(+++) - (---)$ becomes $(---) - (+++)$, which is a different state and is thus odd. Now we can extract the even smaller blocks from H's diagonal and look at each block of momentum in even and odd sectors and analyze the eigenvalues and eigenvectors separately as we have been doing.

7 The Critical Temperature

An exact solution for the eigenvalues of H is known. The equation for the eigenvalues is construction using Λ_m defined below.

$$\Lambda_m = \begin{cases} \sqrt{2(1+\mu^2) - 2(1-\mu^2)\cos\left(\frac{2\pi m}{N}\right)} & \text{if } m \neq 0 \\ -2\mu & \text{if } m = 0 \end{cases} \tag{7.1}$$

In order to evaluate the eigenvalues, we need to introduce a Dirac's ket notation and divide the spectrum into even and odd sectors. At $\mu = 0$, we associate each eigenvalue with a state occupied with particles with certain momenta. Two particles of the same momentum are not allowed within the same ket. For example $|-1, 0, 1>$ is a three particle state consisting of particles with momenta $-1, 0, 1$. $|-1, -1, 0>$ is not an allowed state because two of the particles would have -1 as their momentum. Now we focus upon the division into even and odd sections. In the even sector, momenta must be an odd multiple of $\frac{1}{2}$ and states must contain and even number of particles. In the odd sector, momenta must be an even multiple of $\frac{1}{2}$ and states must contain an odd number of particles. In both cases, $-\frac{N}{2} < m \leq \frac{N}{2}$ and the sum of the particles in a state must equal the momentum group the eigenvalue is in. Now we have all the information

needed to calculate the eigenvalues.

$$\lambda = -\frac{1}{2}\left(\Lambda_{m_1} + \Lambda_{m_2} + \cdots + \Lambda_{m_p}\right) \tag{7.2}$$

The subscripts m are all the values of m that satisfy the requirements for being in the even or odd group. If the m_j momentum is contained in the ket, then the sign in front of Λ_{m_j} is changed to a minus sign. For example, in $N = 3$, the state $|-1, 0, 1>$ has eigenvalue $\lambda = -\frac{1}{2}(\Lambda_{-2} - \Lambda_{-1} - \Lambda_0 - \Lambda_1 + \Lambda_2)$ [3].

8 Relating $\mu = -1, 1$ and 0

Now that we have examined and developed a labeling convention for the eigenvalues of H at $\mu = -1, 0$, and 1, we wish to relate the three points. Figure 4 displays the plots of the eigenvalues for H with $N = 5$ separated by momentum and even or odd status. Only the values for three momentums are displayed because if $p_1 \equiv -p_2 \mod N$, then the plots for p_1 and p_2 are the same. Some general observations are that in even sectors, eigenvalues that converge at $\mu = -1$ also converge to the same point at $\mu = 1$. In fact, the eigenvalues are symmetric about the vertical axis. Additionally, states with n particles at $\mu = -1$ map to n particle states at $\mu = 1$. In the odd case, these results do not hold. There does appear to be some symmetry, as most eigenvalues that converge at $\mu = -1$ also converge at $\mu = 1$. However, not all eigenvalues obey this rule. We suspect that this descepancy is related to the inclusion of the momentum 0 particle in the ket notation at the critical temperature, because its addition or subtraction to a ket causes no change in the associated eigenvalue at $\mu = 0$.

9 Further Questions

Through researching this material, the observations we made suggest that a relatively simple bijection between $\mu = -1$ and $\mu = 1$ could exist. However, the actual problem of finding such a bijection is still of interest. Additionally, the results of this model could prove useful in finding a bijection for the Rogers-Ramanujan identity (43) [2]. First define the following.

$$(q)_0 = 1 \tag{9.1}$$

$$(q)_n = \prod_{k=1}^{n}(1 - q^k) \tag{9.2}$$

$$\sum_{n=0}^{\infty} \frac{q^{n(n+1)}}{(q)_n} = \prod_{n=1}^{\infty} \frac{1}{(1 - q^{5n-2})(1 - q^{5n-3})} \tag{9.3}$$

As N goes to infinity, the number of states at a given energy level at $\mu = 0$ can be written as a generating function. We now define $\mathbf{N}_{\frac{1}{16}}$.

$$\mathbf{N}_{\frac{1}{16}} = \{n \in \mathbf{N} \mid n \equiv \pm 1, \pm 3, \pm 5, \text{ or } \pm 7 \mod 16\} \tag{9.4}$$

Equation (45) counts the number of states at a particular energy in the odd sector. While this equation is not the same as equation (43), it is very similar, suggesting that this physics model may be helpful in finding this bijection.

$$\chi_{\frac{1}{16}} = q^{-\frac{1}{48}+\frac{1}{16}} \sum_{j=0}^{\infty} \frac{q^{j(2j+1)^2}}{(q)_{2j+1}} = q^{-\frac{1}{48}+\frac{1}{16}} \prod_{j \in \mathbf{N}_{\frac{1}{16}}} \frac{1}{(1-q^j)} \tag{9.5}$$

References

[1] Baxter, R. J. (1982). Exactly Solved Models in Statistical Mechanics. London: Academic Press.

[2] Rinat Kedem, Barry M. McCoy, and Ezer Melzer. The sums of Rogers, Schur and Ramanujan and the Bose-Fermi correspondence in (1 + 1)-dimensional quantum field theory. In *Recent progress in statistical mechanics and quantum field theory (Los Angeles, CA, 1994)*, pages 195–219. World Sci. Publ., River Edge, NJ, 1995.

[3] Elliott Lieb, Theodore Schultz, and Daniel Mattis. Two soluble models of an antiferromagnetic chain. *Ann. Physics*, 16:407–466, 1961.

[4] Pierre Pfeuty. The one-dimensional ising model with a transverse field. *Annals of Physics*, 57(1):79 – 90, 1970.

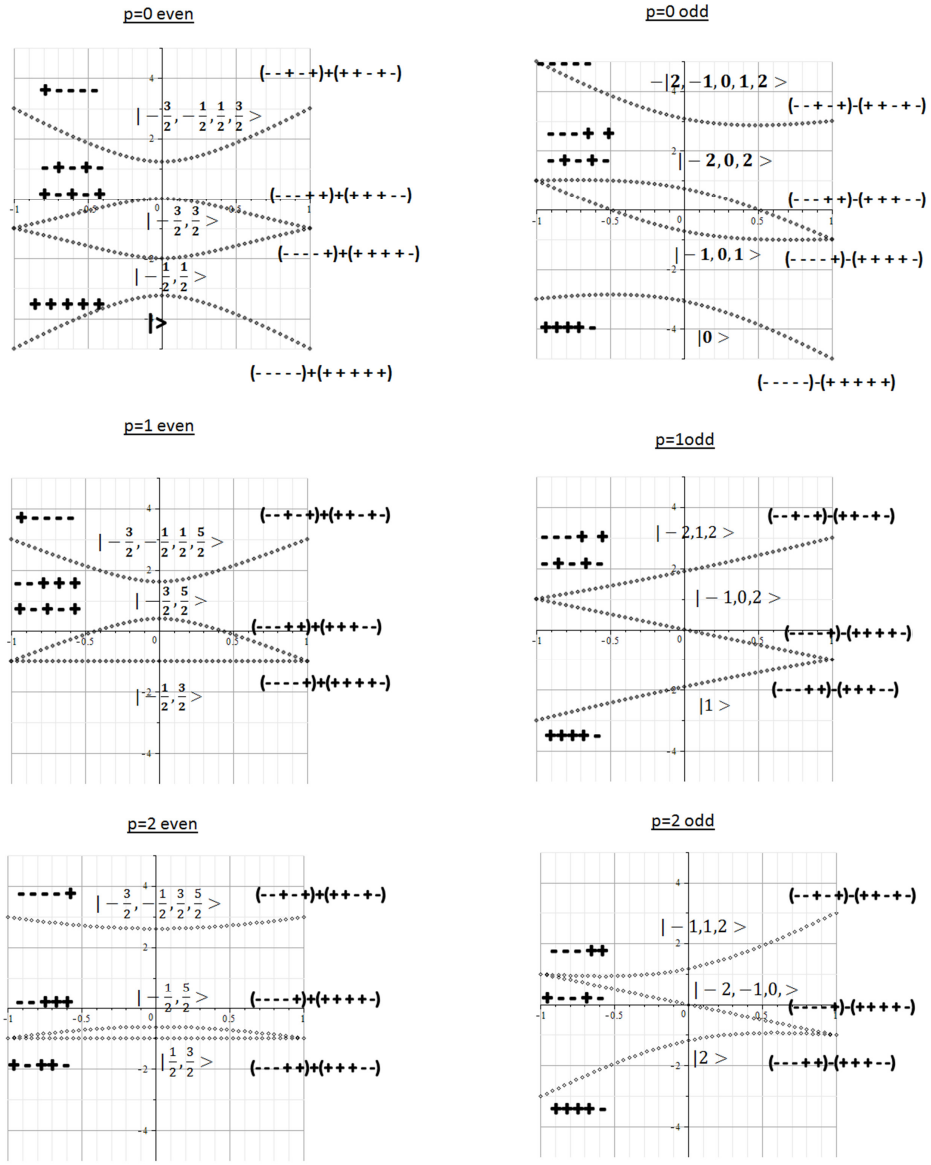
p=0 even
(- - + - +)+(+ + - + -)
+ - - - -
$|-\frac{3}{2},-\frac{1}{2},\frac{1}{2},\frac{3}{2}>$
- + - + -
+ - + - +
(- - - + +)+(+ + + - -)
$|-\frac{3}{2},\frac{3}{2}>$
(- - - - +)+(+ + + + -)
$|-\frac{1}{2},\frac{1}{2}>$
+ + + + +
|>
(- - - - -)+(+ + + + +)
p=0 odd
$-|2,-1,0,1,2>$
(- - + - +)-(+ + - + -)
- - - + +
- + - + -
$|-2,0,2>$
(- - - + +)-(+ + + - -)
$|-1,0,1>$
(- - - - +)-(+ + + + -)
+ + + + -
$|0>$
(- - - - -)-(+ + + + +)
p=1 even
+ - - - -
(- - + - +)+(+ + - + -)
$|-\frac{3}{2},-\frac{1}{2},\frac{1}{2},\frac{5}{2}>$
- - + + +
$|-\frac{3}{2},\frac{5}{2}>$
+ - + - +
(- - - + +)+(+ + + - -)
(- - - - +)+(+ + + + -)
$|-\frac{1}{2},\frac{3}{2}>$
p=1odd
(- - + - +)-(+ + - + -)
- - - + +
$|-2,1,2>$
- + - + -
$|-1,0,2>$
(- - - - +)-(+ + + + -)
(- - - + +)-(+ + + - -)
$|1>$
+ + + + -
p=2 even
- - - - +
(- - + - +)+(+ + - + -)
$|-\frac{3}{2},-\frac{1}{2},\frac{1}{2},\frac{3}{2},\frac{5}{2}>$
- - + + +
$|-\frac{1}{2},\frac{5}{2}>$
(- - - - +)+(+ + + + -)
+ - + + -
$|\frac{1}{2},\frac{3}{2}>$
(- - - + +)+(+ + + - -)
p=2 odd
(- - + - +)-(+ + - + -)
$|-1,1,2>$
- - - + +
$|-2,-1,0,>$
+ - - + -
(- - - - +)-(+ + + + -)
$|2>$
(- - - + +)-(+ + + - -)
+ + + + -

Figure 4: N=5

Geodesics in the Farey Complex

Matthew Mizuhara

Abstract

The Farey complex has as vertices the rational numbers together with the point at infinity, represented as $-1/0 = 1/0$. Given vertices p/q and r/s in lowest terms, join them by an edge if $|ps - rq| = 1$. By this rule, it is possible to consider the combinatorial distance between any pair of extended rational numbers. In this work, we prove a locally deterministic method to calculate a geodesic path between two points, as well as consider the relationship between continued fraction expansions and geodesic paths. These results require nothing more than elementary methods and simple results regarding Möbius transformations. We also construct a recursive algorithm to calculate the number of distinct geodesic paths between two points. We conclude with other interesting, related results as well as provide two distinct programs which can be used to calculate geodesic paths and Farey distances between two extended rational numbers.

1 Introduction

The Farey complex (alternatively the Farey graph), denoted $\mathcal{F}$, has several constructions. Its most elementary representation has as its vertices the extended rational numbers, $\hat{\mathbb{Q}} = \mathbb{Q} \cup \left\{\frac{1}{0} = \frac{-1}{0}\right\}$. We join two vertices $\frac{p}{q}$, $\frac{r}{s} \in \hat{\mathbb{Q}}$ by an edge if and only if $|ps - qr| = 1$. Adjacent vertices are called *Farey neighbors*. Given Farey neighbors $\frac{p}{q}$, $\frac{r}{s} \in \hat{\mathbb{Q}}$, we define a binary operator $\oplus$, called *Farey addition*, by

$$\frac{p}{q} \oplus \frac{r}{s} := \frac{p+r}{q+s}.$$

We call $\frac{p}{q}$ and $\frac{r}{s}$ *Farey parents* of $\frac{p+r}{q+s}$, which is in turn known as the mediant of $\frac{p}{q}$ and $\frac{r}{s}$. It turns out that the mediant is in fact a Farey neighbor to both Farey parents and will always be in reduced terms [Hat1, page 2, 18].

For consistency, we will always assume that any vertex $\frac{p}{q} \in \mathbb{Q}$ is written so that $\gcd(p, q) = 1$, and we identify $\mathbb{Q}$ with $\mathbb{Z} \times \mathbb{N}$, where $(a, b) \Leftrightarrow \frac{a}{b}$. Finally, we write the point at infinity as $\frac{1}{0} = \frac{-1}{0}$ and the point at zero as $\frac{0}{1}$.

As is well-known, the Farey graph is the 1-skeleton of whose 2-simplices are determined by Farey neighbors and their mediant. The Farey complex is isomorphic to the 2-complex given by the (essentially unique) tiling of the hyperbolic plane by ideal triangles [Min1, page 566].

In this work, we derive algorithmic and computational methods to compute the Farey distance between two arbitrary vertices of the Farey graph (as originally proposed in [Pil1]). In Section 2 we introduce the proper notation and

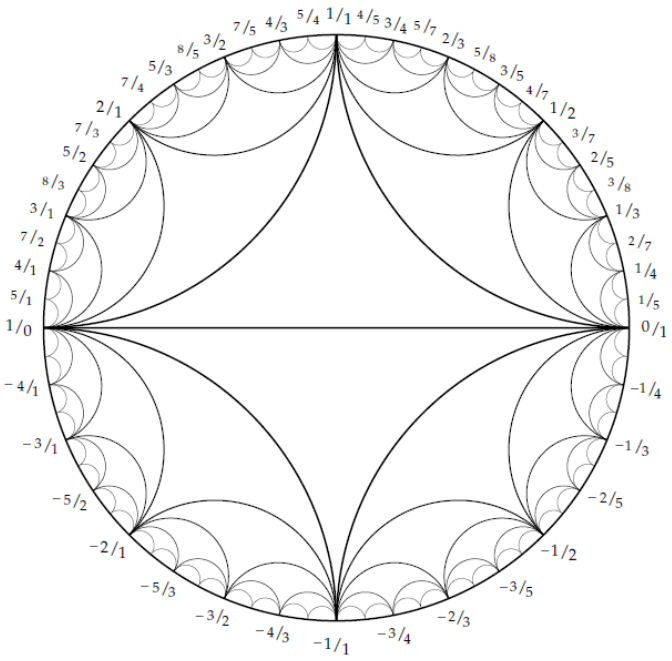

Figure 1: A finite representation of the Farey complex [Hat1, page 1]

language required, as well as present a main theorem which proves a local, deterministic way to construct a geodesic path between two points. In Section 3 we introduce the relationship between the Farey complex and continued fraction expansions, and prove a theorem which calculates the distance from any rational number to 1/0 from the continued fraction expansion. In Section 4 we provide a recursive function which can be used to count the number of geodesics between two vertices and in Section 5 we explore further investigations including an algorithm to construct alternate geodesic paths. Finally, in Section 6 we provide two programs written in Maple code which can be used to calculate paths or distances between vertices.

2 Preliminaries

2.1 Möbius Transformations

A *Möbius transformation* is a function, $f\colon \hat{\mathbb{C}} \to \hat{\mathbb{C}}$, of the form

$$f(z) = \frac{az+b}{cz+d}$$

where a, b, c, d, $\in \mathbb{C}$ and $ad - bc \neq 0$. All Möbius transformations form a group under composition which we denote by Möb($\hat{\mathbb{C}}$). A particularly special subgroup of Möb($\hat{\mathbb{C}}$) is denoted $PSL_2(\mathbb{Z})$ and defined as

$$PSL_2(\mathbb{Z}) := \left\{ z \mapsto \frac{az+b}{cz+d} : a,\, b,\, c,\, d \in \mathbb{Z} \text{ and } ad - bd = 1 \right\}.$$

It is well known that

$$z \mapsto z + 1$$

and

$$z \mapsto \frac{-1}{z}$$

generate $PSL_2(\mathbb{Z})$, so it is often sufficient to prove results only on these two elements. One can show that $PSL_2(\mathbb{Z})$ acts on $\hat{\mathbb{Q}}$ in the obvious way, and so we check further that all elements indeed maintain Farey relations.

Lemma 2.1. *For any $A \in PSL_2(\mathbb{Z})$, if $\frac{p}{q}$ and $\frac{r}{s}$ are Farey neighbors then $A(\frac{p}{q})$ and $A\left(\frac{r}{s}\right)$ are also Farey neighbors.*

Proof. We assume without loss of generality that $ps - qr = 1$. It suffices to prove that the statement holds for the two generating elements of $PSL_2(\mathbb{Z})$. In the first case, we see that $\frac{p}{q} \mapsto \frac{p+q}{q}$ and $\frac{r}{s} \mapsto \frac{r+s}{s}$. It follows that these two numbers are Farey neighbors if and only if

$$(p+q) \cdot s - (r+s) \cdot q = 1.$$

After expansion and cancelation, it is clear that this is equivalent to the hypothesis, so the result holds.
The result holds similarly for the second generator mapping. Hence, it holds for any element of $PSL_2(\mathbb{Z})$ by some composition of the above functions. □

In particular, this result proves that any $A \in PSL_2(\mathbb{Z})$ preserves all edges and hence it preserves all triangles in $\mathcal{F}$. We conclude that $PSL_2(\mathbb{Z})$ is a group of orientation-preserving isometries of the Farey complex. In particular, we show that given any 2-simplex there exists an element of $PSL_2(\mathbb{Z})$ which maps the aforementioned simplex to any other 2-simplex, while maintaining orientation. We first present a result from [Hat1, page 15].

Lemma 2.2. *If p/q, $r/s \in \mathbb{Q}$ are Farey neighbors, then*

$$\frac{p}{q} \oplus \frac{r}{s} \in \left(\frac{p}{q},\, \frac{r}{s} \right).$$

Lemma 2.3. *$PSL_2(\mathbb{Z})$ acts simply transitively on positively oriented, labeled simplices.*

Proof. It suffices to show that we can map any 2-simplex to the 2-simplex defined by the triple of vertices $\frac{0}{1}$, $\frac{1}{1}$, and $\frac{1}{0}$ in any way (while preserving positive orientation). Given some 2-simplex, we can write the vertices as $\frac{p}{q} < \frac{p+r}{q+s} < \frac{r}{s}$ (by Lemma 2.2). It is clear that $\frac{p}{q} < \frac{r}{s}$ if and only if $ps - qr < 0$. Since $\frac{p}{q}$ and $\frac{r}{s}$ are Farey neighbors, we conclude that $ps - qr = -1$. Thus,

$$z \mapsto \frac{-qz + p}{sz - r}$$

precisely maps $\frac{p}{q} \mapsto \frac{0}{1}$, $\frac{p+r}{q+s} \mapsto \frac{1}{1}$, and $\frac{r}{s} \mapsto \frac{1}{0}$. We specially note that this mapping still successfully works in the case that any of the points is initially $\frac{1}{0}$, $\frac{0}{1}$, or $\frac{1}{1}$. Finally, the map

$$z \mapsto \frac{1}{-z + 1}$$

permutes the points $\frac{0}{1}$, $\frac{1}{1}$, and $\frac{1}{0}$ cyclically. So, a composition of the two applicable maps will translate and rotate the 2-simplex as desired. As any Möbius transformation is uniquely determined by three points, we conclude that the resulting map is unique. □

2.2 Properties of $\mathcal{F}$

With these tools, we now characterize the Farey complex by its various relationships and restrictions which we will use to later construct our geodesic path. The following lemma is clear from the disk model of $\mathcal{F}$, however its result will generalize in a useful way.

Lemma 2.4. *Every rational number is adjacent in $\mathcal{F}$ only to other numbers with like sign, excluding $\frac{1}{0}$ and $\frac{0}{1}$.*

Proof. Suppose that there exist two Farey neighbors, $\frac{p}{q}$ and $\frac{r}{s}$, and without loss of generality, that $\frac{p}{q} > 0$ and $\frac{r}{s} < 0$. By our convention of writing extended rational numbers, we then conclude that $r < 0$, $p > 0$, and $q, s \geq 0$. It is clear that $ps - qr > 0$, so we conclude that $ps - qr = 1$. However, $ps \geq 0$ and $-qr \geq 0$, so it must be the case that at least one of ps and $-qr$ is equal to 0. As we assumed neither p/q nor r/s is identically 0, we conclude that $p \neq 0$ and $r \neq 0$. So, it must be the case that either $s = 0$ or $q = 0$. In either case, we conclude that one of the numbers is $\frac{1}{0}$ (or $\frac{-1}{0}$, which is identified with $\frac{1}{0}$). □

So, any path which travels between positive and negative numbers must necessarily travel through either $\frac{1}{0}$ or $\frac{0}{1}$. We define this phenomenon generally as separating the Farey complex and as expected, this holds symmetrically for any edge in $\mathcal{F}$.

Definition 2.5. Given a connected graph $G = (V, E)$ and two adjacent vertices, $a, b \in V$, we say that the edge $\{a, b\}$ is a *vertex separator* of $x, y \in V$ (distinct from a and b) if removing the vertices a and b, along with any edges incident to either vertex separates x and y into distinct, connected components. We say $\{a, b\}$ separates x from y.

Lemma 2.6. *Every edge,* $\left\{\frac{p}{q}, \frac{r}{s}\right\}$*, of* $\mathcal{F}$ *is a vertex separator of every* $x \in (p/q, r/s)$ *from* $y \notin (p/q, r/s)$*.*

Proof. We first prove that $\left\{\frac{1}{0}, \frac{0}{1}\right\}$ is a vertex separator of the desired form. Lemma 2.4 implies that $\frac{1}{0}$ and $\frac{0}{1}$ are the only vertices which are Farey neighbors to both positive and negative numbers. Thus, we conclude that by removing the vertices $\frac{1}{0}$ and $\frac{0}{1}$, there no longer exists a path from any positive number to any negative number, so the graph is disconnected. In other words, every $x \in (0, 1/0)$ is separated from every $y \in (-1/0, 0)$. In general, another way to view the set $(p/q, r/s)$ is as the set of all successive mediants of all adjacent vertices starting with p/q and r/s. As every Möbius transformation preserves Farey relations, the result holds in general by Lemma 2.3. □

Definition 2.7. The *nth extended Stern-Brocot poset*, denoted F_n, is a poset (with the standard $\leq$ ordering, where $-\infty \leq p/q \leq \infty$ for any $p/q \in \mathbb{Q}$) defined inductively as follows:

$$F_0 = \left\{\frac{-1}{0}, \frac{1}{0}\right\},$$

where $-\infty := \frac{-1}{0} \leq \frac{1}{0} =: +\infty$,

$$F_1 = \left\{\frac{-1}{0}, \frac{0}{1}, \frac{1}{0}\right\}$$

and

$$F_{n+1} = F_n \cup \left\{\frac{p}{q} \oplus \frac{r}{s} \colon \frac{p}{q}, \frac{r}{s} \text{ are successive elements in } F_n\right\},$$

when $n \geq 1$. Additionally, we define the *nth level* of the Farey complex, denoted L_n, as the set of all elements which are added to the nth extended Stern-Brocot poset:

$$L_n := F_n \setminus F_{n-1}.$$

For consistency, we maintain that $L_0 := F_0$.

Remark 2.8. We note that for any $n > 1$, it is clear that $F_n \cap \mathbb{Q}^+$ is the $(n-1)$st order Stern-Brocot sequence [GKP1, section 4.5]. By extending the Stern-Brocot sequence to the negative numbers, we have the ability to reconstruct all of the extended rational numbers.

Example 2.9. We list the first few extended Stern-Brocot posets:

$$F_0 = \left\{\frac{-1}{0}, \frac{1}{0}\right\},$$

$$F_1 = \left\{\frac{-1}{0}, \frac{0}{1}, \frac{1}{0}\right\},$$

$$F_2 = \left\{\frac{-1}{0}, \frac{-1}{1}, \frac{0}{1}, \frac{1}{1}, \frac{1}{0}\right\},$$

$$F_3 = \left\{\frac{-1}{0}, \frac{-2}{1}, \frac{-1}{1}, \frac{-1}{2}, \frac{0}{1}, \frac{1}{2}, \frac{1}{1}, \frac{2}{1}, \frac{1}{0}\right\}.$$

For each $n \geq 0$, once we identify $-1/0$ with $1/0$, each extended Stern-Brocot poset, F_n, determines a subset of $\hat{\mathbb{Q}}$ and, therefore, a subcomplex of $\mathcal{F}$; abusing notation, we denote this subcomplex also as F_n.

Lemma 2.10. *Each F_n is convex.*

Proof. It is clear that F_n is connected. Take x, $y \in F_n$ and let γ be a geodesic from x to y. Without loss of generality, we assume $-\infty \leq x < y \leq \infty$, where at least one of the $\leq$ inequalities is strict, or else the result is trivial. Suppose to the contrary that γ passed through $z \in \mathcal{F} \setminus F_n$. Given the cyclic ordering of F_n as determined by the extended Stern-Brocot posets, we know there exists a unique x_0 and its successor y_0, both in F_n satisfying $x_0 < z < y_0$. There are several cases to consider; we first prove the case where

$$x < x_0 < z < y_0 < y.$$

As y_0 is the successor of x_0, it must hold that they are Farey neighbors, so Lemma 2.6 implies that $\{x_0, y_0\}$ separates z from x and y. Thus, any path passing through z must necessarily pass initially through either x_0 or y_0, then pass through z, and finally pass through either x_0 or y_0. It is clear that this is inefficient, and so γ cannot be a geodesic. This is the necessary contradiction.

We now consider the case where

$$x = x_0 < z < y_0 < y.$$

Similar to above, it is obvious that $\{x, y_0\}$ separates z from y. Again, any path through z must necessarily pass initially through x or y_0, then pass through z, and finally pass through either x or y_0. This is again clearly inefficient, drawing the same contradiction. All other cases follow similarly, proving the result. □

We conclude that if we have two numbers, $p/q \in L_n$ and $r/s \in L_m$, then it suffices to construct either F_n or F_m, depending on whether n or m is larger. Once we do so, we know all geodesic paths from p/q to r/s are represented, and so the problem of calculating a geodesic path has been reduced to a finite number of cases. However, if we assume one point is $1/0 \in L_0$, then it is possible to strengthen these results to find a more deterministic method of constructing a geodesic path from any rational number to $1/0$. To do so, we first require the uniqueness of the Farey parents of any rational number.

Lemma 2.11. *Given $\frac{a}{b} \in \mathbb{Q} \setminus \left\{\frac{0}{1}\right\}$, there exists a unique pair $\frac{p}{q}$, $\frac{r}{s} \in \hat{\mathbb{Q}}$ such that*

$$\frac{a}{b} = \frac{p}{q} \oplus \frac{r}{s}$$

where $\frac{p}{q}$ and $\frac{r}{s}$ are Farey neighbors.

Proof. Without loss of generality, we assume $\gcd(a, b) = 1$. By the symmetry in the Farey complex and by Lemma 2.4, it is sufficient to assume all values are non-negative. Now, as a and b are coprime, then the Diophantine equation

$$bp - aq = 1 \tag{2.1}$$

has an infinite number of solutions, by Bézout's Lemma. In particular, it must hold that any pair p and q which solve the equation must be coprime. Rewriting the equation as

$$p(b - q) - q(a - p) = 1 \tag{2.2}$$

it becomes clear that likewise $b-q$ and $a-p$ must also be coprime. But, it is clear that equation (2.2) holds if and only if $\frac{p}{q}$ and $\frac{r}{s} = \frac{a-p}{b-q}$ are Farey neighbors. It only remains to show that there exists a unique solution to (2.1) which satisfies p and $a-p$ having like sign, and that q and $b-q$ are positive. Now, (2.1) implies that any integer solution of p must satisfy

$$bp - 1 \equiv 0 \mod a$$

or, as b has an inverse modulo a,

$$p \equiv b^{-1} \mod a.$$

If we restrict p to the interval $[0, a)$ then there is a unique solution to this equivalence. From this choice, it must hold that p and $a - p$ have like signs. A quick check of cases against (2.2) proves that both q and $b - q$ must be positive. □

Obviously, the Farey parents of a given rational number must live in lower Farey levels than their mediant. As the next result shows, these levels are not completely arbitrary.

Lemma 2.12. *If $\frac{p}{q} \in L_n$ for $n \geq 2$ and if r/s, t/u are as in Lemma 2.11, so that*

$$\frac{p}{q} = \frac{r}{s} \oplus \frac{t}{u},$$

then precisely one of $\frac{r}{s}$, $\frac{t}{u}$ is in L_{n-1} and the other one is in L_k where $k < n-1$. Additionally, the latter number must be a Farey parent of the former number.

Proof. Let $\frac{p}{q} \in L_n$ and $\frac{r}{s}$, $\frac{t}{u}$ be its Farey parents. By our method of construction of the extended Stern-Brocot posets, it is clear that if neither $\frac{r}{s}$ nor $\frac{t}{u}$ were members of L_{n-1} then $\frac{r}{s} \oplus \frac{t}{u} \in L_k$ where $k \leq n-1$, a contradiction. So at least once of $\frac{r}{s}$ and $\frac{t}{u}$ is in L_{n-1}. As each subsequent extended Stern-Brocot poset inserts new numbers between all existing numbers, it cannot hold that there are Farey neighbors with equal level (as a consequence of Lemma 2.6). Hence, one of $\frac{r}{s}$, $\frac{t}{u} \in L_{n-1}$ and the other must be an element of L_k where $k < n-1$. Without loss of generality, $\frac{r}{s} \in L_{n-1}$. However, as $\frac{r}{s}$ and $\frac{t}{u}$ are Farey neighbors, then they appear sequentially in F_{n-1}. In order for these two numbers to appear next to each other, it must hold that there exists some $\frac{v}{w} \in F_{n-2}$, a Farey neighbor of $\frac{t}{u}$, such that $\frac{v}{w} \oplus \frac{t}{u} = \frac{r}{s}$. □

It is now possible to combine Lemmas 2.10 and 2.12 in order to reduce the brute-force search of arbitrary geodesic paths to a binary search when one point is assumed to be $\frac{1}{0}$.

Lemma 2.13. *Every geodesic path from any vertex to the point at infinity must strictly decrease level at each vertex along the path towards infinity.*

Proof. We prove the result by induction. The result is vacuously true for the trivial case where the vertex $p/q = 1/0$ and obvious for the case when $p/q = 0/1$. Assume the result holds for all rational numbers up to level $n-1$. Now, suppose that $p/q \in F_n$ for $n \geq 2$. By Lemma 2.10, we conclude that all geodesics from p/q to $1/0$ must live in F_n. Further, in the case that $p/q \in L_k$ for $k < n$, then the result holds trivially by the induction hypothesis. If $p/q \in L_n$, then in F_n, p/q can only be Farey neighbors with its Farey parents. By Lemma 2.12 and the inductive hypothesis, the result is clear.

□

2.3 Computing a Geodesic Path

By restricting one point to be at $1/0$, we narrow the possible paths from each vertex to only two choices. Unfortunately, for numbers in high levels of the Farey complex, this search becomes exponentially difficult and computationally expensive. The following theorem restricts this path further, and in fact provides a definitive choice to construct a geodesic from any vertex to the point at infinity. Further, this locally deterministic construction generalizes by use of Möbius transformations in order to construct geodesics between arbitrary vertices.

Theorem 2.14. *A geodesic between any $\frac{p}{q} \in \hat{\mathbb{Q}}$ and the point $\frac{1}{0}$ is found by starting at $\frac{p}{q}$ and iteratively moving to the Farey neighbor with lowest level.*

Proof. Given some $\frac{p}{q} \in L_n$, it is sufficient, by Lemma 2.10, to construct the nth partial Farey complex. The result holds by strong induction on the level n. The result is trivial for $n = 0$, as there is a zero-length path from $\frac{1}{0}$ to itself. Likewise, for $n = 1$, the only point in L_1 is $\frac{0}{1}$, which has a length 1 path directly to $\frac{1}{0}$. Similarly, one can exhaustively check that the result holds for all vertices for $n = 2$. Now, suppose that for all k less than or equal to some n, that any points in L_k have a geodesic defined by a path as described above. Now, take any $\frac{p}{q} \in L_{n+1}$. We name the Farey parents $\frac{r}{s}$ and $\frac{t}{u}$. Without loss of generality, $\frac{r}{s} \in L_n$ and $\frac{t}{u} \in L_k$ where $k < n$ (by Lemma 2.12). By the inductive hypothesis, a geodesic exists from $\frac{t}{u}$ to the point at infinity by moving to the Farey neighbor with lowest level. Let this distance be m. Similarly, a geodesic path exists from $\frac{r}{s}$ to the point at infinity. Suppose this distance were $g < m$. Then, from $\frac{t}{u}$, we could create a path through $\frac{r}{s}$ to infinity that had distance $g + 1 \leq m$. But, we know that $\frac{r}{s}$ is in a level higher than $\frac{t}{u}$, so this contradicts Lemma 2.13. Thus, the geodesic path from $\frac{r}{s}$ to infinity is greater than or equal to the geodesic path from $\frac{t}{u}$ to infinity. Thus, it is clear that a geodesic path from $\frac{p}{q}$ must move through $\frac{t}{u}$ in the lower level, as desired. □

Corollary 2.15. *A geodesic in the Farey complex between two arbitrary points, p/q and r/s, can be determined by applying a group element, $A \in PSL_2(\mathbb{Z})$, which sends p/q to $1/0$, constructing a path from $A(r/s)$ to $1/0$ by iteratively moving to the Farey neighbor with lowest level, and then applying A^{-1} to the elements of the path.*

3 Continued Fractions

Given any rational number, there exists a finite simple continued fraction of the form

$$\frac{p}{q} = a_0 + \cfrac{1}{a_1 + \cfrac{1}{a_2 + \cfrac{1}{\ddots + \cfrac{1}{a_n}}}},$$

where a_0 is an integer and for all $i \geq 1$, a_i is a positive integer. To condense the notation for a simple continued fraction, we use the common shorthand

$$\frac{p}{q} = [a_0;\, a_1,\, a_2,\, \ldots,\, a_n].$$

As there are precisely two ways to represent each rational number as a continued fraction, namely

$$\frac{p}{q} = [a_0;\, a_1,\, a_2,\, \ldots,\, a_n,\, 1] = [a_0;\, a_1,\, a_2,\, \ldots,\, a_n + 1],$$

we will assign the shorter expansion as the canonical form. For $p/q \in \mathbb{Q}$, we define p_i/q_i to be the $(i-1)$st convergent of a continued fraction, that is $p_i/q_i := [a_0;\, a_1,\, a_2,\, \ldots,\, a_{i-1}]$, with $p_0/q_0 = 1/0$. In this way $p_{n+1}/q_{n+1} = p/q$. Additionally, for all $m > 0$, if $a_m > 1$ we define "intermediate" values as follows:

$$k_{m,\,\ell} := \frac{\ell \cdot p_m + p_{m-1}}{\ell \cdot q_m + q_{m-1}},$$

where $1 \leq \ell \leq a_m - 1$ and $1 \leq j \leq n$. It is clear that an equivalent way of defining these values inductively. If $a_m > 1$, then

$$k_{m,\,1} = p_m/q_m \oplus p_{m-1}/q_{m-1} \tag{3.1}$$

and

$$k_{m,\,\ell} = k_{m,\,\ell-1} \oplus p_m/q_m \tag{3.2}$$

for $2 \leq \ell \leq a_m - 1$. From these definitions, it follows that the convergents, p_i/q_i, can also be characterized by Farey addition. If $a_m > 1$ then

$$p_{m+1}/q_{m+1} = k_{m,\,a_m-1} \oplus p_m/q_m \tag{3.3}$$

for all $m > 0$. Conversely, if $a_m = 1$, then there are no associated intermediate $k_{m,\ell}$ values, so

$$p_{m+1}/q_{m+1} = p_{m-1}/q_{m-1} \oplus p_m/q_m, \tag{3.4}$$

for all $m > 0$.

Given a rational number $p/q = [a_0; a_1, \ldots, a_n]$, we can use the sequence $(a_0, a_1, \ldots, a_n)$ to build a subcomplex of $\mathcal{F}$, called a Farey chain.

Definition 3.1. Given $p/q = [a_0; a_1, \ldots, a_n] \in \mathbb{Q}$, the *Farey chain* associated to p/q is the subcomplex of $\mathcal{F}$ whose vertices are precisely

$$\bigcup_{k=1}^{n} \{[a_0; a_1, \ldots, a_{k-1}], i \colon 1 \leq i \leq a_k\}.$$

We note that each vertex which correspond to a convergent, p_i/q_i, in the continued fraction expansion is adjacent $a_i - 1$ edges, which join p_i/q_i precisely to each $k_{i,j}$, for $1 \leq j \leq a_i - 1$. This observation leads naturally to the following definition.

Definition 3.2. The *ith fan* is the subcomplex of the Farey chain with vertices

$$\{p_{i-1}/q_{i-1}, p_i/q_i, p_{i+1}/q_{i+1}\} \cup \{k_{i,j} \colon 1 \leq j \leq a_i - 1\}.$$

In particular Hatcher proves the following result which shows that Farey chains are well-defined and consistent with the Farey complex [Hat1, page 15]:

Theorem 3.3. *The convergents for the continued fraction $\frac{p}{q} = [a_0; a_1, a_2, \ldots, a_n]$ are the vertices along a zigzag path consisting of a finite sequence of edges in the Farey diagram, starting at $1/0$ and ending at p/q. The path starts along the edge from $1/0$ to $a_0/1$, then turns left across a fan of a_1 triangles, then right across a fan of a_2 triangles, etc., finally ending at p/q.*

Hence, any path in a Farey chain has a corresponding path which exists in $\mathcal{F}$. For simplicity, we will represent the Farey chain in its geometric "canonical form" as a straight strip of triangles, where the labels are inductively added from left to right; starting with an edge connecting $1/0$ and $p_1/q_1 = a_0$, we calculate successive labels and edges by (3.1), (3.2), (3.3), and (3.4), as well as the values of the a_i.

We present a Farey chain in canonical form below, where the fans are drawn, however the $k_{i,j}$ are left out for clarity.

In particular, by the above observations, it is clear that every vertex in a Farey chain is defined by Farey addition, with exception of the first convergent $p_1/q_1 = a_0$. By Lemmas 2.11, 2.12, and 2.13, it follows that the Farey chain in fact must contain all geodesics between $1/0$ and p/q. We state this formally below.

Lemma 3.4. *For any $p/q \in \mathbb{Q}$, the associated Farey chain contains all geodesics from $1/0$ to p/q.*

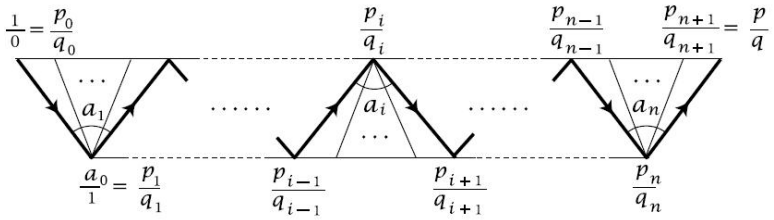

Figure 2: The Farey chain associated to p/q in canonical form

We can now exploit the continued fraction expansion of a rational number in order to calculate the length of any geodesic from said rational number to $1/0$. Often, this distance is the length of the path constructed by the continued fraction convergents, p_i/q_i, however, some exceptional cases can provide a more efficient path. The following theorem provides an exact formulation of the distance in terms of the continued fraction expansion.

Definition 3.5. Given a continued fraction expansion $\frac{p}{q} = [a_0; a_1, a_2, \ldots, a_n] \in \mathbb{Q}$, consider the string given by $\{a_1, a_2, \ldots, a_n\}$. Reading left to right, we define A_i to be the ith maximal subsequence of consecutive 1s. I.e.

$$A_i = \{a_j, a_{j+1}, a_{j+2}, \ldots, a_k\}$$

where $a_j = \cdots = a_k = 1$, $a_{j-1} \neq 1$ (unless $j = 1$), and $a_{k+1} \neq 1$.

Example 3.6. Consider $3588/2203 = [1; 1, 1, 1, 2, 3, 1, 1, 3, 1, 7]$. We have the following subsequences:

$$[1; \underbrace{1, 1, 1}_{A_1}, 2, 3, \underbrace{1, 1}_{A_2}, 3, \underbrace{1}_{A_3}, 7].$$

Theorem 3.7. *Given $\frac{p}{q} = [a_0; a_1, a_2, \ldots, a_n] \in \mathbb{Q}$, the Farey distance from $\frac{p}{q}$ to $\frac{1}{0}$ is given by*

$$n + 1 - \sum_{i=1}^{m} \left\lceil \frac{\#A_i}{2} \right\rceil$$

where there are m distinct subsequences A_i.

Proof. Given some $p/q \in \mathbb{Q}$, we construct its associated Farey chain. By Theorem 2.14, it suffices to construct a path starting from p/q and iteratively moving to the Farey neighbor of lowest level, where Lemma 3.4 implies that this geodesic path exists in the Farey chain. We recall that there are exactly two possible cases:

$$k_{m,\, a_m - 1} \oplus p_m/q_m = p_{m+1}/q_{m+1} \tag{3.5}$$

or

$$p_{m-1}/q_{m-1} \oplus p_m/q_m = p_{m+1}/q_{m+1}. \tag{3.6}$$

By (3.1) and (3.2), it is clear that for any fixed m and any ℓ, if $k_{m,\,\ell} \in L_n$ then $p_m/q_m \in L_k$, where $k < n$. So, in the case of (3.5), the desired geodesic path must pass from p_{m+1}/q_{m+1} to p_m/q_m, by Theorem 2.14. Similarly, in the case of (3.6), the path must pass from p_{m+1}/q_{m+1} to p_{m-1}/q_{m-1}. We recall that p_{m+1}/q_{m+1} is a Farey neighbor to p_{m-1}/q_{m-1} if and only if $a_m = 1$. So, if it were the case that the continued fraction expansion lacked any $a_i = 1$, then the length of the geodesic path would exactly equal the length of the continued fraction expansion. However, if there exists some $m > 0$ such that $a_m = 1$, then Theorem 2.14 implies that the geodesic path moves from p_{m+1}/q_{m+1} directly to p_{m-1}/q_{m-1}, implying that the convergent p_m/q_m is never reached, so we can subtract one from the total distance. However, if $a_{m-1} = 1$ as well, then we note that we cannot again subtract one from the total distance, since p_m/q_m is not a part of the geodesic, and therefore the value of a_{m-1} becomes irrelevant. We conclude, then, that we only can take a shorter route past some p_i/q_i for every odd 1 in a consecutive chain of 1s, with exception, of course, of the leading integer term: if $a_0 = 1$ then there is no sequential point to skip as a short cut. As such, the A_i subsequences are defined for sequences of ones strictly after the first term, and count only the odd numbered terms of the subsequence. This holds for all distinct subsequences of 1s, which proves our result. □

4 Number of Geodesics

The Farey complex is not a unique geodesic space, and as such it would be interesting to calculate precisely how many geodesics exist between two arbitrary rational numbers in $\mathcal{F}$. From Corollary 2.15 it is sufficient to have a mechanism to calculate the number of geodesics from arbitrary rational numbers to $1/0$. Given an arbitrary rational number, p/q, Lemma 3.4 implies that it is sufficient to simply study the Farey chain constructed from the continued fraction expansion of p/q in order to construct all geodesic paths from p/q to $1/0$. In particular, we can consider $p/q = [a_0;\, a_1,\, \ldots,\, a_n]$ as some union of Farey chains:

$$[a_0;\, \ldots,\, a_i] \cup [a_i;\, a_{i+1},\, \ldots,\, a_j] \cup \cdots \cup [a_k;\, \ldots,\, a_n].$$

Here, we must repeat the indices between chains so as to maintain all information. If we let $\mathcal{G}(p/q)$ count the number of geodesics from any p/q to $1/0$, then it is clear from the fundamental counting principle that

$$\mathcal{G}(p/q) \approx \mathcal{G}([a_0;\, \ldots,\, a_i]) \times \cdots \times \mathcal{G}([a_k;\, \ldots,\, a_n]),$$

where some errors may arise from the choice of the subchains due to cases where unions of geodesic paths are no longer geodesics or from instances of double-counting paths. As such, our goal is to quantify how to precisely subdivide Farey chains into fundamental strings without losing information in the process. To facilitate understanding, we recognize that the geometry of the Farey chain

provides all of the necessarily information to count geodesics. We recall that a string of a_is gives rise to a canonical Farey chain. Note that the first term a_0, of a continued fraction expansion does not have any effect on the number of geodesics as it does not define any fans in the Farey chain. As such, we adopt the convention that any string of $[a_1, \ldots, a_n]$ in this section defines an abstract Farey chain without values at the vertices and where each a_i defines the number of subdivisions in a given fan. That is, the following representations are essentially equivalent:

$$[a_0; a_1, a_2, \ldots, a_n] \Leftrightarrow [a_1, a_2, \ldots, a_n],$$

where the use of a semi-colon denotes a simple continued fraction form and the lack of a semi-colon implies a Farey chain without values attached.

Definition 4.1. We define the *left extreme* of a Farey chain as the vertex with lowest Farey level, and analogously define *right extreme* as the vertex with highest Farey level.

If we draw the Farey chain in the canonical form (as in Figure 3) then the left extreme corresponds to the left-most vertex and the right extreme corresponds to the right-most vertex, as expected. We will assume in this section that all Farey chains and subchains (subcomplexes which are also Farey chains) are always drawn in canonical form so that we can more readily discuss directions without ambiguity. Also, we label the vertices as P_i and $K_{i,j}$ to label the same vertices as the p_i/q_i and $k_{i,j}$, respectively, only without numeric value assigned.

Our first result considers an arbitrary Farey chain whose fans all have at least 3 subdivisions.

Lemma 4.2. *If $[a_1, a_2, \ldots, a_n]$ is a string where each $a_i > 2$, then there is a unique geodesic from the left extreme to the right extreme.*

Proof. We prove this by induction on the length of the string, n. For $n = 1$, we assume $a_1 > 2$. Then, we claim that the path from P_0 to P_1 to P_2 is minimal. To see this, we observe that if we instead took a path from P_0 to $K_{1,1}$ then the next step would necessarily have to be to move to the right extreme, P_2 in order to be a geodesic. However, no edge exists from $K_{1,1}$ to P_2 since $a_1 > 2$. So the original path is indeed minimal and unique. To prove the inductive step, assume that the result holds for strings up to length $n - 1$. Then, consider a string of length n where each $a_i > 2$. By the inductive hypothesis, we know that if we consider P_n to be the right extreme, then there exists a unique geodesic from the left extreme to P_n. Now, clearly the edge from P_n to P_{n+1} is the least path so we can adjoin this path to the one constructed by the inductive hypothesis. If another geodesic path existed, then it would have to clearly pass from P_{n-1} to P_{n+1} in two steps, however since $a_n > 2$ then, the $n = 1$ case implies that no such geodesic exists, so the geodesic is indeed unique. □

As Lemma 4.2 implies, then, it is sufficient to understand how Farey chains with fans that have at most 2 subdivisions. We begin with the simple cases, in

the following two lemmas. The first one deals with a Farey chain which has no subdivisions, and the second one deals with Farey chains in which each fan has exactly two subdivisions.

Lemma 4.3. *If* $[a_1\, a_2, \ldots, a_n]$ *is a string where each* $a_i = 1$*, then there are* $\psi(n)$ *geodesics from the left extreme to the right extreme, where*

$$\psi(n) = \begin{cases} \frac{n}{2} + 1 & : n \in 2\mathbb{N} \\ 1 & : n \in 2\mathbb{N} + 1 \end{cases}$$

Proof. We prove this first for the case where n is odd. If $n = 1$ then it is clear that the geodesic is unique. Given some $n \in 2\mathbb{N} + 1$, suppose that the result of unique geodesics holds for all odd integers less than n. Then, the inductive hypothesis states that a unique geodesic exists from the left extreme to P_{n-1}. Then, it is clear that the unique geodesic to P_{n+1} is simply continued from P_{n-1} to P_{n+1} as any other path would necessarily be at least two units longer.
In the case that n is even, we can use a simple counting argument to quickly reason that the function $\frac{n}{2} + 1$ is correct. Given an even length string, we note that there exist two "parallel" lines which are the line of connecting vertices of the form P_{2k}, and the line of connecting vertices of the form P_{2k+1}. Then, it is clear that in order to reach the right extreme from the left extreme in minimal moves, one must travel from P_0 to P_2 to P_4 and so on until at some vertex P_{2k} we move to P_{2k+1} and then continue to P_{2k+3} and so on until we reach the right extreme. It is quick to see that any other path will be less efficient than this family of paths. Clearly, the only free choice made is precisely the move from P_{2k} to P_{2k+1}. As there are n triangles, it is easy to see that there are $\frac{n}{2} + 1$ choices for geodesic paths. □

We recall the Fibonacci sequence, defined recursively as follows:

Definition 4.4. The *Fibonacci sequence*, with nth term denoted $fib(n)$, is defined as

$$fib(0) = 1,$$
$$fib(1) = 1,$$

and

$$fib(n) = fib(n-1) + fib(n-2)$$

for $n \geq 2$.

Lemma 4.5. *If* $[a_1, a_2, \ldots, a_n]$ *is a string where each* $a_i = 2$*, then there are* $fib(n+1)$ *geodesics from the left extreme to the right extreme.*

Proof. As a note, we recall that from Theorem 3.7, the length of the geodesics from left extreme to right extreme would be the distance from $1/0$ to $[0; a_1, a_2, \ldots, a_n]$. This distance is clearly $n + 1$, so we aim to find all paths of length $n+1$. We prove the result by induction. Let $n = 1$. One can quickly check that there are $fib(2) = 2$ minimal paths of length 2 from the left extreme to the right extreme. Similarly, for $n = 2$, one can exhaustively check the paths and

find that there are $fib(3) = 3$ minimal paths of length 3 from the left extreme to the right extreme. So, suppose that the result holds for all $k < n$, where $n \geq 3$. Then, beginning from the left extreme, we have two cases: moving from P_0 to P_1 or moving from P_0 to $K_{1,1}$. In the first case, we use the inductive hypothesis on the string $[a_2, \ldots, a_n]$, so from the point P_1 to the right extreme to conclude that there are $fib(n)$ geodesics of length n. But, any of these geodesics unioned with the single edge from P_0 to P_1 is a path of length $n+1$, and so is a geodesic. Similarly, in the second case, if we move from P_0 to $K_{1,1}$ then moving from $K_{1,1}$ to P_1 would not lead to any geodesic path, so it must be the case that we move from P_0 to $K_{1,1}$ to P_2. Again, the inductive hypothesis implies that there are $fib(n-1)$ geodesics of length $n-1$ from P_2 to the right extreme. Hence, the union of any of these geodesics with the path from P_0 to P_2 through $K_{1,1}$ must be a path of length $n+1$, and hence is a geodesic from left extreme to right extreme. By our construction of cases, we have avoided any double-counting but have been exhaustive. As such, there are $fib(n-1) + fib(n) = fib(n+1)$ geodesics from the left extreme to the right extreme, as desired. □

In order to combine the previous two lemmas, we recognize that the the function used to determine the number of geodesics associated to a string of ones has two very unrelated outputs. For simplicity, it turns out to be useful to consider these cases individually, rather than in one large result. We first consider the case when we have a a string of ones and twos, with an odd number of ones in a row.

Lemma 4.6. *If $[a_1, a_2, \ldots, a_n]$ is a string of odd length such that $a_1 = a_n = 2$ and $a_i = 1$ for all other i, then there is a unique geodesic from the left extreme to the right extreme.*

Proof. If we consider the substring of $[a_2, \ldots, a_{n-1}]$, then Lemma 4.3 implies that there is a unique geodesic from P_1 to P_n. Then, we note that Theorem 3.7 implies that this path unioned with the edges from P_0 to P_1 and P_n to P_{n+1} is a geodesic from the left extreme to the right extreme. To see that it is unique, then it is clear that a different path must, without loss of generality (by symmetry) pass from P_0 to P_2, since if it did not, then it would contradict Lemma 4.3. However, if at any point the path moves from P_{2k} to P_{2k+1}, for $k > 0$, then it is clearly not a geodesic since a shorter path could be found to P_{2k+1}. If it never does so, then the path would be of the form

$$P_0 \to K_{1,1} \to P_2 \to P_4 \to \cdots \to P_{n-1} \to K_{n-1,1} \to P_{n+1}.$$

But the length of this path is two greater than the length of the geodesic previously constructed. Thus, the geodesic of this chain is unique. □

Finally, we prove the most powerful result, which will encompass Lemmas 4.3 and 4.5. First, we introduce necessary notation.

Definition 4.7. Let $[a_1, a_2, \ldots, a_n]$ be a string which alternates between bundles of 2's and even length bundles of 1's with $a_1 = 2$. Then, b_0 is the length

of the maximal consecutive chain of 2's starting from a_1. That is, if i is the minimal i such that $a_i = 1$, then $b_0 = i - 1$. Then, b_1 is the length of the maximal consecutive chain of 1's starting from a_{b_0+1}. We continue this pattern until we exhaust the entire string, so that $\sum b_k = n$.

Example 4.8. Consider the chain [2, 2, 2, 1, 1, 1, 1, 2, 2, 1, 1, 2, 1, 1, 1, 1]. Then,

$$[\underbrace{2, 2, 2}_{b_0}, \underbrace{1, 1, 1, 1}_{b_1}, \underbrace{2, 2}_{b_2}, \underbrace{1, 1}_{b_3}, \underbrace{2}_{b_4}, \underbrace{1, 1, 1, 1}_{b_5}],$$

so $b_0 = 3$, $b_1 = 4$, $b_2 = 2$, $b_3 = 2$, $b_4 = 1$, $b_5 = 4$.

Theorem 4.9. *If $[a_1, a_2, \ldots, a_n]$ is a string with $a_1 = 2$ which alternates between bundles of 2's and even length bundles of 1's, then there are $K_i(b_0, \ldots, b_i)$ geodesics from the left extreme to the right extreme where K_i is defined recursively as:*

$$K_0(b_0) = fib(b_0 + 1)$$

and

$$K_i(b_0, \ldots, b_i) = \begin{cases} K_{i-1}(b_0, \ldots, b_{i-1}) \\ +\psi(b_i - 2) \cdot K_{i-1}(b_0, \ldots, b_{i-1} - 1) & \text{if } i \in 2\mathbb{N} + 1 \\ \\ K_{i-1}(b_0, \ldots, b_{i-1}) \cdot K_0(b_i - 1) \\ +K_{i-2}(b_0, \ldots, b_{i-2} - 1) \cdot K_0(b_i - 2) & \text{if } i \in 2\mathbb{N} \end{cases} \tag{4.1}$$

Proof. We prove this by induction on the index i of K_i. For $i = 0$, the result holds by Lemma 4.5. Then, we have two cases to check, whether i is even or odd. In the case that i is odd, then assume that the recursion holds for all $m < i$. Then, b_i is some bundle of an even number of 1's, and we will call t_0 the left extreme of this bundle, and label successive (from lowest levels to highest levels, i.e. left to right) by successive t_is. We consider two cases: either the geodesic path passes through t_1, or it does not. In the case that it does, the inductive hypothesis states that there are $K_{i-1}(b_0, \ldots, b_{i-1})$ geodesic paths from P_0 to the point t_1. Then, it is clear that the path from t_1 to the right extreme is defined over an odd numbered list of 1's, so Lemma 4.3 implies that the geodesic from t_1 to the right extreme is unique. To see that the union of any of the $K_{i-1}(b_0, \ldots, b_{i-1})$ geodesic paths with the unique geodesic from t_1 to the right extreme is still a geodesic of the entire string, we note that the geodesic constructed from Theorem 3.7 is contained in this set of geodesics, and as all have equal length, they are all geodesics. Alternatively, it is possible that a path is defined from t_0 to t_2. Again, by the inductive hypothesis, there are $K_{i-1}(b_0, \ldots, b_{i-1} - 1)$ geodesics from the left extreme to t_0. We note the special care to avoid double counting any paths from the first set of geodesics already considered by forcing the path to travel from t_0 to t_2. In this case,

we see that Lemma 4.3 implies that there are a total of $\psi(b_i - 2)$ geodesics from t_2 to the right extreme. Again, the union of any geodesic defined by the $K_{i-1}(b_0, \ldots, b_{i-1} - 1)$ term to any of the $\psi(b_i - 2)$ geodesics is a geodesic of the full string since one quickly reasons that the length of any of these strings is equal to the length of the geodesics defined in the first case of the proof. These cases are disjoint and exhaustive, and as such we conclude that there are a total of $K_{i-1}(b_0, \ldots, b_{i-1}) + \psi(b_i - 2) \cdot K_{i-1}(b_0, \ldots, b_{i-1} - 1)$ geodesics as desired.

In the case that i is even, again assume that the recursion holds for all $m < i$. Then, b_i is some bundle of 2's, and we will call t_0 the left extreme of this bundle, and label the following vertices similarly as above. We consider the following two cases: either the path passes through t_1 or it does not. In the case that the path passes through t_1 we see that there are $fib(b_i) = K_0(b_i - 1)$ geodesic paths from t_1 to the right extreme. Then, there are, by the inductive hypothesis, $K_{i-1}(b_0, \ldots, b_{i-1})$ geodesics from the left extreme to t_1. We note that the geodesic as constructed by Theorem 3.7 is included in this set, and so as all paths have the same length, they must all be geodesics. In the case that we do not pass through t_1 then we conclude that we pass from t_0 to $k_{1,0}$ to t_2. We see that there are $fib(b_i - 1) = K_0(b_i - 2)$ geodesics from the right extreme to t_0 in this manner. But, then a geodesic from t_0 to the left extreme has a bundle of an odd number of 1's, so Lemma 4.3 and Lemma 4.6 imply that there is a unique geodesic from t_0 past the bundle of 1's to a bundle of 2's. But, Lemma 4.6 implies that the final 2 in this bundle cannot contribute any new geodesics, so as such there are in fact $K_{i-2}(b_0, \ldots, b_{i-2} - 1)$ geodesics from the left extreme to t_0. Again, the union of these geodesics has the same length as any of the geodesics which pass through t_1, and so each is a new geodesic. So, in total we have constructed exhaustively $K_{i-1}(b_0, \ldots, b_{i-1}) \cdot K_0(b_i - 1) + K_{i-2}(b_0, \ldots, b_{i-2} - 1) \cdot K_0(b_i - 2)$ geodesics. This completes the inductive step and so the result holds for all i. □

Remark 4.10. In the case that $[a_1, \ldots, a_n]$ is a string with $a_1 = 1$ which alternates between even length bundles of 1's and bundles of 2's, then one can quickly reason that we simply take $b_0 = 0$ and apply the theorem above similarly. Also, one can check that the result does not alter for seemingly degenerate cases where $b_i = 1$ or $b_i = 2$, since $fib(0) = fib(1) = 1$.

With the results of Theorem 4.9 and Lemmas 4.2 and 4.3, it is now possible to calculate the number of geodesics from p/q to $1/0$. If $p/q = [a_0; a_1, \ldots, a_n]$, then the number of geodesics to $1/0$ is given by the number of geodesics from left extreme to right extreme of the abstract Farey chain $[a_1, \ldots, a_n]$. Starting from a_1, if $a_1 > 2$, then construct the maximal substring $[a_1, \ldots, a_i]$ where $a_k > 2$ for all $k \leq i$. If $a_1 \leq 2$, then create a maximal substring of the form in Lemma 4.6 or Theorem 4.9. In the case that the string of 2s, $[a_1, \ldots, a_m]$ is followed by an odd number of ones, we simply recall that Lemma 4.2 implies that we can only consider the string $[a_n, \ldots, a_{m-1}]$ as a maximal string of 2s.

We continue this pattern until the entire string $[a_1, \ldots, a_n]$ is divided into fundamental chains. Underlying these choices of partitions are the vertices which are unavoidable by any geodesic path, as determined by Lemmas 4.2, 4.3,

and 4.6. As such, these choices of subchains are exhaustive and non-repetitive. Symbolically:

$$\begin{aligned}\mathcal{G}(p/q) &= \mathcal{G}([a_0;\, a_1,\, \ldots,\, a_i]) \times \mathcal{G}([a_i;\, a_{i+1},\, \ldots,\, a_j]) \\ &\quad \times \cdots \times \mathcal{G}([a_{k-1};\, a_k,\, a_{k+1},\, \ldots,\, a_n]) \\ &= \mathcal{G}([a_1,\, \ldots,\, a_i]) \times \mathcal{G}([a_{i+1},\, \ldots,\, a_j]) \times \cdots \times \mathcal{G}([a_k,\, a_{k+1},\, \ldots,\, a_n]) \\ &= \prod K_\ell,\end{aligned}$$

since $\mathcal{G}([a_m,\, \ldots,\, a_n]) \neq 1$ if and only if $[a_m,\, \ldots,\, a_n]$ is of the form given by Theorem 4.9.

5 Further Investigations

5.1 Diameter of F_n

An interesting question involves calculating the asymptotic behavior of the F_n; we are particularly interested in calculating the diameter of a given F_n as a function of n. For simplicity of notation, we write d_F to be the combinatorial metric on $\mathcal{F}$. We recall the following definition:

Definition 5.1. The *diameter* of F_n is denoted $diam(F_n)$ and defined as

$$diam(F_n) = \max\{d_F(x,\, y)\colon x,\, y \in F_n\}.$$

Intuitively, given some non-trivial F_n, if $x,\, y \in F_n$ satisfy $d_F(x,\, y) = diam(F_n)$, then it should hold that $x,\, y \in L_n$. The converse, however, may not necessarily be true. As such, a characterization of vertices which are inherently far apart would be very useful. Given some p/q, its negative reciprocal $-q/p$ should be one of the furthest points from p/q. It turns out that there will always exist some p/q satisfying the condition that $d_F(p/q, -q/p) = diam(F_n)$. The following lemma constructs these points inductively.

Definition 5.2. We call p/q an *nth level Farey reciprocal* if

$$d_F(p/q,\, -q/p) = n.$$

Proposition 5.3. *For all $n \geq 2$, there exists an nth level Farey reciprocal $p \in L_n$ such that*

$$p = r \oplus t$$

where $r \in L_{n-1}$ and $t \in L_{n-2}$ are an $n-1$st level Farey reciprocal an $n-2$nd level Farey reciprocal, respectively. In particular, $diam(F_n) = n$.

Proof. We let x^* represent the negative reciprocal of x, in this proof. The result holds for our base cases of $n = 2$ and $n = 3$. Assume the result holds up to some $n-1$, and let $r \in L_{n-1}$ be such that $d_F(r,\, r^*) = n-1$ and

$$r = t \oplus u$$

where $t \in L_{n-2}$ and $u \in L_{n-3}$ are an $n-1$st level Farey reciprocal an $n-2$nd level Farey reciprocal, respectively. Then, we claim that

$$p := r \oplus t \in L_n$$

is an nth level Farey reciprocal. Now, we know that $d_F(r, r^*) = n-1$ and $d_F(t, t^*) = n-2$ by construction. As all geodesics between p and p^* live in F_n, then Lemmas 2.10 and 2.6 imply that every geodesic path from p to p^* must travel through some combination of r, r^*, t, and t^*. It is clear that $d_F(r, t^*) \geq n-2$ (and similarly $d_F(r^*, t) \geq n-2$), since if it were not, then we would be able to construct a path of length less than $n-1$ from r to r^*, a contradiction. So, if we consider the four possible cases through which a path can pass from p to p^*, then it is clear that a minimal path will be achieved by

$$p \to t \to \cdots \to t^* \to p^*,$$

since $d_F(t, t^*) = n-2$. We conclude that p is an n level Farey reciprocal.

It remains to show that $diam(F_n) = n$. From the work above, $diam(F_n) \geq n$. Suppose, without loss of generality, that $diam(F_n) = n+1$. Then, there would exist some $p, q \in F_n$ such that $d_F(p, q) = n+1$. Consider

$$p = r \oplus t$$

and

$$q = u \oplus v.$$

Then, $r, t, u, v \in F_{n-1}$. So, the inductive hypothesis implies that the distance between any of the four points must be at most $n-1$. At most, two of the four points can live in L_{n-1}, say $r, u \in L_{n-1}$, by Lemma 2.12. In the worst case, we assume without loss of generality that $d_F(r, u) = n-1$. But as $t, v \notin L_{n-1}$, then the inductive hypothesis on these two points implies that $d_F(t, v) < d_F(r, u)$. So, by constructing a path from p to t to v to q, we conclude that $d_F(p, q) \leq d_F(t, v) + 2 < n+1$. This is a contradiction; we conclude that $diam(F_n) = n$. □

5.2 Alternative Geodesic Algorithm

Theorem 2.14 is convenient because it requires only local information to propagate the geodesic path to $1/0$. The specific path choice and distance, however is dependent on calculating the Farey parents and determining which parent has lower level. Likewise, Theorem 3.7 requires calculating the entire continued fraction expansion. Although such calculations are possible, a continued fraction expansion, for example, could be arbitrarily long, costing an unreasonable amount computational memory. We would like to construct a path whose construction is computationally cheaper and without the need of any oracle machine to compute Farey parents. First note the following inherent symmetry in a Farey chain: given some chain of fans, we can simply rotate or reflect it so as to map the vertex of p/q to $1/0$ and $1/0$ to p/q. In this way, although

the convergents' values are lost, we recognize that every geodesic in the original Farey chain maps to a geodesic in the transformed Farey chain. As the proof of Theorem 3.7 implies, the shape (specifically the subdivisions) of the Farey chain determines the geodesic paths, and not the values of the vertices. Hence, given a geodesic of the Farey chain, we can apply a rotation/reflection in order to construct a geodesic in the new, rotated/reflected Farey chain. These observations are summarized in the following lemma:

Lemma 5.4. *Given $p/q = [a_0; a_1, a_2, \ldots, a_n] \in \mathbb{Q}$, the distance from $1/0$ to p/q is equal to the distance from $1/0$ to $r/s := [b_0; a_n, \ldots, a_2, a_1]$, where $b_0 \in \mathbb{Z}$. Further, all geodesics from $1/0$ to p/q are in bijection with all geodesics from $1/0$ to r/s by reflection/rotation of the associated Farey chains.*

Further, we aim to construct a geodesic which is propagated from $1/0$ to p/q. We use Lemma 5.4 to do so. So, given $p/q = [a_0; a_1, a_2, \ldots, a_n]$, we simply rotate/reflect the associated Farey chain, and use Theorem 3.7 to construct a geodesic from the geometric properties of the Farey chain. Then, we can perform the same rotation/reflection as the beginning in order to retain our original Farey chain with correct labels. Encoding this conjugation action allows us to simply determine a new geometric rule for construction a geodesic from $1/0$ to p/q using only local information.

To do so, we recall that the continued fraction expansion can be recovered from the Euclidean algorithm. Specifically, given $p/q \in \mathbb{Q}$, then the first term of the continued fraction expansion, a_0, satisfies

$$p = a_0 \cdot q + r_0,$$

where $r_0 < q$ by the division algorithm. The next iteration is as follows:

$$q = a_1 \cdot q_1 + r_1,$$

where $r_1 < q_1$ by the division algorithm. So, following the iterative process of the Euclidean algorithm will satisfy the following property:

$$q_i = a_{i+1} \cdot q_{i+1} + r_{i+1},$$

where we continue the process until $r_j = 0$ for some j. Stripping the sequence of a_i terms from these calculations reconstructs the continued fraction expansion of p/q. It is important to note that computing some a_j term only requires information from the calculation of the a_{j-1} term in order to calculate the value of a_{j+1}. This observation, along with the fact that we can construct geodesics geometrically by conjugation, immediately yields the following algorithm to construct geodesic paths. This process only requires a fixed number of values to be stored to memory at any given time, which greatly improves the previous results.

Proposition 5.5. *Given $p/q \in \mathbb{Q}$, a geodesic path from $1/0$ to p/q in $\mathcal{F}$ can be found by iterating steps of the Euclidean algorithm (beginning on p, q and iteratively on their quotients and remainders) and following this algorithm:*

1. *First, simply record a_0 and start the path at $1/0 =: p_0/q_0$.*
    - *If $a_1 > 1$ then continue the path to $a_0/1 =: p_1/q_1$, and continue the algorithm by checking a_2.*
    - *If $a_1 = 1$ then continue the path to $\frac{a_0+1}{1} =: p_1/q_1$, and continue the algorithm by checking a_3.*
2. *In general:*
    - *If the remainder of the Euclidean algorithm computation of a_i is 0, then terminate after the ith loop completes.*
    - *If $a_i > 1$ then continue the path from p_i/q_i to $\frac{a_{i+1}p_i+p_{i-1}}{a_{i+1}q_i+q_{i-1}}$, and continue the algorithm by checking a_{i+1}.*
    - *If $a_i = 1$, then continue the path to $\frac{p_{i-1}+p_{i-2}}{q_{i-1}+q_{i-2}}$, and continue the algorithm by checking a_{i+2}.*

6 Programs

6.1 Height Function

It turns out that computing the Farey level of a rational number is quite difficult, as it requires computing successive F_n until said rational number is constructed. However, most of our results do not require the specific Farey level of a rational number so much as a comparison of Farey levels between two numbers. As such, we recall the following measure of complexity of a rational number, as defined by Silverman and Tate, and explore its relation to Farey levels.

Definition 6.1 ([ST1])**.** The *height* of a rational number, $\frac{p}{q}$, is given by the function $H\colon \hat{\mathbb{Q}} \to \mathbb{Z}$ defined by

$$H\left(\frac{p}{q}\right) = \max\{|p|, |q|\}.$$

Lemma 6.2. *If $\frac{a}{b} \in \mathbb{Q} \setminus \left\{\frac{0}{1}, \frac{\pm 1}{1}\right\}$ has Farey parents $\frac{p}{q}$ and $\frac{r}{s}$, then*

$$H\left(\frac{a}{b}\right) > \max\left\{H\left(\frac{p}{q}\right), H\left(\frac{r}{s}\right)\right\},$$

and furthermore

$$H\left(\frac{p}{q}\right) \neq H\left(\frac{r}{s}\right).$$

Proof. As $\frac{p}{q}$ and $\frac{r}{s}$ are Farey neighbors, by Lemma 2.4 they must necessarily have like sign, which implies that

$$|p + r| = |p| + |r|$$

and

$$|q+s| = |q| + |s|.$$

Also, since $\frac{0}{0} \notin \hat{\mathbb{Q}}$, we deduce that $H(m)$ must be strictly positive for any $m \in \hat{\mathbb{Q}}$. Now, it is clear that

$$H\left(\frac{a}{b}\right) = \max\{|p+r|, |q+s|\} = \max\{|p|+|r|, |q|+|s|\} \geq |p|+|r| \geq |p|.$$

Similarly, one can show that $H\left(\frac{a}{b}\right)$ is greater than or equal to any of $|r|$, $|q|$, or $|s|$. So, it must hold that

$$H\left(\frac{a}{b}\right) \geq H\left(\frac{p}{q}\right)$$

and

$$H\left(\frac{a}{b}\right) \geq H\left(\frac{r}{s}\right).$$

Suppose that there were equality in either case. Without loss of generality, we assume that

$$H\left(\frac{a}{b}\right) = H\left(\frac{p}{q}\right) = |p|.$$

So $\left|\frac{p}{q}\right| > \frac{1}{1}$ and $|p| = H\left(\frac{a}{b}\right) = |p+r| = |p| + |r|$, so $|r| = 0$. But, this implies that $\frac{r}{s} = \frac{0}{1}$. But this is impossible since $\frac{p}{q}$ and $\frac{r}{s}$ are Farey neighbors, and it cannot hold that $\frac{r}{s}$ is a Farey neighbor with a number greater than $\frac{1}{1}$. So, the inequality must be strict in this case. The other case follows similarly if we assume

$$H\left(\frac{a}{b}\right) = H\left(\frac{p}{q}\right) = |q|.$$

This leads to a similar contradiction where $\frac{r}{s} = \frac{1}{0}$ and $\frac{p}{q} < \frac{1}{1}$. This proves the first part of the claim. To prove that $H\left(\frac{p}{q}\right) \neq H\left(\frac{r}{s}\right)$ it is necessary to consider $\frac{p}{q}$ and $\frac{r}{s}$ as elements in levels of the Farey complex. Lemma 2.12 implies that the two numbers cannot be in the same level of the Farey complex. Thus $\frac{p}{q}$ is a Farey parent of $\frac{r}{s}$ or vice versa. We assume, without loss of generality, that $\frac{p}{q}$ is a Farey parent of $\frac{r}{s}$. So, there exists a Farey neighbor to $\frac{p}{q}$, say $\frac{p'}{q'}$, such that

$$\frac{r}{s} = \frac{p}{q} \oplus \frac{p'}{q'}.$$

But, the work from the first part of the claim implies that

$$H\left(\frac{p}{q}\right) > H\left(\frac{r}{s}\right),$$

so the claim is established. □

Lemma 2.12 and Lemma 6.2 together immediately lead to the following equivalence:

Proposition 6.3. *If $\frac{p}{q}$ and $\frac{r}{s}$ are Farey neighbors, then $H\left(\frac{p}{q}\right) < H\left(\frac{r}{s}\right)$ if and only if $\frac{p}{q}$ is in a lower level than $\frac{r}{s}$.*

6.2 Maple Code

The following are a series of procedures written in Maple code which act in two classes. The first class of programs forms the first method of computation of Farey distance utilizing the results of Theorem 2.14. In this method, the computational time is longer, but for small calculations, it is more beneficial because it also includes a list containing the vertices of the path. Of course, the program could be made faster by not incorporating this list, however it would still be less efficient than the second class of programs. This second class of programs only returns a single number which is the Farey distance between two points. It is much faster and relies on the results of Theorem 3.7.

6.2.1 Method 1

```
LinfFarey := proc (r)::list;
local d, f, i, p1, p2, q;
description "Creates a list of points along the geodesic
             path from r to infinity";
q := r; d := [ ]; f := 1;
if q < 0 then
     q := -q;
     f := -1;
end if;
do
if q = infinity then
     if f = -1 then
          for i to nops(d) do
               d[i] := -d[i];
          end do;
     end if;
break;
elif q = 0 then
     d := [op(d), 0];
     if f = -1 then
          for i to nops(d) do
               d[i] := -d[i];
          end do;
     end if;
break;
elif q = 1 then
     d := [op(d), 1];
     if f = -1 then
          for i to nops(d) do
```

```
               d[i] := -d[i];
          end do;
     end if;
break;
elif numer(q) = 1 then
     d := [op(d), q];
     d := [op(d), 0];
     if f = -1 then
          for i to nops(d) do
               d[i] := -d[i];
          end do;
     end if;
break;
elif denom(q) = 1 then
     d := [op(d), q];
     if f = -1 then
          for i to nops(d) do
               d[i] := -d[i];
          end do;
     end if;
break;
else
     d := [op(d), q];
     igcdex(numer(q), denom(q), 'x', 'y');
     p1 := -y/x; p2 := (numer(q)+y)/(denom(q)-x);
     if abs(-y)+abs(x) < abs(numer(q)+y)+abs(denom(q)-x) then
          q := p1;
     else q := p2;
     end if;
end if;
end do;
return d;
end proc;

LFarey := proc (t, r)::list;
local dis, i;
description "Creates a list of points along the geodesic from
             t to r"
if t = infinity then
     dis := Reverse([op(LinfFarey(r)), t]);
elif r = infinity then
     dis := [op(LinfFarey(t)), r];
else
     igcdex(numer(r), denom(r), 'a', 'b');
     dis := LinfFarey((a*t+b)/(denom(r)*t-numer(r)));
     for i to nops(dis) do
```

```
          dis[i] := (numer(r)*dis[i]+b)/(denom(r)*dis[i]-a);
     end do;
     dis := [op(dis), r];
end if;
return dis;
end proc;
```

6.2.2 Method 2

```
countones := proc (mylist::list, b::integer)::integer;
local c, i;
description "Counts the number of consecutive ones in a list
             starting from a given index";
c := 0;
for i from b to nops(mylist) do
     if mylist[i] = 1 then
          c := c+1
     else
          break;
     end if;
end do;
return c;
end proc;
```

```
infFarey := proc (q::rational)::integer;
local dis, ct, clist, k, i;
description "Computes the distance from an arbitrary rational number to 1/0";
if abs(q) = 1 then
     dis := 1;
     return dis;
     break;
end if;
clist := cfrac(abs(q), quotients);
dis := nops(clist);
clist := clist[2 .. ];
while member(1, clist, 'k') do
     ct := countones(clist, k);
     dis := dis-ceil((1/2)*ct);
     clist := clist[k+ct .. ]
end do;
return dis;
end proc;
```

```
Farey := proc (q, r)::integer;
local dis;
description "Finds the Farey distance between two arbitrary rational numbers";
if (q = r) or (q=infinity and r=-infinity) or (q=-infinity and r=infinity) then
```

```
     dis := 0;
elif q = infinity then
     dis := infFarey(r);
elif r = infinity then
     dis := infFarey(q);
else
     igcdex(numer(q), denom(q), 'x', 'y');
     dis := infFarey((-x*r-y)/(denom(q)*r-numer(q)));
end if;
return dis;
end proc;
```

7 Acknowledgements

The author would like to extend his deepest thanks to Professor Kevin Pilgrim, whose guidance and support led to wonderful inspiration and mathematical advancement. He also extends gratitude to Indiana University for the accommodations and facilities so generously provided, as well as to the National Science Foundation for their continued support of REU programs.

References

[GKP1] R.L. Graham, D.E. Knuth, and O. Patashnik, *Concrete Mathematics: A Foundation for Computer Science*, Addison-Wesley, Reading, MA, 1989.

[Hat1] A. Hatcher, *Topology of Numbers*, in preparation (2011), available at *http://www.math.cornell.edu/ hatcher/TN/TNpage.html*

[Min1] Y. N. Minksy, *The classification of punctured-torus groups*, Ann. of Math. (2) **149** (1999), 559–626.

[Pil1] K. Pilgrim, *distance formula in Farey graph?*, MathOverflow (2010), available at *http://mathoverflow.net/questions/33002*

[ST1] J.H. Silverman and J.T. Tate, *Rational Points on Elliptic Curves*, Springer, 1992.

.

Combinatorial Expansion Factors

Rachel Moger-Reischer

1 Introduction

Consider the two-sphere S^2 described as in [1] as a square pillowcase.

Definition 1.1. A *square pillowcase* is the 2-sphere obtained by gluing two square tiles by a homeomorphism of their edges.

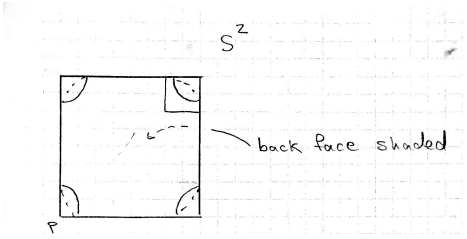

Figure 1: A square pillowcase

We call this cell complex Q_0. We will discuss our own subdivision rule shortly, but first we consider the motivation for our project; namely, some other, simpler examples of cell complexes that develop as a result of subdivision rules.

The idea of having a cell structure on a square pillowcase is one that has been seen before, most notably in the Lattés examples. As with the Lattés examples, we will look at a subdivision rule iterated repeatedly, where our definition of a subdivision rule is that of Cannon, Floyd, Kenyon, and Parry in [1].

Definition 1.2. (Cannon, Floyd, Kenyon, & Parry) A *finite subdivision rule* consists of:

1. a finite two-dimensional cell complex S_R (called the *model subdivision complex*);
2. a subdivision $R(S_R)$;
3. a continuous cellular map $\sigma_R : R(S_R) \to S_R$ (called the *subdivision map*), which restricts to a homeomorphism on each open cell of $R(S_R)$.

A number of variations on the Lattés subdivision rule are given on [2]. In looking at any particular example, we can consider the combinatorial distance

across the cell complex at a fixed level n, where n is the number of iterations of the subdivision rule. By combinatorial distance, we simply mean the number of tiles one must cross in getting from one side to the other. Complex though some of these variations are, nonetheless a minimal path across each example crosses 2^n tiles.

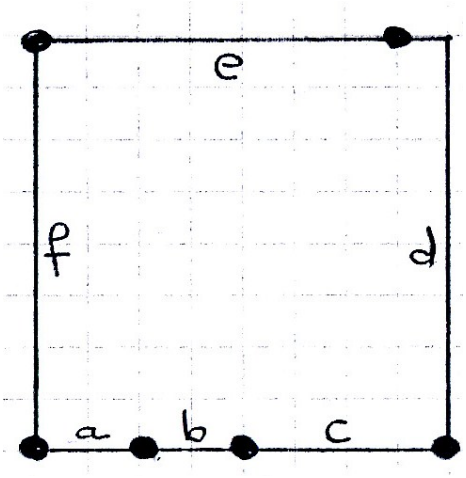

Figure 2: Q_0

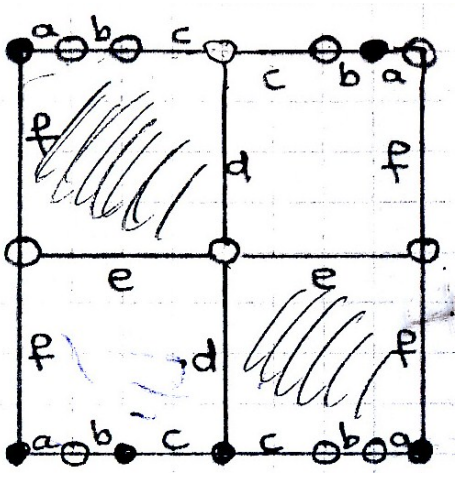

Figure 3: Q_1

Thinking that it might be interesting to look for a subdivision rule that does not have this property, we developed the subdivision rule and the corresponding series of cell complexes that are the topic of this paper. We call the cell complex

after n iterations of the subdivision rule Q_n. We sought a more complicated cell complex that might have minimal combinatorial distance less than 2^n. Thus, rather than having the two faces of the square pillowcase be squares, we let them be hexagons where the six edges are labeled a, b, c, d, e, f and the vertices are placed as in fig: 2. The set of all edges at level n is denoted $E(Q_n)$ and the set of all vertices at level n is denoted $V(Q_n)$. We note that the definition of square pillowcase preserves all labels and orientations of edges.

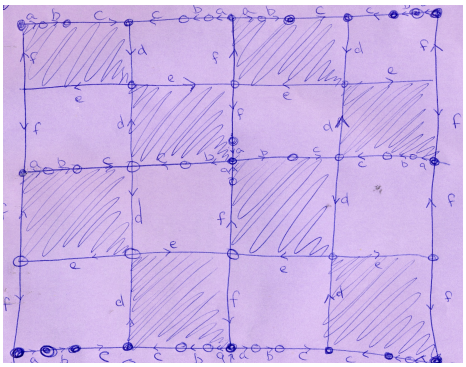

Figure 4: Q_2

Our subdivision rule is one which maps edges of Q_n to edges of Q_{n+1} as follows:

- $a \mapsto a, b$
- $b \mapsto c$
- $c \mapsto c, b, a$
- $d \mapsto f, f, a$
- $e \mapsto b, c, c, b, a$
- $f \mapsto f, f$

where the order of the labels of the new edges reflects their order with respect to the orientation of the original edges.

We then draw two additional edges—one from the vertex that is between what were the b and c edges of the previous iteration to the new vertex between the two new c edges on what was the e edge of the previous iteration and the other from the new vertex between the two f edges created from what was the f edge of the previous iteration to the new vertex between the two f edges that were created from what was a d edge the previous iteration. These two new edges intersect at a vertex. The first becomes two new d edges and the second becomes two new e edges.

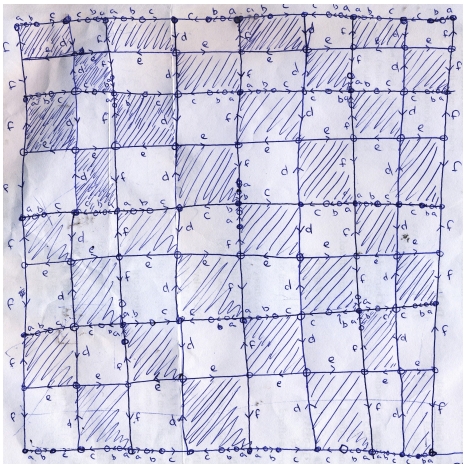

Figure 5: Q_3

Our subdivision rule is a member of the one parameter family that is formally defined and shown to exist in [3].

Iterating this subdivision rule yields the cell complexes depicted in fig: 3, fig: 4, fig: 5, and fig: 6.

What interests us, then, is the growth rate of the minimal distance $D(n)$ from one side of Q_n to an opposite side. This can be articulated in terms of the limit $\lim_{n\to\infty} D(n)^{\frac{1}{n}}$, which we know to exist by previous work in the area. Because the faces of Q_0 are hexagons, what is meant by opposite sides is non-obvious.

Definition 1.3. We say that two sides of Q_0 are *opposite* if they share no vertices. We define a *side* of Q_n to be union of the edges between two of the vertices at level n that were vertices of Q_0. Sides of Q_n are *opposite* if the corresponding sides of Q_0 were opposite.

2 Paths, Bands, and Shortcuts

As we iterate our subdivision rule, we often find it convenient to look at particular subsets of Q_n. Let t_i be some tile of Q_n. By $E(t_i)$ we denote the set of all edges of t_i and by $V(t_i)$ we denote the set of all vertices of t_i.

Definition 2.1. We define a *path* β at level n, denoted β_n,to be a sequence of tiles such that for any two tiles t_i and t_{i+1}, $V(t_i) \cap V(t_{i+1}) \neq \emptyset$.

Definition 2.2. We define a *band* to be a sequence of connected tiles, where by connected we mean that the tiles t_i and t_{i+1} are such that $E(t_i) \cap E(t_{i+1}) \neq \emptyset$.

The distinction, then, between bands and paths is this: while successive tiles in a band must share an edge, successive tiles in a path need only share a vertex.

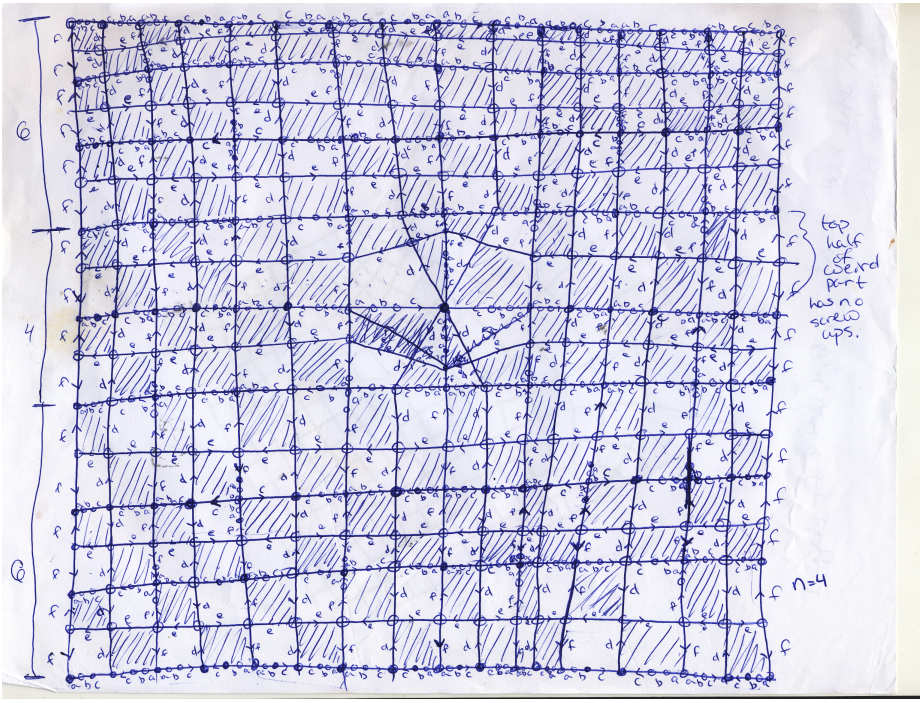

Figure 6: Q_4

Thus, it is clear that the set of all bands on Q_n is a proper subset of the set of all paths.

Let A_β be the set of all a edges traversed by a path β. We define B_β, C_β, D_β, E_β, and F_β similarly. Let A be the set of all a edges in Q_n, B the set of all b edges, and so forth.

Definition 2.3. We say that a band is *horizontal* if for all tiles t_i and t_{i+1} we have that $(E(t_i) \cap E(t_{i+1})) \cap (D \cup F) \neq \emptyset$.

This is to say that a band is horizontal if every pair of adjacent tiles shares either a d edge or an f edge.

Definition 2.4. A path β_n is called *horizontal* if $\beta_n \subseteq b_n$, where b_n is a horizontal band.

As may be observed in fig: 6, unlike with the Lattés examples, it is possible from one side of Q_n to an opposite side while crossing less than 2^n tiles. Notice that the point at the very center of the complex, call it P, has valence strictly greater than 4.

Definition 2.5. We say that a point p has *valence* m at level n if $p \in V(Q_n)$ and the number of edges that have p as a vertex is equal to m.

Points with valence greater than 4 the observed warping, which we'll call a shortcut, at the center of Q_4. This leads us to formally define the concept.

Definition 2.6. A path β_n has *shortcut* at point p_l and stage i, denoted $sc_{p_l,i}$, if

1. $sc_{p_l,i}$ is a horizontal subpath of β_n;
2. for any two tiles t_j and t_{j+1} with the property that $E(t_j) \cup E(t_{j+1}) = \{f, a, b, c\}$, we have $t_j \notin \beta_n$ and $t_{j+1} \notin \beta_n$;
3. $p_l \in V(t_j)$ for some tile $t_j \in \beta_n$;
4. at level n, p has valence strictly greater than 4;
5. $p_l \in V(Q_k)$, where k is the minimum level such that $val_k(p_l) > 4$;
6. the stage i is given by $i = n - k$.

We note that $p_l \in V(c_l)$, where c_l is some subcomplex of Q_n containing $sc_{p_1,i}$. Thus, the point p_l serves to locate the shortcut on the cell complex.

Definition 2.7. We call the point p_l in a shortcut $sc_{p_l,i}$ the *central point* of $sc_{p_l,i}$.

3 Finding the Minimal Distance

In this section, we will first look at some special paths and the distance along them. We conjecture that these paths are minimal on Q_n.

3.1 Calculating the Distance Along Some Special Paths

Here we will calculate the distance along a special set of paths, for any $n = 4m$, where $m \in \mathbf{N}$.. We note that, since we are concerned with the limit as n approaches infinity of this minimal distance, it will suffice to look at this distance for all multiples of 4.

By $d_{d,f}(\beta_{n_i})$ we denote the distance from an edge d to an edge f along a subpath β_{n_i} of a path β_n through a subcomplex c_i. We will denote the minimal distance across c_i in the d, f direction $D_{d,f}(c_i)$.

Let the central point of the shortcut that develops at level $n = 4$ be denoted P. Let $U, L \subset Q_4$ be such that U and L are horizontal bands and $sc_{P,1} \subseteq U \cup L$. Note that under subdivision U and L are subcomplexes of Q_n. We define a set of paths Γ_n on for $n = 4m$, where $m \in \mathbf{N}$, recursively as follows:

1. Γ_4 is the set of paths on Q_4 with the following properties:
   (a) $\gamma_4 \subset U \cup L$;
   (b) the central point P is a vertex of t_7 and of t_8;

(c) γ_4 uses the shortcut $sc_{P,1}$;

(d) $E(t_{14} \cap D \neq \emptyset$.

We note that each tile of γ_4 is a copy of Q_0. Under subdivision it will form a subcomplex of Q_n, which, after an additional four subdivisions when $n = 8$, the subcomplex will be a copy of all of Q_4. In general, at level n these subcomplexes will be copies of Q_{n-4}.

2. Γ_n is the set of paths on Q_n with the following properties:

   (a) $\gamma_n \subseteq \gamma_{n-4}$;

   (b) the subpath γ_{n_j} of γ_n contained in each subcomplex c_j of Q_n that was a tile $t_j \in \gamma_{n-4}$ follows a path that replicates the path γ_{n-4} traverses across all of Q_{n-4} unless the subcomplex $c_j \subseteq sc_{P,i}$ at level n, in which case the tile t_j at level $n-4$ behaves in four possible distinct ways with regard to the tiles t_{j-1} and t_{j+1}. Namely:

      i. the tile t_j shares an edge with t_{j-1} and an edge with t_{j+1};

      ii. the tile t_j shares an edge with t_{j-1}, but only a vertex with t_{j+1};

      iii. t_j shares a vertex only with t_{j-1}, but shares an edge with t_{j+1};

      iv. t_j shares vertices only with t_{j-1} and t_{j+1}.

      The behavior of t_j at level $n-4$ determines the behavior of the subpath γ_{n_j} at level n. If (i), then γ_{n_j} replicates γ_{n-4}. If (ii), then let γ_{n_j} replicate γ_n until the central point p_j of the central shortcut $sc_{p_j,i}$ is reached at which time continue diagonally to the vertex shared with c_{j+1}. If (iii), then let γ_{n_j} proceed diagonally from the vertex shared with c_{j-1} to the central point p_j of the central shortcut $sc_{p_j,i}$ of the subcomplex c_j and then replicate γ_{n-4}. If (iv), let γ_{n_j} cross c_j strictly diagonally, crossing 16 tiles.

We believe that the minimal distance is realized by following any path $\gamma_n \in \Gamma_n$ through the cell complexes that develop within the two central horizontal bands of Q_4, namely U and L, under subdivision.

Theorem 3.1. *Let $\gamma_n \in \Gamma_n$ be arbitrary. If the number of subdivisions n is such that $n = 4m$ for some $m \in \mathbf{N}$, then the distance along any path γ_n is equal to $X(n)$, where $X(n)$ is defined recursively by*

$$X(4) = 14 \text{ and}$$

$$X(n) = 13 \cdot X(n-1) + 2^{(n-4)}.$$

Proof. We will use induction on m. Let γ_n be defined as in our claim and let $\gamma_{n_i} \subseteq \gamma_n$ denote the sub-path of γ_n that is contained in a subcomplex c_i. Counting gives the length of γ_4 to be 14.

Consider $m = 2$. We note that every tile, t_i, along the middle horizontal edge of Q_4 is a copy of Q_0. Thus, after another 4 subdivisions, that is when $m = 2$, each of these subcomplexes is a copy of Q_4. Hence for each subcomplex

$c_i \notin sc_4$, we have $d_{d,f}(\gamma_{4_i}) = 14$. Since there are 12 subcomplexes $c_i \notin sc_4$, we have a total distance of $12 \cdot 14$.

Now consider the subcomplexes within the shortcut itself. Notice that if we are to use the shortcut $sc_{P,4}$ our path must cut through the point at the center of the shortcut complex. But since the subcomplexes within $sc_{P,4}$ are themselves copies of Q_4, each contains a shortcut $sc_{p,1}$. So our path must pass through the central point of these shortcut complexes as well. Hence, we traverse a path that is just like those for the subcomplexes not in sc_4 until we reach this center point of $sc_{p,1}$, crossing through 7 tiles. We then cut diagonally to the center point of $sc_{P,4}$. Since shortcuts only exist in the d, f direction, we cross 8 more tiles. The other subcomplex in sc_4 is the mirror image of the first, so crossing it, we cross 8 tiles diagonally to get to the center point of this subcomplex's $sc_{p,1}$ and then cross another 7 tiles. Thus, $d_{d,f}(\gamma_{n_{sc_4}}) = 14 + 16 = 14 + 2^4$.

Adding the distances across the subcomplexes $c_i \notin sc_4$ and those $c_i \in sc_4$, we have $d_{d,f}(\gamma_8) = 12 \cdot 14 + 14 + 2^4 = 13 \cdot 14 + 2^{8-4} = X(8)$. Hence, the base case holds.

Now suppose that our claim is satisfied after $n - 4 = 4(m - 1)$ subdivisions. Since each of the 12 tiles along the middle horizontal edge of Q_4 is a copy of Q_0, in Q_n these subcomplexes are copies of Q_{n-4}. Hence, for each subcomplex $c_j \notin sc_{P,n-4}$, we have $dd, f(c_j) = d_{d,f}(n - 4)$. Thus, the total distance across the subcomplexes $c_j \notin sc_{P,n-4}$ is $12 \cdot d_{d,f}(n - 4)$.

Next consider the subcomplexes inside the shortcut $sc_{P,n-4}$. Noting that, as with the $n = 8$ case, we wish our path to pass through the center point of $sc_{P,n-4}$, we cut across the first subcomplex, call it c_m where $m \in \mathbf{N}$ is fixed, as for the other subcomplexes $c_j \notin sc_{P,n-4}$ until we reach the central point of c_m, crossing $\frac{d_{d,f}(n-4)}{2}$ tiles. We then cut diagonally to the center point of $sc_{P,n-4}$. Since short cuts exist only in the d, f direction, this is just like cutting diagonally across a grid. We note that c_m has width equal to $\frac{1}{16}$ of Q_n. Thus, this diagonal distance is $\frac{2^n}{2^5}$. Because the other subcomplex within $sc_{P,n-4}$ is the reflection of c_m, we have a total distance across $sc_{P,n-4}$ of $2(\frac{D_{d,f}(n-4)}{2} + 2^{n-5}) = D_{d,f}(n - 4) + 2^{n-4}$.

Therefore, the total distance $d_{d,f}(\gamma_n) = X(n)$ for all $n = 4m$, as desired. □

3.2 The Limit

The recursive function that gives the distance along a path $\gamma_n \in \Gamma_n$ may be written explicitly. Although the explicit formulation fails to capture the direct behavior of γ_n, it makes the behavior of the limit $\lim_{n\to\infty} (D(n))^{\frac{1}{n}}$ clear.

Proposition 3.2. *Let $n = 4m$ for $m \in \mathbf{N}$ and recall the expression $X(n)$ defined recursively by*

$$X(4) = 14 \text{ and}$$

$$X(n) = 13 \cdot X(n - 1) + 2^{(n-4)}.$$

If we let $y_m = X(4m)$, this may be stated explicitly as $y_m = \frac{2}{3} \cdot 13^m + \frac{1}{3} \cdot 2^4 m$.

Proof. We note that $X(n+4) = 13 \cdot X(n) + 2^n$, which we rewrite as $X(4(m+1)) = 13 \cdot X(4m) + 2^{4m}$. Let $y_m = X(4m)$. Then $y_{m+1} = 13y_m + 2^{4m} = 13y_m + 16^m$ with $y_1 = 14$. Since y_{m+1} is the sum of homogeneous part $y^h_{m+1} = 13y_m$ and non-homogeneous part $y^p_{m+1} = 16^m$, we can deal with these two parts separately. We note that y^h_{m+1} has general solution $y^h_m = C \cdot 13^m$ for some constant C. We may write $y^p_m = A \cdot 2^{4m}$. Plugging this into the original equation for y_{m+1} we obtain $A \cdot 16^{m+1} = 13(A \cdot 16^m) + 16^m$. Dividing through by the 16^m term, we get $A \cdot 16 = 13A + 1$. Equivalently, $A = \frac{1}{3}$. Thus, the general solution to y_{m+1} is given by $y_m = C \cdot 13^m + \frac{1}{3} \cdot 16^m$. Plugging in our initial condition gives $14 = C \cdot 13 + \frac{1}{3} \cdot 16$. Solving for C we find $C = \frac{2}{3}$. Therefore, $y_m = \frac{2}{3} \cdot 13^m + \frac{1}{3} \cdot 2^4 m$, as desired. □

Now that we have the distance formula in a form that we can comfortably manage, we proceed to find the limit.

Theorem 3.3. *Given* $y_m = \frac{2}{3} \cdot 13^m + \frac{1}{3} \cdot 16^m$*, we have* $\lim_{m \to \infty} (y_m)^{\frac{1}{m}} = 16$.

Proof. Consider that

$$\begin{aligned}\left(\frac{2}{3} \cdot 13^m + \frac{1}{3} \cdot 16^m\right)^{\frac{1}{m}} &= \left(16^m \left(\frac{2}{3} \cdot \left(\frac{13}{16}\right)^m + \frac{1}{3}\right)\right)^{\frac{1}{m}} \\ &= 16 \left(\frac{2}{3} \cdot \left(\frac{13}{16}\right)^m + \frac{1}{3}\right)^{\frac{1}{m}},\end{aligned}$$

so $\lim_{m \to \infty} \left(\frac{2}{3} \cdot 13^m + \frac{1}{3} \cdot 16^m\right)^{\frac{1}{m}} = 16 \lim_{m \to \infty} \left(\frac{2}{3} \cdot \left(\frac{13}{16}\right)^m + \frac{1}{3}\right)^{\frac{1}{m}}$. Now consider that for all m:

$$\begin{aligned}\left(\frac{13}{16}\right)^m &< 1 \\ \frac{2}{3}\left(\frac{13}{16}\right)^m &< \frac{2}{3} \\ \frac{2}{3}\left(\frac{13}{16}\right)^m + \frac{1}{3} &< 1.\end{aligned}$$

Also, clearly $\frac{1}{3} < \frac{2}{3}\left(\frac{13}{16}\right)^m + \frac{1}{3}$. Since $\lim_{m \to \infty} \left(\frac{1}{3}\right)^{\frac{1}{m}} = 1$ and $\lim_{m \to \infty} 1^{\frac{1}{m}} = 1$, we have $\lim_{m \to \infty} \left(\frac{2}{3} \cdot \left(\frac{13}{16}\right)^{\frac{1}{m}} + \frac{1}{3}\right)^{\frac{1}{m}} = 1$, by the Squeeze Theorem. Hence, $\lim_{m \to \infty} \left(\frac{2}{3} \cdot 13^m + \frac{1}{3} \cdot 16^m\right)^{\frac{1}{m}} = 16$, as desired. □

3.3 Relevant Linear Algebra

We will next show that the paths $\gamma_n \in \Gamma_n$ are minimal. We will use an argument from linear algebra, so we introduce some concepts here.

Definition 3.4. We say that a matrix A is *non-negative*, and write $A \geq 0$, if the entry $a_{i,j} \geq 0, \forall i, j$.

We can consider vectors in a similar vein.

Definition 3.5. Let v be some vector in an arbitrary vector space V. We define v to be *non-negative*, and write $v \geq 0$, if $w_i \geq 0, \forall i$.

This allows us to order both matrices and vectors with the ordinary partial order. That is, it follows directly from the definitions that, for $n \times m$ matrices A and B, we have $A \leq B$ if and only if $B - A \geq 0$. Similarly, for vectors $v, w \in V$, we have $v \leq w$ if and only if $w - v \geq 0$.

Lemma 3.6. *Let A and B be $n \times m$ matrices such that $A, B \geq 0$ and let $v, w \in V$, where V is an n-dimensional vector space, with $v, w \geq 0$. If $A \leq B$ and $v \leq w$, then $Av \leq Bw$.*

Proof. We note that A, B non-negative implies that $a_{i,j}, b_{i,j} \geq 0, \forall i, j$ and v, w non-negative implies that $v_i, w_i \geq 0, \forall i$. Since $A \leq B$, we have $a_{i,j} \leq b_{i,j}, \forall i, j$ and, similarly, $v \leq w$ gives $v_i \leq w_i, \forall i$. Thus, $a_{i,j}v_i \leq b_{i,j}w_i, \forall i, j$. Hence,

$$\sum_{j=1}^{m} a_{i,j}v_i \leq \sum_{j=1}^{m} b_{i,j}w_i, \forall i.$$

This is equivalent to $Av \leq Bw$, by definition. □

A similar result holds for powers of non-negative square matrices.

Corollary 3.7. *Let A and B be $n \times n$ matrices such that $A, B \geq 0$ and let $v, w \in V$, where V is an n-dimensional vector space, with $v, w \geq 0$. If $A \leq B$ and $v \leq w$, then $A^n v \leq B^n w$.*

Proof. Note that for any non-negative square matrix M and any $n \in \mathbf{N}$ we have that M^n is also non-negative. The result now follows directly from our lemma. □

3.4 The Minimal Distance

Before continuing to the main result, we remind the reader that previous results have shown that the combinatorial distance on a cell complex such as Q_n is proportionally the same whether we count tiles or edges. In this argument, we find it more convenient to count edges.

Since the edges that $\gamma_n \in \Gamma_n$ traverses are all a, b, or c edges, we look at these edges under our subdivision rule to obtain the transition matrix

$$A = \begin{bmatrix} 1 & 0 & 1 \\ 1 & 0 & 1 \\ 0 & 1 & 1 \end{bmatrix}.$$

Note that $A \geq 0$.

Let a vector v_{β_n} be associated to each path β_n. Define v_{β_n} as $v_{\beta_n} = \begin{bmatrix} a_{\beta_n} \\ b_{\beta_n} \\ c_{\beta_n} \end{bmatrix}$, where $a_{\beta_n} = |A_{\beta_n}|$, $b_{\beta_n} = |B_{\beta_n}|$, and $c_{\beta_n} = |C_{\beta_n}|$. We note that $0 \leq v_{\gamma_4} = \begin{bmatrix} 14 \\ 14 \\ 14 \end{bmatrix}$ for any path $\gamma_4 \in \Gamma_4$.

Theorem 3.8. *A path $\gamma_n \in \Gamma_n$ is minimal for all $n \geq 4$.*

Proof. Given any path from the original f side of Q_0 to the original d side of Q_0, either it reaches the d side on the top of Q_n or on the right hand side of Q_n. Call the set of all paths that reach d on the top $\mathfrak{A}_n$ and call the set of paths that reach d on the right hand side $\mathfrak{B}_n$.

First consider the paths $\alpha_n \in \mathfrak{A}_n$. In particular, we will show that our result holds for all such paths. Let the path through the topmost horizontal band of Q_n through the vertex separating the sides d and e of Q_0 be called α'_n. Notice that, when $n = 4$, $d_{d,f}(\alpha'_4) = 14 = d_{d,f}(\gamma_4)$. Further, this distance the minimum distance for all paths $\alpha_4 \in \mathfrak{A}_4$. Equivalently, $v_{\alpha'_4} < v_{\alpha_4}$ for all $\alpha_4 \in \mathfrak{A}_4$ such that $\alpha_4 \neq \alpha'_4$. By the definition of a transition matrix, $v_{\alpha_n} = A^{n-4} v_{\alpha_4}$ for all $n > 4$, where we remember that

$$A = \begin{bmatrix} 1 & 0 & 1 \\ 1 & 0 & 1 \\ 0 & 1 & 1 \end{bmatrix}.$$

Thus, $v_{\alpha'_n} = A^{n-4} v_{\alpha'_4} < A^{n-4} v_{\alpha_4} = v_{\alpha_n}$ for all $\alpha_n \neq \alpha'_n$ and all $n > 4$, by 3.7 to 3.6. Hence, it is sufficient to show that $v_{\gamma_n} \leq v_{\alpha'_n}$. But this is already clear from the fact that $v_{\alpha'_4} = v_{\gamma_4}$ and from 3.7.

Now consider the paths $\beta_n \in \mathfrak{B}_n$. Note that $0 \leq \begin{bmatrix} 14 \\ 14 \\ 16 \end{bmatrix} \leq v_{\beta_4}$ for all such paths $\beta_4 \notin \Gamma_4$, so $v_{\gamma_4} < v_{\beta_4}$ for all $\beta_4 \notin \Gamma_4$. By the definition of a transition matrix, we have $v_{\gamma_n} = A^{n-4} v_{\gamma_4}$ for all $n > 4$. Since $A \geq 0$, we have $A^{n-4} \geq 0$ for all $n > 4$. Thus, $v_{\gamma_n} = A^{n-4} v_{\gamma_4} < A^{n-4} v_{\beta_4} = v_{\beta_n}$, where β_n is any path satisfying $\beta_n \notin \Gamma_n$. In other words, the distance along γ_n is minimal, as desired. □

References

[1] Cannon, J. W.; W. J. Floyd; R. Kenyon; and W. R. Parry. *Constructing Rational Maps from Subdivision Rules*. Brown University Mathematics. 3 August 2011. *http://www.math.brown.edu/ rkenyon/papers/ratsub.pdf*

[2] Coloring Booklets from Finite Subdivision Rules. Floyd, W. J. The Department of Mathematics at Virginia Tech. 3 August 2011. *http://www.math.vt.edu/people/floyd/coloring/*

[3] Haissinsky, Peter and Kevin M. Pilgrim. *Examples of Coarse Expanding Conformal Dynamical Systems*. To appear, proceedings of the conference "Dynamical Systems II, Denton 2009", special volume of *Discrete and Continuous Dynamical Systems*.

.

Statistical Consistency of the Method of Maximum Parsimony

Frederick Robinson and Elizabeth Ann Housworth

Abstract

We record our progress to date on the second parsimony conjecture of Mike Steel. That conjecture states that if binary characters have the same probability, p, of changing on each branch of a phylogeny, then for p sufficiently small and independent of the number of taxa related by the phylogeny, maximum parsimony is statistically consistent. That is, maximum parsimony will return the correct phylogeny with probability increasing to one as the amount of data observed on the extant taxa increases to infinity.

Introduction

Phylogenetics is the study of how different species are related. An important question in phylogenetics is how to recover a tree (phylogeny) describing how species are related, given characteristics (characters) of all the species involved. Throughout this paper, we will be concerned only with binary (0/1) characters.

The phylogeny estimation method with which we are concerned is maximum parsimony. It selects the phylogeny(ies) which involve the fewest number of changes in the character states needed to explain the observed species data – the most parsimonious ones. It is well-known that a phenomenon called long branch attraction (see [3] can cause maximum parsimony to return incorrect phylogenies no matter how many characters are observed at the species tips, leading to the method of maximum parsimony being inconsistent in some circumstances. However, any method, including the method of maximum likelihood, can be inconsistent if the data do not conform to the model assumptions (see [2], for instance). Our goal is to describe the assumptions under which the method of maximum parsimony is guaranteed to recover the original phylogenetic. It is already known that given a fixed number n of species on a phylogeny, there is a corresponding probability of character change, p_n, so that if the true probability of change, p, satisfies $0 < p < p_n$, then maximum parsimony is a consistent method for estimating the phylogeny.

Our goal is to show that there is a p_0 independent of the number of species related by the phylogeny, so that if the probability of change, p, satisfies $0 < p < p_0$, maximum parsimony is consistent, thus proving a conjecture of Steel [6].

Main Result

Our goal is to prove the following conjecture of Steel [6].

Conjecture: Consider taxa character sequences generated on a phylogeny with all branches having equal length, p, signifying the probability a binary character changes on the branch. If $p < 0.01$, then the method of maximum parsimony on the resulting taxon data is statistically consistent; i.e. maximum parsimony returns the correct phylogeny with probability tending to one as the number of characters observed increases to infinity.

To prove this result, we have created a probabilistic version of the definition of a one-clustering introduced in Chai and Housworth (2011) [1]. Before we define a one-clustering, we will clarify the other terminology we will use in this work. There are multiple trees involved in this work. One is the real, or true, tree on which the data, or random variables, are created by randomly flipping bits (0 to 1 or 1 to 0) on each edge, independently, with probability p. The result of this process is character sequences or random variables on the species tips of the tree which are observable.

The phylogeny we recreate using the method of maximum parsimony is a second tree which cannot agree with the real tree in the sense that the reconstruction of the sequences or random variables at the interior nodes cannot fully agree with their real counterparts. However, we will say that the maximum parsimony tree is equivalent to the real tree if both trees have the same collection of splits. A third tree will replace the most parsimonious resolutions at the interior nodes with close approximations to those and will be defined further below.

We now give some more formal definitions. We will view nodes in these trees as random variables. Again, there are the random variables on the real tree generated by the probabilistic process and random variables on the most parsimonious tree generated as the most parsimonious reconstruction of the random variables at the tips. We will identify vertices in trees by their corresponding random variables.

Definition 0.9 (degree)**.** The degree of a vertex a in a tree T is the number of edges connected to a and will be denoted $\deg_T(a)$.

Definition 0.10 (edge weight)**.** The weight of an edge connecting two vertices a and b is the expected distance between a and b: $d(a, b) = E(|a - b|)$.

Definition 0.11 (score)**.** The expected score of a tree T is the sum of the weights of the edges in T and is denoted by $score(T)$.

Definition 0.12 (depth)**.** The depth of a vertex a in a tree T is the minimum over degree 1 vertices b of the number of edges in the path from a to b and is denoted $\text{depth}_T(a)$. The degree 1 vertices themselves have depth 0.

Definition 0.13 (cherry)**.** A cherry in a tree T consists of two vertices a and b each connected by an edge to a common vertex q. The vertex $q = q(a, b)$ is called the root of the cherry.

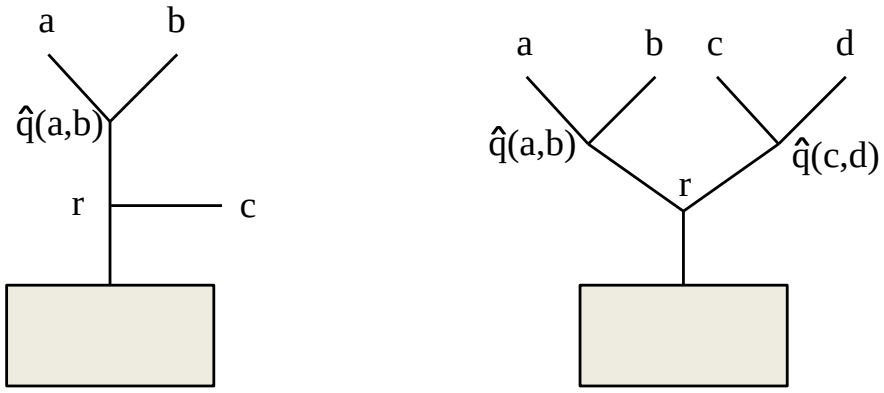

Figure 1: Two cases: the asymmetric case on the left with a cherry attached to an observed leaf sequence and the symmetric case on the right with two cherries attached together.

Definition 0.14 (external cherry)**.** An external cherry in a tree T consists of two degree 1 vertices a and b each connected by an edge to a common vertex $q = q(a, b)$. The only distinction between a cherry and an external cherry is that, for a cherry, a and b need not be leaves in T. This is a non-standard use of the term.

Definition 0.15 (approximate cherry root)**.** If vertices a and b form a cherry with root $q = q(a, b)$, then any other sequence $\hat{q} = \hat{q}(a, b)$ which is within $5p^2$ of $q = q(a, b)$ is an approximate cherry root.

Definition 0.16 (properly fully resolved)**.** A spanning tree T of N taxa sequences is properly fully resolved if the vertex associated with each taxon has degree 1 and all other vertices have degree 3.

We now explore the joint distribution that two parsimonious assignments that form a cherry in T equal or do not equal the real value at the cherry root. We proceed using an iterative argument.

In the initial case, considering the depth 1 vertices, we see that T has one of the following two structures. Call a pair of cherries the symmetric case and the cherry attached to a leaf as the asymmetric case. Note that the leaf vertex in the asymmetric case even when iterating is always an observed taxon sequence (our iterative process always leaves cherries behind.)

The process of constructing the most parsimonious sequences at each interior node requires a forward looking process followed by a backward looking process. We can give approximate parsimony values by just looking in a small neighborhood of a node. We prove further below that these roots are, in fact, approximate parsimony roots as defined above.

In the asymmetric case, an approximate parsimony root is

$$\hat{q}(a,b) = \begin{cases} a & \text{if } a = b \\ c & \text{if } a \neq b \end{cases}$$

In the symmetric case, an approximate parsimony root for a and b is

$$\hat{q}(a,b) = \begin{cases} a & \text{if } a = b \text{ or } (a \neq b \text{ and } c \neq d) \\ c & \text{if } a \neq b \text{ and } c = d \end{cases}$$

Similarly, an approximate parsimony root for c and d is

$$\hat{q}(c,d) = \begin{cases} c & \text{if } c = d \text{ or } (a \neq b \text{ and } c \neq d) \\ a & \text{if } c \neq d \text{ and } a = b \end{cases}$$

To prove that these are indeed approximate parsimony roots and are close to the real random variables, we consider the joint distribution of the random variables indicating whether, in the asymmetric case, $\hat{q}(a,b) = r$ and $c = r$, and in the symmetric case, $\hat{q}(a,b) = r$ and $\hat{q}(c,d) = r$. Since we need to be able to iterate this argument we go ahead and give the general iteration formulas. These are quite complicated looking but are relatively straightforward to obtain by conditioning on whether the real roots above r are equal to r or to $1-r$. We let superscripts (1) denote the previous iteration of this joint distribution on the left and (2) denote the previous iteration of this joint distribution on the right in the symmetric case. The joint distribution without superscripts is the current distribution. The subscripts indicate whether the random variables agree with r or disagree with r.

In the asymmetric case, these iterative formulas are based on two cases: whether $r(a,b) = r$ or $r(a,b) = 1-r$, where $r(a,b)$ is the real (probabilistic) outcome at cherry root of a and b.

$$\begin{aligned} P_{r,r} &= (1-p)^2 \left[P^{(1)}_{r,r} + P^{(1)}_{r,(1-r)} + P^{(1)}_{(1-r),r} \right] \\ &\quad + p(1-p) \left[P^{(1)}_{(1-r),(1-r)} + P^{(1)}_{r,(1-r)} + P^{(1)}_{(1-r),r} \right] \\ &= P\left(\hat{q}(a,b) = r, c = r\right) \end{aligned} \tag{A1}$$

$$\begin{aligned} P_{r,(1-r)} &= p(1-p) \left[P^{(1)}_{r,r} \right] + p^2 \left[P^{(1)}_{(1-r),(1-r)} \right] \\ &= P\left(\hat{q}(a,b) = r, c = 1-r\right) \end{aligned} \tag{A2}$$

$$\begin{aligned} P_{(1-r),r} &= (1-p)^2 \left[P^{(1)}_{(1-r),(1-r)} \right] + p(1-p) \left[P^{(1)}_{r,r} \right] \\ &= P\left(\hat{q}(a,b) = 1-r, c = r\right) \end{aligned} \tag{A3}$$

$$
\begin{aligned}
P_{(1-r),(1-r)} &= (1-p)p\left[P^{(1)}_{(1-r),(1-r)} + P^{(1)}_{r,(1-r)} + P^{(1)}_{(1-r),r}\right] \\
&\quad + p^2\left[P^{(1)}_{r,r} + P^{(1)}_{r,(1-r)} + P^{(1)}_{(1-r),r}\right] \\
&= P\left(\hat{q}(a,b) = 1-r, c = 1-r\right)
\end{aligned} \tag{A4}
$$

In the symmetric case, these iterative formulas are:

$$
\begin{aligned}
P_{r,r} &= (1-p)^2\left[P^{(1)}_{r,r}P^{(2)}_{r,r} + P^{(1)}_{r,r}\left(P^{(2)}_{r,(1-r)} + P^{(2)}_{(1-r),r}\right)\right. \\
&\quad \left. + \left(P^{(1)}_{r,(1-r)} + P^{(1)}_{(1-r),r}\right)P^{(2)}_{r,r} + P^{(1)}_{r,(1-r)}P^{(2)}_{r,(1-r)}\right] \\
&\qquad\qquad (r(a,b) = r(c,d) = r) \\
&\quad + p(1-p)\left[P^{(1)}_{r,r}P^{(2)}_{(1-r),(1-r)} + P^{(1)}_{r,r}\left(P^{(2)}_{r,(1-r)} + P^{(2)}_{(1-r),r}\right)\right. \\
&\quad \left. + \left(P^{(1)}_{r,(1-r)} + P^{(1)}_{(1-r),r}\right)P^{(2)}_{(1-r),(1-r)} + P^{(1)}_{r,(1-r)}P^{(2)}_{(1-r),r}\right] \\
&\qquad\qquad (r(a,b) = r, r(c,d) \neq r) \\
&\quad + p(1-p)\left[P^{(1)}_{(1-r),(1-r)}P^{(2)}_{r,r} + \left(P^{(1)}_{r,(1-r)} + P^{(1)}_{(1-r),r}\right)P^{(2)}_{r,r}\right. \\
&\quad \left. + P^{(1)}_{(1-r),(1-r)}\left(P^{(2)}_{r,(1-r)} + P^{(2)}_{(1-r),r}\right) + P^{(1)}_{(1-r),r}P^{(2)}_{r,(1-r)}\right] \\
&\qquad\qquad (r(a,b) \neq r, r(c,d) = r) \\
&\quad + p^2\left[P^{(1)}_{(1-r),(1-r)}P^{(2)}_{(1-r),(1-r)} + \left(P^{(1)}_{r,(1-r)} + P^{(1)}_{(1-r),r}\right)P^{(2)}_{(1-r),(1-r)}\right. \\
&\quad \left. + P^{(1)}_{(1-r),(1-r)}\left(P^{(2)}_{r,(1-r)} + P^{(2)}_{(1-r),r}\right) + P^{(1)}_{(1-r),r}P^{(2)}_{(1-r),r}\right] \\
&\qquad\qquad (r(a,b) \neq r, r(c,d) \neq r) \\
&= P\left(\hat{q}(a,b) = r, \hat{q}(c,d) = r\right)
\end{aligned} \tag{S1}
$$

$$
\begin{aligned}
P_{r,(1-r)} &= (1-p)^2\left[P^{(1)}_{r,r}P^{(2)}_{(1-r),(1-r)} + P^{(1)}_{r,(1-r)}P^{(2)}_{(1-r),r}\right] \\
&\quad + p(1-p)\left[P^{(1)}_{r,r}P^{(2)}_{r,r} + P^{(1)}_{r,(1-r)}P^{(2)}_{r,(1-r)}\right] \qquad (r(a,b) = r, r(c,d) \neq r) \\
&\quad + p(1-p)\left[P^{(1)}_{(1-r),(1-r)}P^{(2)}_{(1-r),(1-r)} + P^{(1)}_{(1-r),r}P^{(2)}_{(1-r),r}\right] \\
&\qquad\qquad (r(a,b) \neq r, r(c,d) = r) \\
&\quad + p^2\left[P^{(1)}_{(1-r),(1-r)}P^{(2)}_{r,r} + P^{(1)}_{(1-r),r}P^{(2)}_{r,(1-r)}\right] \qquad (r(a,b) \neq r, r(c,d) \neq r) \\
&= P\left(\hat{q}(a,b) = r, \hat{q}(c,d) = 1-r\right)
\end{aligned} \tag{S2}
$$

$$
\begin{aligned}
P_{(1-r),r} = (1-p)^2 &\left[P^{(1)}_{(1-r),(1-r)}P^{(2)}_{r,r} + P^{(1)}_{(1-r),r}P^{(2)}_{r,(1-r)}\right] && \text{(S3)}\\
+ p(1-p) &\left[P^{(1)}_{(1-r),(1-r)}P^{(2)}_{(1-r),(1-r)} + P^{(1)}_{(1-r),r}P^{(2)}_{(1-r),r}\right] \\
& && (r(a,b) = r, r(c,d) \neq r)\\
+ p(1-p) &\left[P^{(1)}_{r,r}P^{(2)}_{r,r} + P^{(1)}_{r,(1-r)}P^{(2)}_{r,(1-r)}\right] && (r(a,b) \neq r, r(c,d) = r)\\
+ p^2 &\left[P^{(1)}_{r,r}P^{(2)}_{(1-r),(1-r)} + P^{(1)}_{r,(1-r)}P^{(2)}_{(1-r),r}\right] && (r(a,b) \neq r, r(c,d) \neq r)\\
= P&\left(\hat{q}(a,b) = 1-r, \hat{q}(c,d) = r\right)
\end{aligned}
$$

$$
\begin{aligned}
P_{(1-r),(1-r)} = (1-p)^2 &\left[P^{(1)}_{(1-r),(1-r)}P^{(2)}_{(1-r),(1-r)} + P^{(1)}_{(1-r),(1-r)}\left(P^{(2)}_{r,(1-r)} + P^{(2)}_{(1-r),r}\right)\right. \\
& && \text{(S4)}\\
&\left. + \left(P^{(1)}_{r,(1-r)} + P^{(1)}_{(1-r),r}\right)P^{(2)}_{(1-r),(1-r)} + P^{(1)}_{(1-r),r}P^{(2)}_{(1-r),r}\right] \\
& && (r(a,b) = r(c,d) = r)\\
+ p(1-p) &\left[P^{(1)}_{(1-r),(1-r)}P^{(2)}_{r,r} + \left(P^{(1)}_{r,(1-r)} + P^{(1)}_{(1-r),r}\right)P^{(2)}_{r,r}\right. \\
&\left. + P^{(1)}_{(1-r),(1-r)}\left(P^{(2)}_{r,(1-r)} + P^{(2)}_{(1-r),r}\right) + P^{(1)}_{r,(1-r)}P^{(2)}_{(1-r),r}\right] \\
& && (r(a,b) = r, r(c,d) \neq r)\\
+ p(1-p) &\left[P^{(1)}_{r,r}P^{(2)}_{(1-r),(1-r)} + P^{(1)}_{r,r}\left(P^{(2)}_{r,(1-r)} + P^{(2)}_{(1-r),r}\right)\right. \\
&\left. + \left(P^{(1)}_{r,(1-r)} + P^{(1)}_{(1-r),r}\right)P^{(2)}_{(1-r),(1-r)} + P^{(1)}_{(1-r),r}P^{(2)}_{r,(1-r)}\right] \\
& && (r(a,b) \neq r, r(c,d) = r)\\
+ p^2 &\left[P^{(1)}_{r,r}P^{(2)}_{r,r} + \left(P^{(1)}_{r,(1-r)} + P^{(1)}_{(1-r),r}\right)P^{(2)}_{r,r}\right. \\
&\left. + P^{(1)}_{r,r}\left(P^{(2)}_{r,(1-r)} + P^{(2)}_{(1-r),r}\right) + P^{(1)}_{r,(1-r)}P^{(2)}_{r,(1-r)}\right] \\
& && (r(a,b) \neq r, r(c,d) \neq r)\\
= P&\left(\hat{q}(a,b) = 1-r, \hat{q}(c,d) = 1-r\right)
\end{aligned}
$$

Note that initially, the probability two observed tips equal the true root value is $(1-p)^2$, the probability a specific one equals the true root value and the other one does not is $p(1-p)$ and the probability neither equals the true root value is p^2. Plugging this into the formulas above gives the following first set of joint distributions in the asymmetric and symmetric cases.

$$
\begin{array}{ll}
\hat{q}(a,b)\backslash c & \begin{array}{cc} r & 1-r \end{array} \\
\begin{array}{l} r \\ 1-r \end{array} & \begin{pmatrix} 1-2p(1-p)-p^3 & p(1-3p(1-p)) \\ p(1-p)^2 & 3p^2(1-p) \end{pmatrix}
\end{array}
$$

and

$$\begin{array}{lcc} \hat{q}(a,b)\backslash\hat{q}(c,d) & r & 1-r \\ r & 1-2p(1-p)-2p^2(1-p)^2 & p(1-p)-2p^2(1-p)^2 \\ 1-r & p(1-p)-2p^2(1-p)^2 & 6p^2(1-p)^2 \end{array}$$

We prove several inequalities:

Theorem 0.17. *For $p < 0.01$,*

- $2p^2 \leq P_{(1-r),(1-r)} \leq 7p^2$
- $p - 4p^2 \leq \min\left(P_{(1-r),r}, P_{r,(1-r)}\right) \leq \max\left(P_{(1-r),r}, P_{r,(1-r)}\right) \leq p + 4p^2$
- $1 - 2p - 15p^2 \leq P_{r,r} \leq 1 - 2p + 6p^2$

Proof. Note that the initial joint distributions satisfy these inequalities. Proceeding by induction, we will show that after each iteration described above the resulting joint distribution still satisfies these inequalities.

In the asymmetric case, the lower and upper bounds on $P_{(1-r),(1-r)}$ are obtained by plugging in the relevant lower and upper bounds (assumed true by induction) into (A4):

$$2p^2 \leq 3p^2 - 10p^3 - 15p^4 \leq P_{(1-r),(1-r)} \leq 3p^2 + 13p^3 + 3p^4 \leq 7p^2$$

which is true for $p < .088$.

Similarly, lower and upper bounds for $P_{(1-r),r}$ and $P_{r,(1-r)}$ are obtained by plugging in the relevant lower and upper bounds (assumed true by induction) into (A3) and (A2):

$$p - 4p^2 \leq p - p^2 - 15p^3 + 15p^4 \leq P_{(1-r),r} \leq p + 4p^2 - 2p^3 - 3p^4 \leq p + 4p^2$$

which is true for $p < .27$ and

$$p - 4p^2 \leq p - 3p^2 - 11p^3 + 15p^4 \leq P_{r,(1-r)} \leq p - 3p^2 + 12p^3 - 3p^4 \leq p + 4p^2$$

which is true for $p < .10$.

Finally, lower and upper bounds for $P_{r,r}$ are obtained via the lower and upper bounds for $P_{(1-r),(1-r)}$, $P_{(1-r),r}$, and $P_{r,(1-r)}$ obtained for this iteration just above:

$$1 - 2p - 15p^2 \leq P_{r,r} \leq 1 - 2p + 6p^2$$

Similarly, in the symmetric case, he lower and upper bounds on $P_{(1-r),(1-r)}$ are obtained by plugging in the relevant lower and upper bounds (assumed true by induction) into (S4):

$$\begin{aligned} 2p^2 &\leq 6p^2 - 30p^3 - 65p^4 + 300p^5 + 225p^6 \\ &\leq P_{(1-r),(1-r)} \\ &\leq 6p^2 + 54p^3 + 139p^4 + 78p^5 + 9p^6 \leq 7p^2 \end{aligned}$$

for $p < .01$.

We omit demonstrating the bounds on $P_{(1-r),r)}$ as it is identical to $P_{r,(1-r)}$. Using (S2) we see that

$$\begin{aligned} p - 4p^2 &\leq p - 3p^2 - 36p^3 + 85p^4 + 165p^5 - 225p^6 \\ &\leq P_{r,(1-r)} \\ &\leq p + 3p^2 + 8p^3 + 64p^4 + 21p^5 - 9p^6 \leq p + 4p^2 \end{aligned}$$

for $p < .03$.

Again, using the bounds just obtained, we obtain the following bounds on $P_{r,r}$:

$$1 - 2p - 15p^2 \leq P_{r,r} \leq 1 - 2p + 6p^2$$

□

Proposition 0.18. *The approximate cherry root $\hat{q}(a, b)$ is an approximate parsimony root*

Proof. Note, that in the asymmetric case, our choice of $\hat{q}(a, b)$ is one of at most two equally parsimonious choices. Thus, up to ambiguity in the choice of the most parsimonious value, our choice gives no error. In the symmetric case, our choice for $\hat{q}(a, b)$ can be wrong, but only in the case where both the left and right cherries contain one left zero and one left one. The joint distribution calculation above gives that this happens with probability less than $4(p + 4p^2)^2 \leq 5p^2$ if $p < 0.01$. □

Proposition 0.19. *We also claim that $d(\hat{q}(a, b), r(a, b)) \leq 16p^2$.*

Proof. To see this, condition when necessary on the outcome of $r(a, b)$ and $r(c, d)$:

$$
\begin{aligned}
P\left(\hat{q}(a,b) \neq r(a,b)\right) &= P^{(1)}_{(1-r),(1-r)} + P^{(1)}_{(1-r),r}\left(P^{(2)}_{r,(1-r)} + P^{(2)}_{(1-r),r}\right) \\
&\quad + (1-p)^2\left(P^{(1)}_{r,(1-r)} + P^{(1)}_{(1-r),r}\right)P^{(2)}_{(1-r),(1-r)} \\
&\qquad\qquad (r(a,b) = r(c,d) = r)) \\
&\quad + p(1-p)\left(P^{(1)}_{r,(1-r)} + P^{(1)}_{(1-r),r}\right)P^{(2)}_{r,r} \\
&\qquad\qquad (r(a,b) = r, r(c,d) \neq r) \\
&\quad + p(1-p)\left(P^{(1)}_{r,(1-r)} + P^{(1)}_{(1-r),r}\right)P^{(2)}_{r,r} \\
&\qquad\qquad (r(a,b) \neq r, r(c,d) = r)) \\
&\quad + p^2\left(P^{(1)}_{r,(1-r)} + P^{(1)}_{(1-r),r}\right)P^{(2)}_{(1-r),(1-r)} \\
&\qquad\qquad (r(a,b) \neq r, r(c,d) \neq r) \\
&\leq 15p^2 + 32p^3 + 20p^4 + 72p^5 - 32p^6 \\
&\leq 16p^2
\end{aligned}
$$

for $p < 0.01$.

In the asymmetric case, the calculation is simpler:

$$
\begin{aligned}
P\left(\hat{q}(a,b) \neq r(a,b)\right) &= P^{(1)}_{(1-r),(1-r)} + \left(P^{(1)}_{(1-r),r} + P^{(1)}_{r,(1-r)}\right)P(c \neq r(a,b)) \\
&= P^{(1)}_{(1-r),(1-r)} + \left(P^{(1)}_{(1-r),r} + P^{(1)}_{r,(1-r)}\right)2p(1-p) \\
&\leq 11p^2 + 12p^3 - 16p^4 \\
&\leq 16p^2
\end{aligned}
$$

for all $p \leq 1$.

Thus, our approximate parsimony roots are within $5p^2$ of one of the choices for their most parsimonious counterparts and also within $16p^2$ of the roots generated by the real (probabilistic) process when $p < 0.01$. The fact that the most parsimonious roots are close to the real, probabilistic, roots, gives that the most parsimonious phylogeny is a probabilistic one-clustering.

□

Conjecture: Any connected, fully resolved one-clustering on 3 or more taxa gives the corresponding fully resolved phylogeny as the unique most parsimonious phylogeny with the ancestral sequences uniquely determined by the one-clustering.

Summary and Conclusions

In the discrete case considered by Housworth and Chai [1], the notion of one clustering allows for a peeling argument where the true tree T, and the test tree T' are simultaneously broken down (peeled) while keeping track of the score of the removed branches. The argument shows that the total score of T' is always greater than that of T, unless $T' = T$. This approach is likely adaptable to the problem at hand, and will lead to a proof of the conjecture. We hope to refine our notion of probabilistic one clustering to allow an adaptation of this argument to the current problem.

We have a partial proof that maximum parsimony is consistent. It remains to adapt the pealing argument used in a similar, discrete problem to work in the probabilistic realm.

Acknowledgements

We thank Mike Steel for posting interesting conjectures in phylogenetics on his website.

References

[1] J. Chai and E.A. Housworth, (2011), On the number of binary characters needed to recover a phylogeny using maximum parsimony, Bulletin of Mathematical Biology 73, 1398-1411.

[2] J. Chang, (1996), Inconsistency of evolutionary tree topology reconstruction methods when substitution rates vary across characters, Mathematical Biosciences 13, 189-216.

[3] J. Felsenstein, (2004), Inferring Phylogenies, Sinauer Associates, Inc., Sunderland, MA.

[4] M.D. Hendy, L.R. Foulds, and D. Penny, (1980), Proving phylogenetic trees minimal with l-clustering and set partitioning, Mathematical Biosciences 51, 71-88.

[5] R.J. Lipman, R.E. Tarjan, (1979), A separator theorem for planar graphs, SIAM Journal of Applied Mathematics 36, 177-189.

[6] M. Steel, (2000), Sufficient Conditions for two tree reconstruction techniques to succeed on sufficiently long sequences, SIAM Journal of Discrete Mathematics 14, 36-48.